NASA Tech Briefs

Official Publication of
National Aeronautics and
Space Administration
Volume 15 Number 8

Transferring Technology
to Industry and
Government
August 1991

Advanced Telerobots:
Tougher
Stronger
Smarter

THE ONLY TAPE DRIVE THAT PUTS 25GB ON A SINGLE 8MM TAPE.

Do you wish you could find a backup system with enough capacity, speed, and sophistication to backup unattended?

Could you recreate a document from scratch in the time it takes you to restore it?

FAST BACKUP, FAST RESTORE.

Introducing the CY-8500, the 8mm tape drive that gives you up to 25 GB on a single tape. And with transfer rates of up to 90 MB per minute, backup takes less time, frees resources, and makes frequent backup simple and convenient.

And that's not all. The CY-8500 offers fast file search capability. So you get the advantages of high capacity and fast transfer rates plus the ability to locate and restore your files quickly – about 75 times faster than normal speed.

TRUE "PLUG-AND-PLAY" COMPATIBILITY WITH:

Alliant	DEC Unibus	PC 386/ix
Alpha Micro	Gould	PC MS-DOS
Altos	HP	PC
Apollo	IBM AS/400	Xenix/Unix
Arix	IBM Mainframe	Pertec
AT&T	IBM RISC/6000	Plexus
Basic-4	IBM RT	Prime
Concurrent	IBM S/38	Pyramid
Convergent	Macintosh	Sequent
DataGeneral	McDonnell Douglas	Silicon Graphics
DEC 3100	NCR	Sun
DEC BI-Bus	Novell	Unisys
DEC HSC	OS/2	Wang
DEC Q-Bus	PS/2	*and more*
DEC TU/TA81		

CONFIGURATION FLEXIBILITY.

The state-of-the-art liquid crystal display gives you complete drive status information. Command under execution, transfer rate, tape remaining, and ECC are presented in a clear easy-to-read format. By offering such features as data compression – for five times the storage capacity per tape – and data encryption – giving you data access control – the CY-8500 adapts to your company's growing needs. We'll adapt to your site requirements too, with rack mounting options and cable lengths of up to 80 feet.

PROVEN TECHNOLOGY.

Best of all, the CY-8500 offers peace of mind. 8mm helical scan technology, designed for data recording, gives you demonstrated performance and reliability. Not an adaptation of an audio recording format.

The CY-8500 is part of a complete family of tape backup products that range in capacity from the 150 MB ¼″ cartridge streamer to the 2 TB cartridge handling system. All backed up by our in-house technical support group and 12-month warranty. For more information on how you can enjoy the best value in tape backup, call today at 804/873-0900.

CONTEMPORARY CYBERNETICS Group

Circle Reader Action No. 411

Rock Landing Corporate Center · 11846 Rock Landing, Newport News, VA 23606 · 804/873-0900 · FAX 804/873-8836

YOU CAN DEVELOP ADA CODE WITHOUT ADAMAT.™ OF COURSE, YOU CAN SKYDIVE WITHOUT THIS, TOO.

The fact is, when you write Ada code without using AdaMAT™ you're really putting the quality of your code at great risk. To be frank, you're actually inviting poorly written, unclear and inconsistent code that guarantees errors during development.

AdaMAT is quite simply, the most valuable and crucial software engineering tool that is available today to Ada program developers. It is the only tool for the prevention of errors during development. AdaMAT analyzes Ada code and evaluates it using key quality characteristics that are based on the most effective use of the language.

With the use of AdaMAT, potential errors are detected prior to testing. It lets programmers insure the quality of their code earlier in development when errors are much less time-consuming and costly to fix. So avoid the pitfalls. Get your project in on time and right on budget. Write clean, consistent, accurate, reliable Ada code. And do it whether you're developing in the Rational, VAX, SUN, or SCO/UNIX environments. Call us today at 1-800-522-7321 for complete infomation. We'd jump at the chance to tell you all about the immediate benefits you'll receive using AdaMAT for your Ada development.

DRC® DYNAMICS RESEARCH CORPORATION

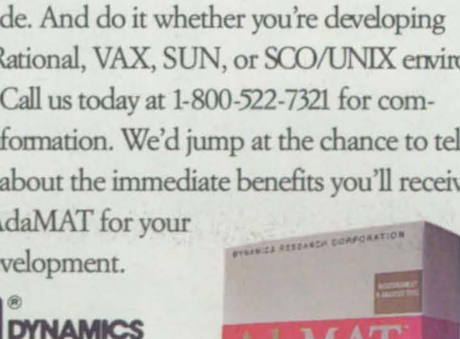

AdaMAT. The code word for quality Ada.

Dynamics Research Corporation, 60 Frontage Road, Andover, MA 01810

Circle Reader Action No. 601


MORE HIGH PRECISION FITTINGS THAN ANYWHERE ELSE IN THE WORLD.
VICI
Valco Instruments Co. Inc.
P.O. Box 55603, Houston, TX 77255 USA
Telephone (713) 688-9345
Telefax (713) 688-8106 Telex 79-0033 VALCO HOU
VICI AG
Valco Europe
Untertannberg 7 CH-6214 Schenkon, Switzerland
Telephone (045) 21 68 68
Telefax (045) 21 30 20 Telex 868342 VICI CH
Circle Reader Action No. 498

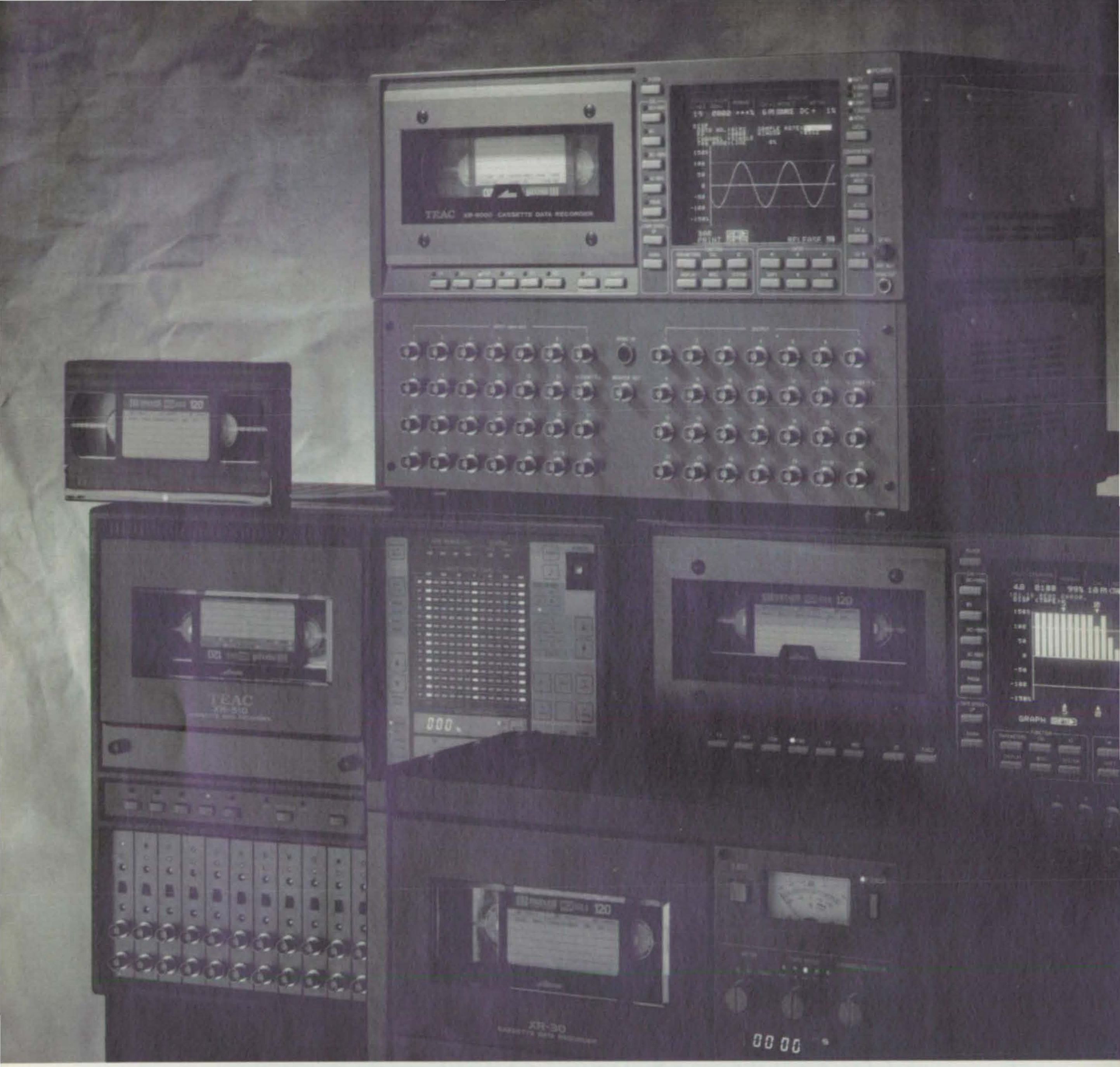

...ONE GIANT STEP FOR ENGINEERING

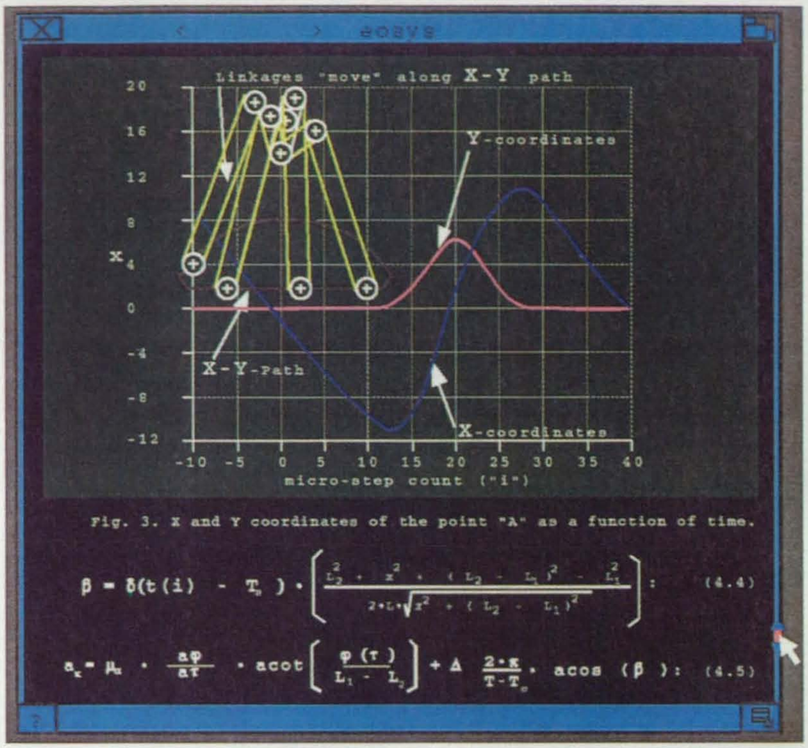

A revolutionary PC based software so advanced, it will change the way you solve day to day engineering problems.

POWERFUL COMBINATION UNDER "ONE ROOF"

EOSys is a new engineering language and application package...but EOSys is more...the combination of E-Language with its applications and utilities is synergistic. The result is a powerful combination of capabilities assembled in one easy to use package. Its integrated design uniquely combines vivid graphics, mathematical capabilities, full scope editor and recalculation capabilities by use of E-Language.

EASY TO LEARN AND USE

This powerful, easy to learn and use language is modeled after the human thought process. EOSys is based on English and math, so if you can read and write in English, you can understand and use EOSys.

ONE GIANT STEP FOR ENGINEERS AND SCIENTISTS

E-Language allows you to write applications and support many of your technical needs. With EOSys you don't have to be an expert programmer. The only thing required is creativity. The power and expressiveness of E-Language allows you to attack problems you would not have dreamed of solving with Computer Aided Engineering programs currently on the market.

ADVANCED COMPONENTS

EOSys is state of the art, featuring a windowing WYSIWYG environment, parametric modeling, on the fly reconfigurable keymap, mouse interface and on line help. Plus, EOSys provides important basic facilities such as natural user interface, 350 commonly used functions, and solving equations including the creation, editing, and solving of complex formulas and graphics. EOSys will print all analysis in presentation quality documents using regular laser printers.

Call us for a free EOSys interactive demo disk, available in 5-1/4 and 3-1/2 inch diskettes.
Dial 1-800-EOSys-21, that's 1-800-367-9721.
Available for IBM/AT™ and compatibles.
Thirty day unconditional money back guarantee.

EO Systems, Inc.
1333 Blue Hills Avenue
Bloomfield, CT. 06002

For 3-1/2 Inch Diskettes Circle Reader Action No. 598. For 5-1/4 Inch Diskettes Circle Reader Action No. 595.

NASA Tech Briefs

Transferring Technology to Industry and Government

August 1991
Volume 15 Number 8

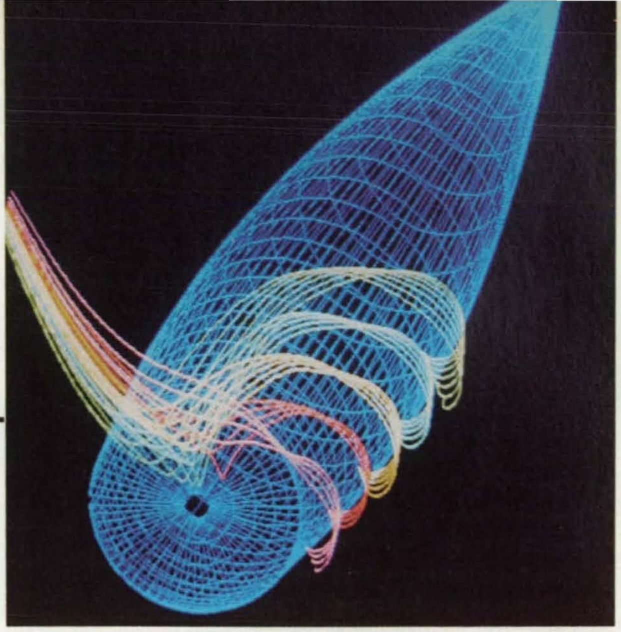

Graphic courtesy Ames Research Center

Ames scientists used computational fluid dynamics (CFD) techniques to produce this solution to the incompressible, viscous flow past an ogive/cylinder. See the tech brief on page 73.

SPECIAL FEATURES

TECHNICAL SECTION

DEPARTMENTS

On The Cover: Odetics' new high-strength, dexterous robot arm, designed for dangerous jobs such as space truss assembly, satellite servicing, and hazardous waste site cleanup. A hierarchical control system developed under NASA contract continuously optimizes the arm position for the task at hand. Turn to page 11.

(Photo courtesy Odetics Inc.)

Jet Propulsion Laboratory has created a testbed for next-generation robotic systems (page 30).

Photo courtesy Jet Propulsion Laboratory

NASA Tech Briefs, ISSN 0145-319X, USPS 750-070, copyright © 1991 in U.S., is published monthly by Associated Business Publications Co., Ltd., 41 E. 42nd St., New York, NY 10017-5391. The copyrighted information does not include the individual tech briefs which are supplied by NASA. Editorial, sales, production and circulation offices at 41 East 42nd Street, New York, NY 10017-5391. Subscription for non-qualified subscribers in the U.S. , Panama Canal Zone, and Puerto Rico, $75.00 for 1 year; $125.00 for 2 years; $200.00 for 3 years. Single copies $10.00. Foreign subscriptions one-year U.S. Funds $150.00. Remit by check, draft, postal, express orders or VISA, MasterCard, and American Express. Other remittances at sender's risk. Address all communications for subscriptions or circulation to NASA Tech Briefs, 41 East 42nd Street, New York, NY 10017-5391. Second-class postage paid at New York, NY and additional mailing offices. **POSTMASTER: please send address changes to NASA Tech Briefs, 41 E. 42nd Street, Suite 921, New York, NY 10017-5391.**

NASA Tech Briefs

Official Publication of National Aeronautics and Space Administration

ABP BPA

NASA Tech Briefs:

Published by	**Associated Business Publications**
Editor-in-Chief/Publisher	**Bill Schnirring**
Associate Publisher	**Frank Nothaft**
Editor	**Joseph T. Pramberger**
Managing Editor	**R.J Laer**
Associate Editor	**Sarah L.Gall**
Assistant Editor	**Justina Cardillo**
Assistant Editor	**Patrick Corbett**
Technical Advisor	**Dr. Robert E. Waterman**
Production Manager	**Rita Nothaft**
Traffic Manager	**James E. Cobb**
Art Director	**Pierre Granier**
Circulation Manager	**Cheryl Cohen**
Advertising Coordinator	**Daniel Murphy**
Telecommunications Specialist	**Evelyn Mars**
Reader Service Manager	**Sylvia Valentin**

Briefs & Supporting Literature:
Provided to National Aeronautics and Space Administration by **International Computers & Telecommunications, Inc.**, NY, NY with assistance from **Logical Technical Services**, NY, NY

Technical/Managing Editor	**Ted Selinsky**
Art Director	**Luis Martinez**
Administrator	**Elizabeth Texeira**
Chief Copy Editor	**Lorne Bullen**
Staff Writers/Editors	**Dr. James Boyd, Dr. Larry Grunberger, Dr. Theron Cole, Jordan Randjelovich, George Watson, Oden Browne**
Graphics	**Zinaida Gimpeleva, Vernald Gillman, Pamela Baynham, Charles Sammartano**
Editorial & Production	**Bill Little, Ivonne Valdes, Susan Kyu Oh, Frank Ponce**

NASA:
NASA Tech Briefs are provided by the National Aeronautics and Space Administration, Technology Utilization Division, Washington, DC:

Administrator	**Richard H. Truly**
Assistant Administrator for Commercial Programs	**James T. Rose**
Deputy Assistant Administrator(Programs)	**Frank E. Penaranda**
Deputy Director TU Division(Publications Manager)	**Leonard A. Ault**
Manager, Technology Utilization Office, NASA Center For AeroSpace Information	**Walter M. Heiland**

Associated Business Publications
41 East 42nd Street, Suite 921, New York, NY 10017-5391
(212) 490-3999 FAX (212) 986-7864

President	**Bill Schnirring**
Executive Vice President	**Frank Nothaft**
Vice President	**Domenic A. Mucchetti**
Operations Manager	**Rita Nothaft**
Controller	**Felecia Lahey**
Systems Analyst	**Patrick Wolfert**

Advertising:
New York Office:(212) 490-3999 FAX (212) 986-7864

Director of Advertising Sales	**Domenic A. Mucchetti**
Account Executive (NY,NJ)	**Brian Clerkin** at (201) 366-2751
Account Executive (VA,DC,MD,DE,WV)	**John D. Floyd, CBC** at (215) 399-3265
Account Executive	**Debby Crane** at (201) 967-9838
Regional Manager (Midwest)	**Paul Lesher,CBC** at (312) 296-2040
Account Executive (Northwest)	**Bill Hague** at (206) 858-7575
Regional Sales Manager (South)	**Douglas Shaller** at (212) 490-3999
Account Executives (Eastern MA,NH,ME,RI)	**Paul Gillespie** at (508) 429-8907; **Bill Doucette** at (508) 429-9861
Account Executives (Western MA,CT,VT)	**George Watts** at (413) 253-9881

Account Executives (Calif.,AZ,NV,NM)
for Area Codes 714/619 **Tom Murphy**
for Area Codes 213/818/805/602/702/505 **Robert D'Alexander** at (213) 372-2744
for Area Codes 408/415/916/209/707 **Elizabeth Cooper** at (415) 673-5123

NTBM-Research Center

Account Supervisor	**Lourdes Del Valle**

Editorial Notebook

We're delighted to report that Technology 2001, the second national technology transfer conference and exhibition, promises to be an even bigger success than last year's inaugural show, Technology 2000. Already more exhibit space has been reserved in the San Jose Convention Center than was used last year in Washington, DC, and all indications are that attendance will be at least 50 percent higher than at Technology 2000.

Expanded to three days, December 3-5, Technology 2001 will have three times the exhibit space and nearly ten times the meeting space as Technology 2000, to accommodate the large number of presentations and exhibits by federal laboratories, their contractors, and other companies and universities with innovative, commercially-promising technologies available for transfer. Some 50 federal labs have signed on to exhibit and/or present papers, representing NASA, the Environmental Protection Agency, and the departments of Agriculture, Commerce, Defense, Energy, Health and Human Services, Interior, Transportation, and Veterans Affairs.

The latest news is that this year an interagency government group (the agencies that comprise the FCCSET* Committee on Industry and Technology) will hold a meeting on Intelligent Processing Equipment (IPE) concurrently with Technology 2001. IPE is one of four key technologies for advanced manufacturing identified by the National Critical Technologies Panel in a recent report to President Bush. It includes a broad range of computer-controlled equipment designed to improve the efficiency of manufacturing processes such as machining, forming, welding, heat-treating, inspecting, and material handling.

Through symposia, exhibits, and government-industry discussion sessions, the IPE meeting will report on current federal R&D efforts in intelligent processing and begin to identify private sector needs in this area. This will lay the groundwork for the transfer of IPE technology to industry.

Participants will include many of the federal agencies I listed earlier, as well as the Office of Science and Technology Policy and the Office of Management and Budget. Arrangements are also being considered for a lunch or breakfast talk by a nationally-recognized expert in advanced manufacturing.

Further details on the IPE meeting will appear in next month's *NASA Tech Briefs*. For more information on the Technology 2001 conference, turn to the section in this issue beginning on page 33. ❒

Bill Schnirring

* *The Federal Coordinating Council on Science, Engineering, and Technology*

Building Smarter, Tougher Telerobots

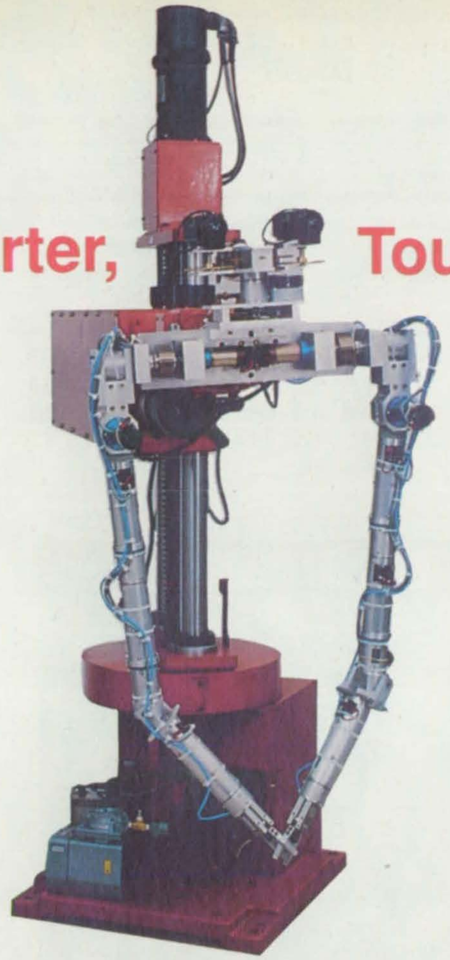

A new prototype robot features two dexterous arms, a movable head, two CCD cameras for producing stereoscopic views, and an articulated lower body.
Photo courtesy Scientific Research Associates

Whether space-borne or Earth-bound, advanced robotic systems will save humans time and money, and spare them from health hazards and tedium. These intelligent machines will build structures in orbit, clean up toxic wastes on Earth, and perform repetitive manufacturing tasks. And that's just the beginning, according to **Dr. Neville Marzwell**, the technical manager of several NASA Small Business Innovation Research (SBIR) contracts that aim to produce smarter, stronger robots. "The rapid evolution of robotics technology promises to widen the scope of its application to space commercialization, mining, and exploration," Marzwell said.

Marzwell is a member of the Robotics and Automation Systems section at NASA's Jet Propulsion Laboratory. JPL provides international leadership in robotics, producing state-of-the-art technology in areas such as teleoperated and supervisory control, planning and scheduling, robotic inspection, enhanced sensory systems, and artificial intelligence. Marzwell, a JPL employee since 1982, applies this expertise to NASA's mission of space exploration. His primary focus is development and implementation of semiautonomous systems for assembling space structures and servicing spacecraft.

Through remote operation of robotic systems, humans can guide many phases of space construction and exploration without the high risk and cost of manned space flight. "It is only by considering cost in the planning phases of these enormous projects that we will realize the vast potential of space exploration," said Marzwell, who holds a PhD in applied physics from the California Institute of Technology.

Many of the latest robotics advances can also be applied terrestrially. In recent years, NASA has increasingly promoted the timely transfer of space technology to industry, where robots can assume dangerous or difficult tasks. This drive to share knowledge has led to Marzwell's involvement in various SBIR projects. "Through these relationships," he said, "NASA helps the small business community bring technology to market."

Having scanned robotics technology around the globe, Marzwell considers it the most promising way to increase business productivity. "Implementing robotic automation has a multiplier effect on investments by reducing and avoiding human error and by affording 24-hour production," he explained. "We can greatly increase our standard of living by automating the manufacture of key industrial components."

Such promise, he said, can be realized through mechanical systems combining autonomous with teleoperative functions. Autonomous operation, useful for simple or repetitive jobs such as unscrewing bolts, is prohibitively expensive for singular complex tasks. These are better accomplished with human guidance. The ideal system will combine or alternate between autonomy and teleoperation, depending on the task.

One such flexible system has been developed through an SBIR contract with Scientific Research Associates. The robot has 18 degrees of freedom, stereoscopic real-time vision, two cooperatively dexterous arms, and expandable shoulders, all of which enable it to perform complex mechanical tasks. Its arms can wield various tools and perform precise functions such as replacing microelectronic chips and circuit boards. Moreover, artificial intelligence enables the robot to learn from its mistakes by storing data from previous tasks. Although modular in design for ease of repair and upgrading, the robot's many subcomponents work in harmony under the guidance of a local area network (LAN) computer system.

A second type of manipulator, developed for JPL by Odetics Inc., is also highly dexterous but designed to carry much heavier loads. The lightweight, high-strength arm features seven degrees of freedom and can lift 50 pounds at Earth gravity. Originally developed to lift and transport large assembly

(continued on page 92)

Dr. Neville Marzwell oversees several SBIR projects aimed at producing smarter, stronger robots for space and industrial applications.
Photo courtesy JPL

New Product Ideas

New Product Ideas are just a few of the many innovations described in this issue of *NASA Tech Briefs* and having promising commercial applications. Each is discussed further on the referenced page in the appropriate section in this issue. If you are interested in developing a product from these or other NASA innovations, you can receive further technical information by requesting the TSP referenced at the end of the full-length article or by writing the Technology Utilization Office of the sponsoring NASA center (see page 14). NASA's patent-licensing program to encourage commercial development is described on page 14.

Zero-Spring-Rate Mechanism/ Air Suspension Cart

A zero-spring-rate mechanism/air suspension cart is to be used for ground testing of flexible, "mass-critical" articles like lightweight spacecraft undergoing such large motions as slewing, translation, and telescoping/retraction. The cart is very small compared to a test article and is easily adapted to most test facilities.
(See page 69)

Integral Plug-Type Heat-Flux Gauge

A new heat-flux gauge eliminates measurement errors caused by temperature discontinuities. Unlike a conventional gauge, the new gauge is not screwed or welded into place, but instead a thermoplug and annulus are electrical-discharge-machined into the specimen material.
(See page 72)

Compact Apparatus for Growth of Protein Crystals

A compact vapor-diffusion apparatus for the growth of protein crystals would enable experimenters to initiate and terminate growth by remote or automatic control at prescribed times. The apparatus would have few moving parts and would contain no syringes.
(See page 51)

Making High-Pass Filters for Submillimeter Waves

A micromachining-and-electroforming process makes rigid metal meshes with cells that range in size from 0.002 in. (0.05 mm) to 0.05 in. (1.27 mm) square. These meshes are used as high-pass filters (dichroic plates) for submillimeter electromagnetic waves.
(See page 83)

Stirling-Cycle Cooling for Tunable Diode Laser

A miniature Stirling-cycle cooler has been shown to be effective in continuously cooling a PbSnTe tunable diode laser to a stable operating temperature near 80 K. Such small, compact coolers can simplify laboratory diode-laser spectroscopy and instruments for use aboard aircraft and balloons.
(See page 16)

Preventing Aim at an Undesired Target

An avoidance-control-logic subsystem prevents an instrument from aiming at an undesired target. The subsystem could be used to protect delicate photodetectors in a servocontrolled infrared spectrometer or imaging instrument against damage from excessively bright object.
(See page 24)

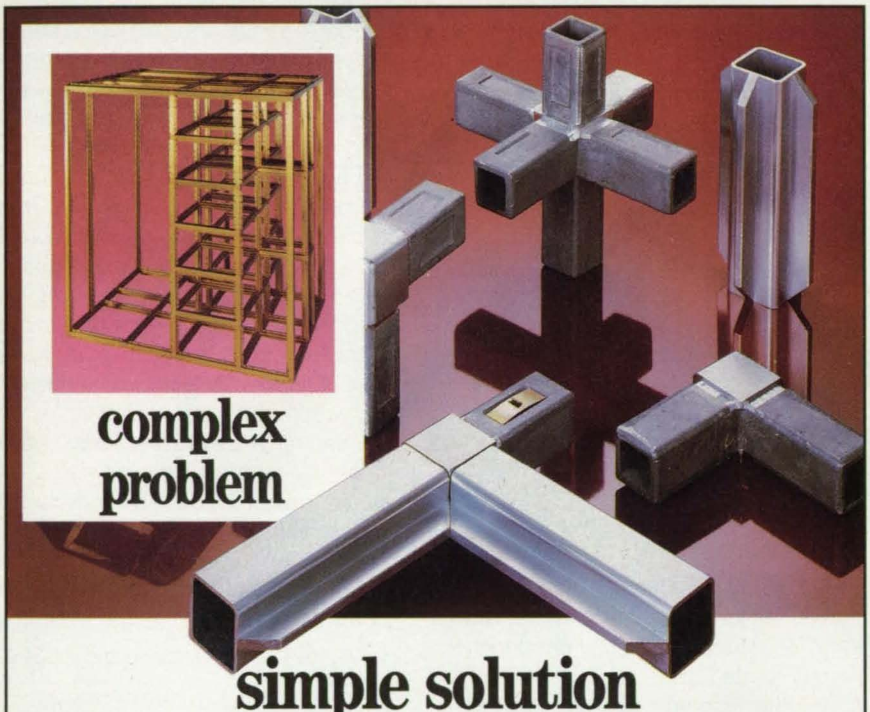

HOW YOU CAN BENEFIT FROM NASA's TECHNOLOGY UTILIZATION SERVICES

If you're a regular reader of TECH BRIEFS, then you're already making use of one of the low-and no-cost services provided by NASA's Technology Utilization (TU) Network. But a TECH BRIEFS subscription represents only a fraction of the technical information and applications/engineering services offered by the TU Network as a whole. In fact, when all of the components of NASA's Technology Utilization Network are considered, TECH BRIEFS represents the proverbial tip of the iceberg.

We've outlined below NASA's TU Network—named the participants, described their services, and listed the individuals you can contact for more information relating to your specific needs. We encourage you to make use of the information, access, and applications services offered by NASA's Technology Utilization Network.

How You Can Utilize **NASA's Industrial Applications Centers**—A nationwide network offering a broad range of technical services, including computerized access to over 100 million documents worldwide.

You can contact NASA's network of Industrial Applications Centers (IACs) for assistance in solving a specific technical problem or meeting your information needs. The "user friendly" IACs are staffed by technology transfer experts who provide computerized information retrieval from one of the world's largest banks of technical data. Nearly 500 computerized data bases, ranging from NASA's own data base to Chemical Abstracts and INSPEC, are accessible through the ten IACs located throughout the nation. The IACs also offer technical consultation services and/or linkage with other experts in the field. You can obtain more information about these services by calling or writing the nearest IAC. User fees are charged for IAC information services.

Aerospace Research Center (ARAC)
Indianapolis Center for Advanced Research
611 N. Capitol Avenue
Indianapolis, IN 46204
Dr. F. Timothy Janis, Director
(317) 262-5036

Central Industrial Applications Center/NASA (CIAC)
Rural Enterprises, Inc.
Post Office Box 1335
Durant, OK 74702
Dr. Dickie Deel, Director
(405) 924-5094
(800) 658-2823 (toll-free U.S.)

Science and Technology Research Center (STRC)
Post Office Box 12235
Research Triangle Park, NC 27709-2235
H.L. (Lynn) Reese, Director
(919) 549-0671

NASA Industrial Applications Ctr. 823 William Pitt Union
University of Pittsburgh
Pittsburgh, PA 15260
Lani Hummel
Executive Director
(412) 648-7000

Southern Technology Applications Center (STAC)
Post Office Box 24
Progress Ctr., One Progress Blvd.
Alachua, FL 32615
J. Ronald Thornton, Director
(904) 462-3913
(800) 354-4832 (FL only)
(800) 225-0308 (toll-free US)

NASA/UK Technology Technology Applications Center
University of Kentucky
109 Kinkead Hall
Lexington, KY 40506-0057
William R. Strong, Director
(606) 257-6322

NERAC, Inc.
One Technology Drive
Tolland, CT 06084
Dr. Daniel U. Wilde, President
(203) 872-7000

Technology Application Center (TAC)
University of New Mexico
Albuquerque, NM 87131
Dr. Stanley A. Morain, Director
(505) 277-3622

NASA Industrial Applications Center
University of Southern California
Research Annex
3716 South Hope Street
Los Angeles, CA 90007-4344
Robert Stark, Director
(213) 743-6132
(800) 642-2872 (CA only)
(800) 872-7477 (toll-free US)

NASA/SU Industrial Applications Center
Southern University Department of Computer Science
Post Office Box 9737
Baton Rouge, LA 70813-9737
Dr. John Hubbell, Director
(504) 771-6272
(504) 771-4950

If you represent a public sector organization with a particular need, you can contact NASA's Application Team for technology matching and problem solving assistance. Staffed by professional engineers from a variety of disciplines, the Application Team works with public sector organizations to identify and solve critical problems with existing NASA technology. **Technology Application Team, Research Triangle Institute, P.O. Box 12194, Research Triangle Park, NC 27709; *Dr. Doris Rouse, Director,* (919) 541-6980**

How You Can Access Technology Transfer Services At NASA Field Centers: **Technology Utilization Officers & Patent Counsels**—Each NASA Field Center has a Technology Utilization Officer (TUO) and a Patent Counsel to facilitate technology transfer between NASA and the private sector.

If you need further information about new technologies presented in NASA Tech Briefs, request the Technical Support Package (TSP). If a TSP is not available, you can contact the Technology Utilization Officer at the NASA Field Center that sponsored the research. He can arrange for assistance in applying the technology by putting you in touch with the people who developed it. If you want information about the patent status of a technology or are interested in licensing a NASA invention, contact the Patent Counsel at the NASA Field Center that sponsored the research. Refer to the NASA reference number at the end of the Tech Brief.

Ames Research Ctr.
Technology Utilization Officer:Geoffrey S. Lee
Mail Code 223-3
Moffett Field, CA 94035
(415) 604-4044
Patent Counsel:
Darrell G. Brekke
Mail Code 200-11
Moffett Field, CA 94035
(415) 604-5104

Lewis Research Center
Technology Utilization Officer: Anthony F. Ratajczak
Mail Stop 7-3
21000 Brookpark Road
Cleveland, OH 44135
(216) 433-2225
Patent Counsel:
Gene E. Shook
Mail Code LE-LAW
21000 Brookpark Road
Cleveland, OH 44135
(216) 433-5753

John C. Stennis Space Center
Technology Utilization Officer: Robert Barlow
Code HA-30
Stennis Space Center, MS 39529
(601) 688-2042

John F. Kennedy Space Center
Technology Utilization Officer: Thomas M. Hammond
Mail Stop PT-PMO-A
Kennedy Space Center, FL 32899
(407) 867-3017
Patent Counsel:
Bill Sheehan
Mail Code PT-PAT
Kennedy Space Center, FL 32899
(407) 867-2544

Langley Research Ctr.
Technology Utilization Officer: Joseph J. Mathis Jr.
Deputy Head, TU Office
Mail Stop 139A
Hampton, VA 23665
(804) 864-2484
Patent Counsel:
George F. Helfrich
Mail Code 279
Hampton, VA 23665
(804) 864-3523

Goddard Space Flight Center
Technology Utilization Officer: Donald S. Friedman
Mail Code 702.1
Greenbelt, MD 20771
(301) 286-6242
Patent Counsel:
R. Dennis Marchant
Mail Code 204
Greenbelt, MD 20771
(301) 286-7351

Jet Propulsion Lab.
NASA Resident Office
Technology Utilization Officer: Arif Husain
Mail Stop 180-801
4800 Oak Grove Drive
Pasadena, CA 91109
(818) 354-4862
Patent Counsel:
Thomas H. Jones
Mail Code 180-801
4800 Oak Grove Drive
Pasadena, CA 91109
(818) 354-5179
Technology Utilization Mgr. for JPL: Dr. Norman L. Chalfin
Mail Stop 156-211
4800 Oak Grove Drive
Pasadena, CA 91109
(818) 354-2240

George C. Marshall Space Flight Center
Technology Utilization Officer: Ismail Akbay
Code AT01
Marshall Space Flight Center, AL 35812
(205) 544-2223
Fax (205) 544-3151
Patent Attorney:
William L. Broad
Mail Code CC01
Marshall Space Flight Center, AL 35812
(205) 544-0021

Lyndon B. Johnson Space Center
Technology Utilization Officer: Dean C. Glenn
Mail Code IC-4
Houston, TX 77058
(713) 483-3809
Patent Counsel:
Edward K. Fein
Mail Code AL3
Houston, TX 77058
(713) 483-4871

NASA Headquarters
Technology Utilization Officer: Leonard A. Ault
Code CU
Washington, DC 20546
(703) 557-5598
Assistant General Counsel for Patent Matters: Robert F. Kempf, Code GP
Washington, DC 20546
(202) 453-2424

A Shortcut To Software: **COSMIC®**—For software developed with NASA funding, contact COSMIC, NASA's Computer Software Management and Information Center. New and updated programs are announced in the Computer Programs section. COSMIC publishes an annual software catalog. For more information call or write: **COSMIC®**, 382 East Broad Street, Athens, GA 30602 *John A. Gibson, Dir.*, (404) 542-3265.

If You Have a Question..**NASA Center For AeroSpace Information** can answer questions about NASA's Technology Utilization Network and its services and documents. The CASI staff supplies documents and provides referrals. Call, write or use the feedback card in this issue to contact: **NASA Center For AeroSpace Information,** Technology Utilization Office, P.O. Box 8757, Baltimore, MD 21240-0757. *Walter M. Heiland, Manager*, (301) 859-5300, Ext. 245.

Electronic Components and Circuits

Switched-Capacitor Voltage Multiplier

High voltage is generated without a transformer

NASA's Jet Propulsion Laboratory, Pasadena, California

A dc-to-dc power converter multiplies the input supply potential by a factor of nearly 40, without using a transformer. The converter is suitable for high-voltage, low-current applications. During tests, the converter stepped-up 90 V dc from a dry battery to 3.3 kV dc, at currents up to several microamperes.

The converter (see figure) includes a first bank of five capacitors, C_1 through C_5, a second bank of eight capacitors, C_6 through C_{13}, and a filter capacitor, C_f. The capacitors are connected to each other through a network of optically isolated solid-state switching devices, r_1 through r_{20} and s_1 through s_{19}. A controller that contains transistor/transistor-logic integrated circuits generates a two-phase switch-controlling signal.

At the beginning of the first half cycle, the r switches are turned off and the s switches are turned on, thereby connecting C_1 through C_5, in parallel, to the input voltage, V_i, and disconnecting these capacitors from the others. These capacitors quickly charge up to V_i. At the beginning of the next half cycle, the s switches are turned off and the r switches are turned on; this disconnects C_1 through C_5 from the power supply and connects them in series so that, in combination, they act as an intermediate source of voltage $V_i' = 5V_i$. At the same time, C_6 through C_{13} are connected in parallel to the series combination of C_1 through C_5, thereby charging C_6 through C_{13} to nearly the intermediate source voltage V_i'.

At the beginning of the next half cycle (which is the same as the first half cycle), C_6 through C_{13} are connected to each other in series, disconnected from C_1 through C_5, and connected to C_f and the load. The series combination of C_6 through C_{13} acts as a source of voltage $8V_i' = 40V_i$. This source voltage charges C_f, which in turn supplies current to the load. In practice the actual voltage gain is slightly less than 40. The reasons for this reduction are as follows: Because of non-zero conductance, a small amount of intra-circuit current exists during the off state of the solid-state relay; this gives rise to unwanted discharge of the capacitors. Secondly, the present switching frequency is rather low (125 Hz), and so the time the relays remain on or off is much higher than the charging time of the capacitors, resulting in poor utilization of the capacitors. A better gain figure and a lower percentage ripple are bound to occur if higher frequency of is used.

The proposed dc-to-high voltage dc converter has the following attributes. The design does not make use of transformers or inductors but instead effects voltage boost-up by capacitive energy transfer. The circuit is primarily made up of banks of capacitors, connected by a network of integrated-circuit relays. The converter is functionally a linear voltage amplifier with a fixed gain figure. It is truly bipolar in operation (the input voltage and the output voltage have the same polarity). The output is fully floating, and there is excellent dc isolation between the input and output terminals.

This work was done by Govind Sridharan of Caltech for **NASA's Jet Propulsion Laboratory**. *For further information, Circle 78 on the TSP Request Card.*

Inquiries concerning rights for the commercial use of this invention should be addressed to the Patent Counsel, NASA Resident Office - JPL [see page 14]. Refer to NPO-17994.

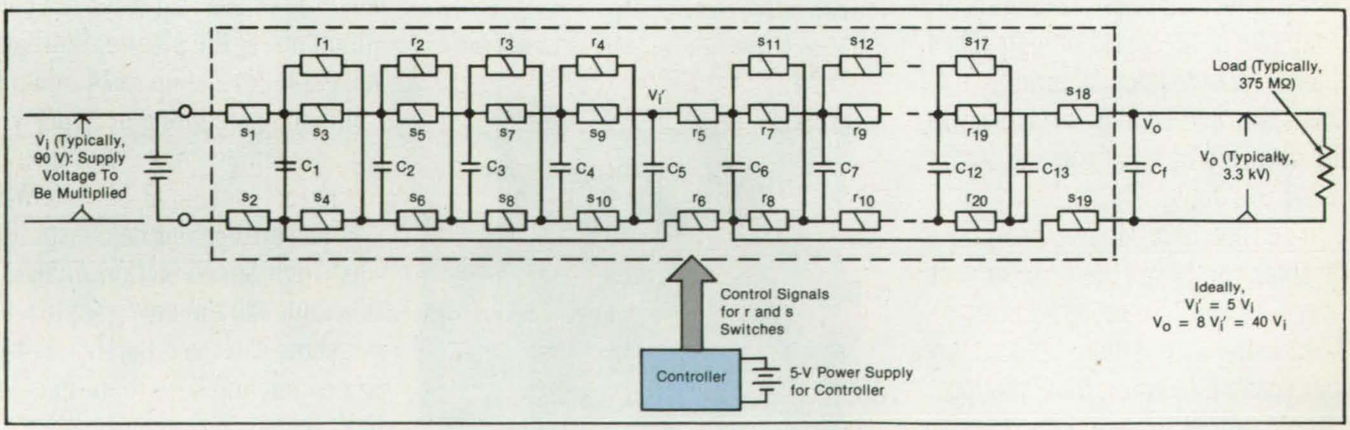

Capacitors in Two Banks are alternately charged in parallel and discharged in series. This switching-and-charging action multiplies the input voltage V_i by a factor of as much as 40.

Stirling-Cycle Cooling for Tunable Diode Laser

Small coolers can simplify laboratory spectroscopy and lighten airborne instruments.

NASA's Jet Propulsion Laboratory, Pasadena, California

A miniature Stirling-cycle cooler has been shown to be effective in continuously cooling a PbSnTe tunable diode laser to a stable operating temperature near 80 K. The cooler — a commercially available unit — occupies a volume of only 80 in.^{3}

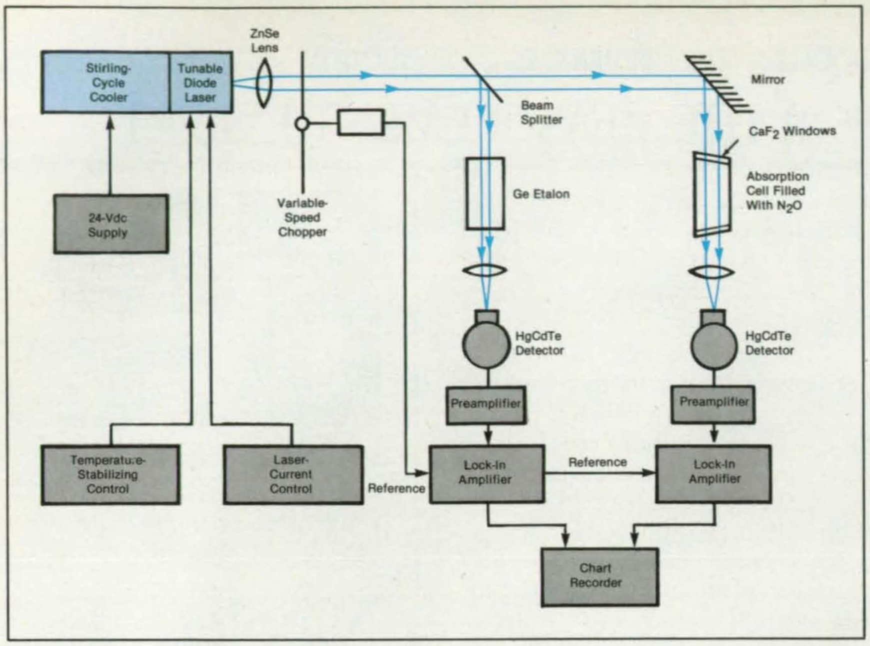

Figure 1. This **Infrared-Absorption** apparatus was used to measure the short-term frequency drift of the tunable diode laser by reference to a known spectral line of N_2O.

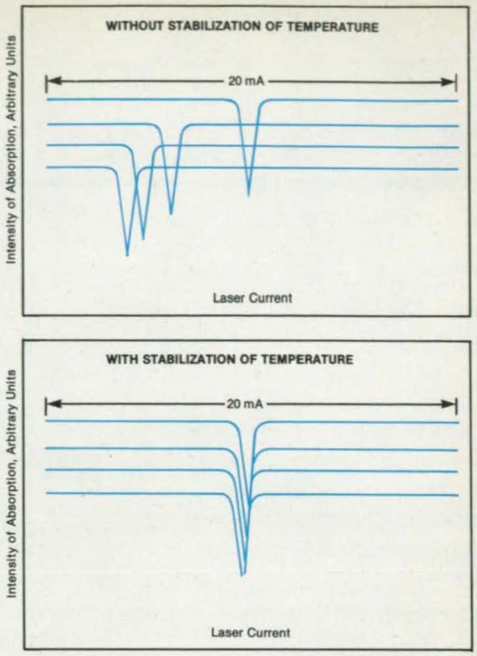

Figure 2. The **Intensity of Absorption** in the 1187.8787 cm^{-1} absorption line of N_2O was measured as a function of laser current. These scans were recorded at intervals of 2 min.

(1,300 cm^3) and weighs only 3 lb (1.4 kg). Such small, compact coolers can simplify laboratory diode-laser spectroscopy and instruments for use aboard aircraft and balloons.

Continuous stabilization of the temperature near 80 K and minimization of acoustic coupling are required to keep the laser output within a narrow frequency band for a long time in a typical scientific or military application. Although liquid nitrogen cools to 77 K with minimal acoustic coupling, cooling ceases when the liquid evaporates. A conventional mechanical cryogenic system can provide the required continuous cooling, but is much larger [7,500 in.^{3} (1.2×10^5 cm^3)] and heavier [170 lb (77 kg)] and produces sufficient undesired acoustic coupling to increase the half bandwidth of the laser output to the range of 30 to 50 MHz.

The combination of the PbSnTe tunable diode laser and the Stirling-cycle cooler was demonstrated in the infrared-absorption apparatus illustrated schematically in Figure 1. The laser, excited with currents ranging from 130 to 180 mA, operated at a wavelength near 8.4 μm. The laser was mounted on a copper block attached to the cold finger of the Stirling-cycle cooler. For additional stabilization of temperature, a heater wire was attached to the side of the block opposite the laser and a temperature-sensing silicon diode was mounted on the block midway between the heater wire and the laser. The cooler took about 1 h to bring the temperature from ambient down to about 80 K and about 1 additional hour to stabilize the temperature within ±1 mK of a steady value.

The short-term frequency drift of the laser was measured in the spectroscopic apparatus by use of the 1187.8787 cm^{-1} (wavelength 8.41836797 μm) spectral line of the N_2O gas in the absorption cell. Without stabilization of the temperature, this spectral line was observed to drift to lower laser currents, indicating slow warming of the laser. When the temperature was stabilized, this spectral line remained near a fixed laser current (see Figure 2). The half bandwidth of the laser output was 21 ±2 MHz — about 10 to 30 MHz narrower than that of a laser cooled by a conventional mechanical cryogenic system.

This work was done by Santo S. Durso, Randy D. May, Matthew A. Tuchscherer, and Christopher R. Webster of Caltech for **NASA's Jet Propulsion Laboratory.** *For further information, Circle 137 on the TSP Request Card.* *NPO-18045*

Five-Segment Interconnection for Electromigration Tests

A test pattern would conform to standards.

NASA's Jet Propulsion Laboratory, Pasadena, California

A proposed integrated-circuit conductive pattern (see figure) is intended for use in electromigration lifetime testing of the interconnection lines of integrated circuits. The pattern is designed for the collection of statistics on electromigration from the smallest possible area. It includes 5 interconnection segments with Kelvin voltage taps, with a total of 12 contact pads, and provides for simultaneous measurements on all of the segments. The pattern attempts to minimize thermal gradients within each segment and conforms to the guidelines on electromigration test structures promulgated by the National Institute of Standards and Technology (NIST).

The critical design parameters are the width, W, and the length, L, of each of the test lines (the five segments); the width, W_C, and the length, L_C, of the lines that make contact with the ends of the test lines; and the width, W_I, of the current taps. From the NIST guidelines, $L = 800$ μm. To minimize the thermal gradients at the ends of the test lines, $W_C = 2W$, while $L_C = 10W$. To minimize both spatial and temporal nonuniformities in heating, the widths of the current taps should satisfy the relationship $W_I \geq 10W$; in the figure, $W_I = 15W$ is used.

The separation between adjacent test lines is not critical. The larger the separation, the smaller the thermal interaction between the test lines. However, even at separations as wide as 1,000 μm, this thermal coupling cannot be ignored and must be included in the analysis of the results of the test. In the figure, the separation between adjacent test lines is 10W.

The U-shaped pieces that join adjacent test lines should be uniform in design to facilitate the mathematical modeling of the flow of current in resistance thermometry. A less-critical design parameter is the width, W_U, of the arms of the U-shaped

AT&T's DSP3 Parallel Processor: every cubic foot, a gigaflop.

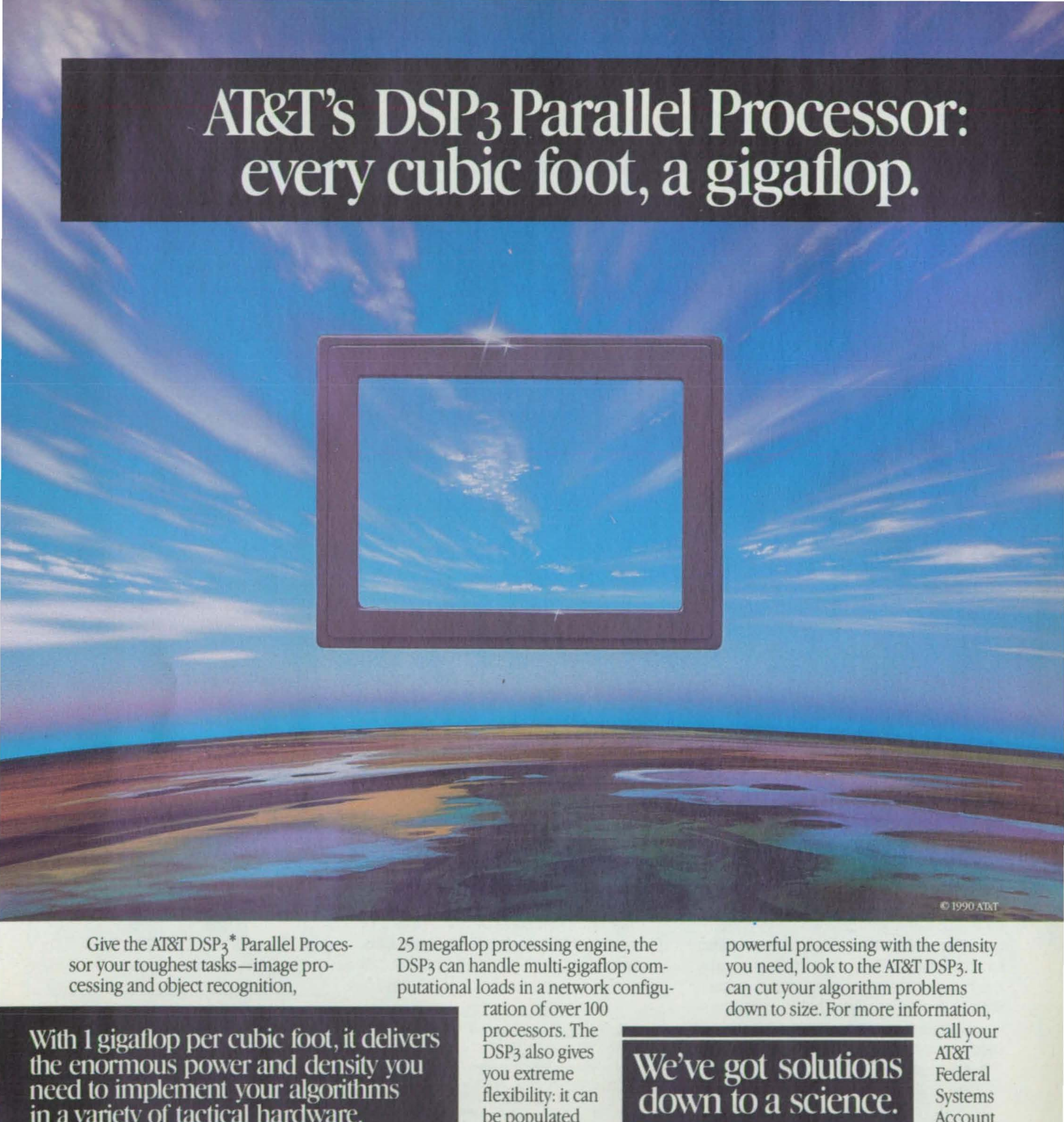

Give the AT&T DSP3* Parallel Processor your toughest tasks—image processing and object recognition, beamforming, neural networking, speech recognition, synthetic aperture radar—and it'll handle the problem with speed and ease.

With 1 gigaflop per cubic foot, it delivers the enormous power and density you need to implement your algorithms in a variety of tactical hardware.

The DSP3 delivers 1 gigaflop per cubic foot of active area (up to 3.2 gigaflops in a single array). With an advanced package that gives you 800 megaflops in only 9 cubic inches.

Speed? 40 megabytes/second on each of four channels for an aggregate bandwidth of up to 160 megabytes/second.

Capacity is also maximized. Using a 25 megaflop processing engine, the DSP3 can handle multi-gigaflop computational loads in a network configuration of over 100 processors. The DSP3 also gives you extreme flexibility: it can be populated with one to eight boards, each with 16 processing nodes, providing 400 megaflops of power and four megabytes of memory.

AT&T's DSP3 gives you access to high-level language software such as a C compiler and a wide library of signal processing subroutines. And it leads the industry in price per megaflop. Plus, of course, you get the unparalleled support and service of AT&T Bell Laboratories and AT&T Field Applications Engineers.

So, for realtime parallel processing, powerful processing with the density you need, look to the AT&T DSP3. It can cut your algorithm problems down to size. For more information, call your AT&T Federal Systems Account Executive, or 1 800 553-8805. (N.C. residents, call collect: 919 697-9580.)

We've got solutions down to a science.

*Developed in part under a DARPA sponsored contract.

AT&T
The right choice.

Circle Reader Action No. 665

pieces: W_U should equal or exceed W_C. In the figure, $W_U = 4W = 2W_C$.

The contact-pad pattern shown in the figure has twice the height of the pattern of contact-pad probes now in use at several foundries that make GaAs integrated circuits. This new pattern should facilitate both bonding and probing.

Given the size of the contact-pad pattern and the foregoing design criteria, W is constrained to be less than about 3 μm. To use wider test lines, one would have to decrease the distance between them or use fewer of them.

This work was done by David J. Hannaman and Martin G. Buehler of Caltech for **NASA's Jet Propulsion Laboratory**. *For further information, Circle 141 on the TSP Request Card.*
NPO-18105

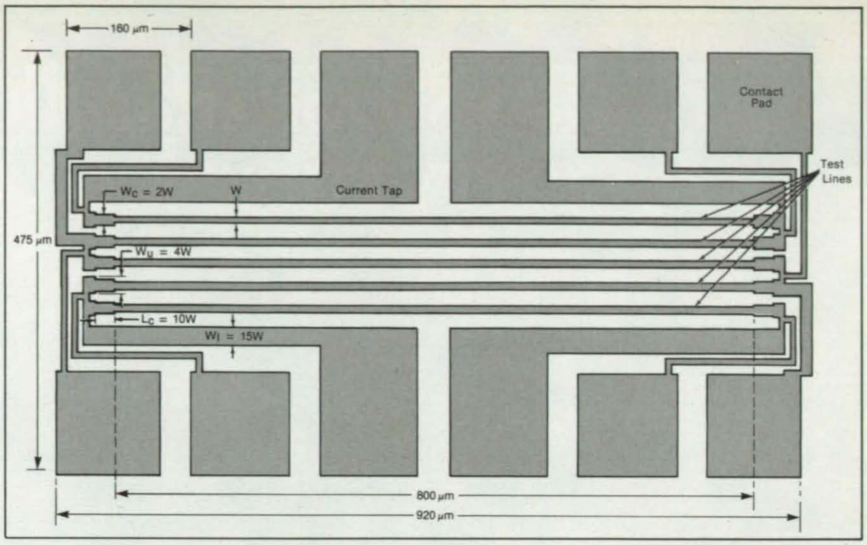

This **Integrated-Circuit Conductive Pattern** is designed for measurements that generate data on electromigration in the test lines.

Reducing Cross-Polarized Radiation From a Microstrip Antenna

Electromagnetic modes of higher order are suppressed.

NASA's Jet Propulsion Laboratory, Pasadena, California

A change in the configuration of the feed of a nominally linearly polarized microstrip-patch transmitting array antenna reduces the cross-polarized component of its radiation. It is desirable to reduce the cross-polarized component because this component can adversely affect the symmetry of the radiated beam and because it produces little or no useful signal power in another antenna aligned to receive in the expected polarization.

To make it operable over a wide frequency band, a microstrip antenna is usually constructed on a thick dielectric substrate. Unfortunately, a thick substrate supports the higher-order electromagnetic modes that give rise to asymmetry and cross polarization. Previously, all the microstrip patches in an array antenna were fed in the same phase, at the same location relative to the center of each patch (see Figure 1). This asymmetrical arrangement can result in significant excitation of higher-order modes. In the new configuration, the patches are fed on opposing sides, in opposite phases. This combination of spatial symmetry and temporal asymmetry causes the copolarized components of radiation from the fundamental modes of the patches to reinforce each other and the cross-polarized components of radiation from the higher-order modes to cancel each other.

To test this concept, two microstrip antennas like those shown in Figure 1 were constructed. The patches were 3.025-in. (7.68-cm) squares, and the substrate was 1/2-in. (12.7-mm)-thick foam with a dielectric constant of 1.05. The antennas were designed to resonate at frequencies from 1.55 to 1.66 GHz, and the distance between the elements along both principal axes was 0.6 wavelength at the middle frequency.

Figure 2 contains plots of measured and calculated intensities of the copolarized and cross-polarized components of radiation from the two antennas in the magnetic-field plane of the nominal radiated beam. These plots show clearly that the cross-polarized component is reduced by the new feed configuration.

This work was done by John Huang of Caltech for **NASA's Jet Propulsion Laboratory**. *For further information, Circle 126 on the TSP Request Card.* *NPO-18147*

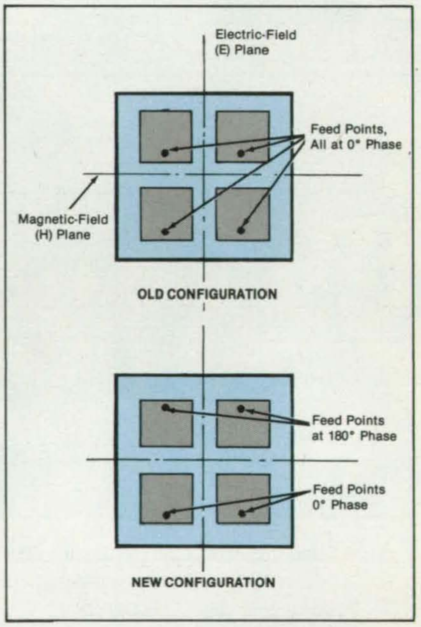

Figure 1. **Linearly-Polarized 2-by-2 Microstrip Antennas** can be fed in several alternative configurations, including the two shown here. The old configuration favored the generation of electromagnetic modes of higher order; the new configuration suppresses them.

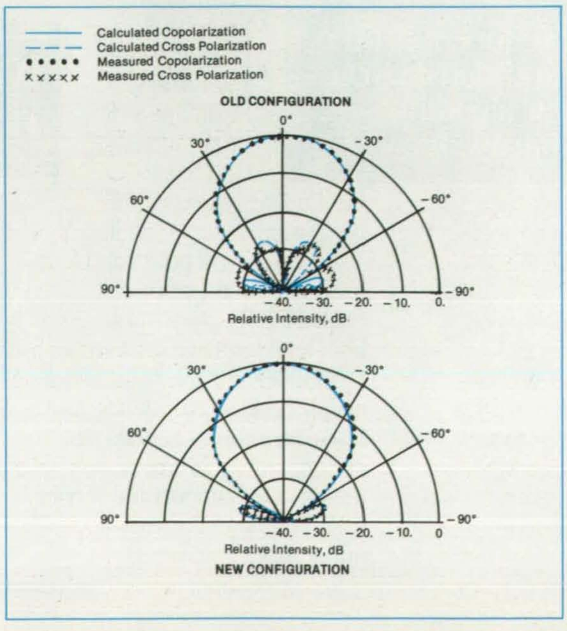

Figure 2. These **H-Plane Radiation Patterns** were produced at a frequency of 1.55 GHz by antennas like those described in Figure 1 and the text. The O° line is perpendicular to the plane of the antenna.

Spatial Light Modulator Would Serve as Electronic Iris

The brightness of the image would be adjustable in many discrete steps.

Marshall Space Flight Center, Alabama

In a proposed technique for controlling the brightness of an image formed by a lens, a spatial light modulator would serve as a segmented, electronically variable aperture. The technique offers several advantages: The spatial light modulator could be controlled remotely and would respond faster than a motorized iris or other remotely controlled mechanical iris does. Unlike an iris, the spatial light modulator could be configured so as not to vary the depth of field appreciably. Unlike a lead lanthanum zirconate titanate crystal, which could also be used to control the brightness, a spatial light modulator does not require high voltage.

A spatial light modulator is a two-dimensional array of electro-optical elements, each of which can be switched between a state of transparency or a state of opacity

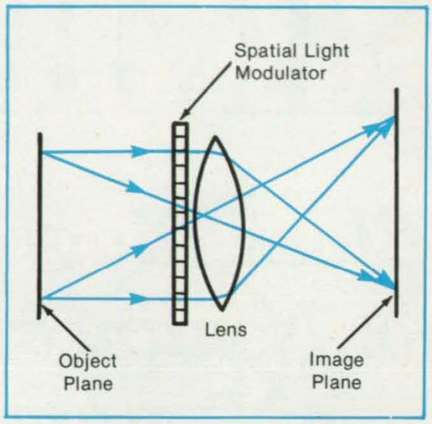

A **Spatial Light Modulator** placed at or near the principal plane of a lens would act as a segmented, electronically variable aperture.

(intermediate states are not available). A typical device of this type contains 128 by 128 elements. In the proposed technique, the spatial light modulator would be placed in or near the principal plane of the lens (see figure).

If all the elements of the spatial light modulator were transparent, the image would be at full brightness. If one of the elements were made opaque, all of the image rays passing through that element would be stopped. Inasmuch as each point of the principal plane receives light from all points of the object plane, the opacity of that element would reduce the overall intensity of the image somewhat. Similarly, the image could be darkened further by making more elements opaque.

Provided that the spatial light modulator covered the full aperture of the lens but no more, the brightness of the image could thus be reduced or increased in a large number of increments (e.g., 128^2 = 16,384) from full opacity to full transparency. The depth of field would not be affected appreciably as long as the elements were turned transparent or opaque in a random spatial pattern. However, if it were desired to mimic an iris and vary the depth of field, this could be done by turning the elements on or off in a pattern that approximated an opening or closing circle of transparency surrounded by opacity.

This work was done by David A. Gutow of Rockwell International Corp. for **Marshall Space Flight Center**. *No further documentation is available.*

Inquiries concerning rights for the commercial use of this invention should be addressed to the Patent Counsel, Marshall Space Flight Center [see page 14]. Refer to MFS-29758.

Betavoltaics of Increased Power

Long-lived cells would derive power from radioactive sources.

NASA's Jet Propulsion Laboratory, Pasadena, California

Batteries of newly developed betavoltaic cells have been proposed as long-lived sources of power of the order of watts. Intended for use aboard spacecraft, batteries of this type might also be used, for example, in surgically implanted devices requiring high power. Heretofore, betavoltaics have been used in surgically implanted devices — specifically, heart pacemakers, but these consume powers of no more than a few microwatts.

A betavoltaic cell functions analogously to a photovoltaic cell, except that the role of the photons is played by energetic electrons (β particles) generated by the radioactive decay of a suitable material. The β particles traverse the cell, losing kinetic energy and creating pairs of holes and electrons. Those holes and electrons that lie within a diffusion length of the p/n junction of the cell are swept across the junction and contribute to the output current of the cell. An equivalent circuit for such a cell is identical to that of a solar photovoltaic cell.

Previously, betavoltaics were not considered for supplying powers of the order of watts because available materials provided low energy-conversion efficiencies and were vulnerable to damage by the high-energy incident β particles. However, the energy-conversion efficiencies of recently developed betavoltaic cells are appreciably greater than those of the previous cells. In addition, it appears that betavoltaic cells can be produced economically in quantity by use of solar-cell technology.

The figure illustrates a conceptual betavoltaic cell and battery. The cell would be a simple p/n-junction device to which a layer of β-emitting material would be attached. There would be an optimum thickness for the β-emitting layers: each layer would have to be thick enough to emit a sufficient number of particles, but diminishing returns would be reached at thicknesses great enough to result in the reabsorption of the emitted particles. A battery would contain a stack of β-emitting layers interspersed with enough p/n-junction devices to stop most of the β particles. The battery would be encased in a suitable β-backscattering material to prevent any β particles from escaping.

A GaP betavoltaic cell has been developed. GaP is believed to be particularly suitable because it has relatively wide energy-band gaps of 2.2 eV (indirect) and 2.7 eV (direct) and because a wide gap is associated with the ability to resist damage by the β particles. The GaP cell is a p/n device, grown and diffused by liquid-phase epitaxy. The measured power-conversion efficiency for the particular cell is 8.4 percent, and the theoretically attainable power-conversion efficiency of GaP cells in general is almost 25 percent.

The most suitable source of β particles for high power applications appears to be ^{90}Sr (which has a half life of 28 years). Preliminary calculations indicate that a battery with ^{90}Sr sources could be made to have an initial specific power of about 3 W/kg. Similar calculations for cells made with ^{204}Tl β emitters (half life 4 years) indicate an initial specific power as high as 8 W/kg.

This work was done by Frederick S. Pool and Paul Stella of Caltech for **NASA's Jet Propulsion Laboratory**. *For further information, Circle 32 on the TSP Request Card.*

NPO-17817

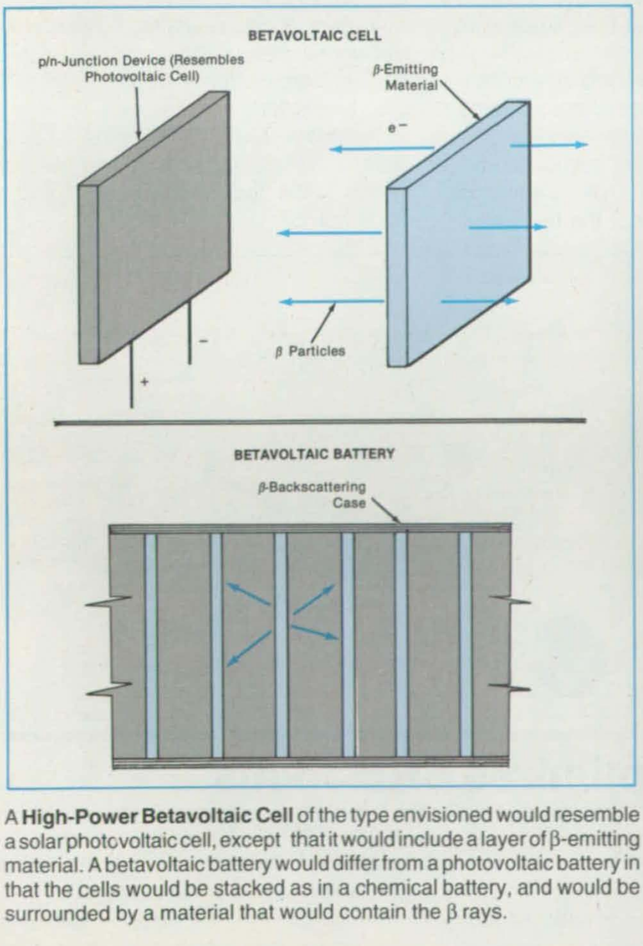

A **High-Power Betavoltaic Cell** of the type envisioned would resemble a solar photovoltaic cell, except that it would include a layer of β-emitting material. A betavoltaic battery would differ from a photovoltaic battery in that the cells would be stacked as in a chemical battery, and would be surrounded by a material that would contain the β rays.

Electronic Systems

Preventing Aim at an Undesired Target

Avoidance-control logic interrupts normal attitude-control logic when necessary.

NASA's Jet Propulsion Laboratory, Pasadena, California

An electronic system that controls changes in the orientation of an optical instrument includes an avoidance-control-logic subsystem that prevents the instrument from aiming at an undesired target. For example, it could be used to protect delicate photodetectors in a servocontrolled infrared spectrometer or imaging instrument against the damage that could occur if the instrument were aimed at the Sun or another excessively bright object.

In stationary operation, another part of the overall control system controls the torque applied to the instrument in such a way as to minimize the angular error between the line of sight of the instrument and the commanded line of sight. When the instrument is commanded to turn to a new line of sight, signals from rotation-rate sensors (e.g., gyroscopes) are processed into transformed coordinates and used along with the angle-error signals to control the slew — the rapid turn through most of the angular interval between the old and new commanded orientations (see Figure 1). To obtain the shortest possible rotation, the line of sight is ordinarily slewed in the plane that contains the old and new commanded lines of sight. The desired motion is obtained by controlling the applied torques so as to make the instrument rotate about a slewing axis perpendicular to this plane.

The instrument is equipped with a Sun sensor that indicates the orientation of the line of sight to the Sun relative to the line of sight of the instrument. The avoidance control logic does not affect the motion until and unless, at some point along the slewing trajectory, these two lines of sight come within an angle θ of each other; that is, the avoidance-control logic remains inoperative until the line of sight of the instrument enters a cone of avoidance of half apex angle θ about the line of sight to the Sun.

Once activated, the avoidance control logic interrupts the normal control logic. It then calculates a succession of temporary slewing axes and associated actuator torques so as to make the line of sight follow the shorter of the two trajectories around the cone of avoidance. Once sensors indicate that the line of sight has reached the end of the trajectory around the cone of avoidance, the avoidance control logic is deactivated, the normal control logic resumes operation, and the instrument starts to turn again on the original slewing axis toward the new commanded target.

This work was done by Neil E. Goodzeit of General Electric Co. for **NASA's Jet Propulsion Laboratory**. *For further information, Circle 91 on the TSP Request Card.*

In accordance with Public Law 96-517, the contractor has elected to retain title to this invention. Inquiries concerning rights for its commercial use should be addressed to

William H. Meise, Patent Counsel
General Electric Co.
One Independence Wage
P.O. Box 2023
Princeton, N.J. 08540

Refer to NPO-18077, volume and number of this NASA Tech Briefs *issue, and the page number.*

Figure 1. The **Slew-Control System** includes avoidance-control logic, which overrides the slew-control error generator when the line of sight of the instrument comes within a cone of avoidance around the line of sight to the Sun.

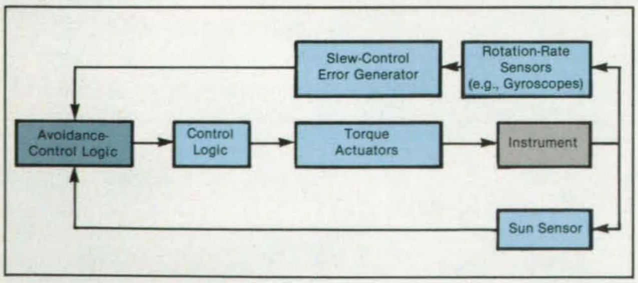

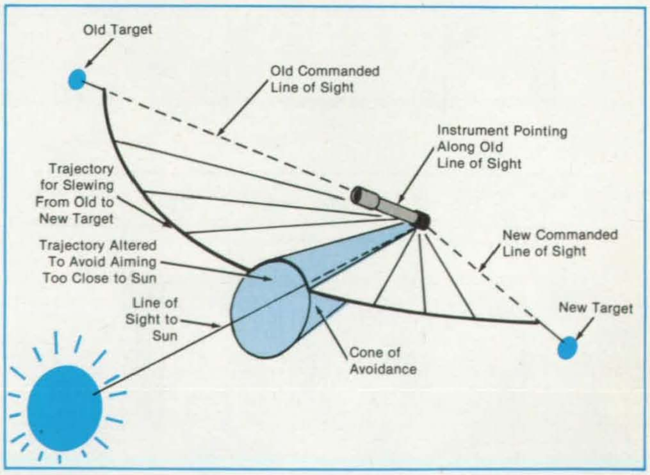

Figure 2. The **Normal Slewing Trajectory** is interrupted by the avoidance-control logic, which computes actuator torques that take the line of sight around the cone of avoidance.

Distributed-Computer System Optimizes SRB Joints

Productivity is enhanced fourfold.

Langley Research Center, Hampton, Virginia

Initial calculations of a redesign of the joint on the solid rocket booster (SRB) that failed during the Space Shuttle tragedy showed that the redesign increased the weight. Optimization techniques were to be applied to determine whether the weight could be reduced while keeping the joint closed and limiting the stresses. To enable engineers to examine as many alternatives

as possible, an analysis system was developed by use of existing software that coupled structural analysis with optimization computations.

The software of this system was designed to be executable on a network of computer workstations. This system took advantage of the parallelism offered by the finite-difference technique of computing gradients to enable several workstations to contribute simultaneously to the solution of the problem. The resulting system reduced the time to complete one optimization cycle from 2 hours to one-half hour, with a potential of reducing it to 15 minutes.

The major tools used for this project were the hardware (DEC MicroVAX computer workstations and DEC 11/785 minicomputer), the software (PROSSS, Programming System for Structural Synthesis), and the networks (DECnet and LaRCNET).

PROSSS, a system of computer programs that combines structural analysis and optimization, was chosen as the software tool because the majority of the code in PROSSS was independent of the type of problem being solved. In addition, PROSSS had been converted earlier to run on the workstations and had been verified with the standard test cases. EAL (Engineering Analysis Language) was chosen for the structural analysis.

The workstations and central minicomputer complex were connected by the two networks. The DECnet (the DEC software and hardware that enable different DEC operating systems to operate as a network) connected the workstations through an Ethernet circuit. The LaRCNET is the local-area network developed specifically for NASA's Langley Research Center to provide a center-wide capability for transferring data files among distributed systems of computers from multiple vendors.

Initially, PROSSS was executed sequentially on a single workstation. With a four-workstation distributed system, time was decreased by approximately a factor of 4. One workstation was used as the controlling system. The front processor, run as a stand-alone program on the controlling workstation, was modified to loop through the design variables, perturbing them one at a time and creating a separate file for each design variable with the changed shape in the form of updated joint locations. All workstations were sent a command file with checks to prevent them from executing until all of the required data were available. Once the analysis of the mathematical model with a perturbed shape was completed, an EAL library file containing the objective function, stresses, and reactions was sent to the controlling workstation. If the model was optimized, the system stopped; otherwise, it looped back to the front processor to begin a new cycle with a new shape determined by the change in the design variables.

The software system that couples structural analysis and optimization has been successfully distributed over this network of workstations. By distributing the workload over four workstations instead of just one, the time required to complete an optimization cycle decreased from 2 hours to one-half hour. Because of the enhanced productivity achieved with the distributed system, engineers were able to test more alternatives in a shorter time. The key features were the effective use of redundancies in hardware (multiple workstations and two networks) and flexible software, which enabled the optimization to proceed with minimal delay and decreased overall time to completion.

This work was done by James L. Rogers, Jr., Katherine C. Young, and Jean-Francois M. Barthelemy of **Langley Research Center**. *Further information may be found in NASA TM-89108 [N87-19022], "Distributed Computer System Enhances Productivity for SRB Joint Optimization."*

Copies may be purchased [prepayment required] from the National Technical Information Service, Springfield, Virginia 22161, Telephone No. (703) 487-4650. Rush orders may be placed for an extra fee by calling (800) 336-4700.

LAR-14311

Video Pipeline Tree for Scan Conversion of Triangles

Scenes containing many polygons could be generated in real time.

Ames Research Center, Moffett Field, California

A video pipeline subsystem having a branched structure would perform the scan conversion of polygons in images generated by computers. Heretofore, the conversion of computer-generated image coordinates, brightnesses, and colors of polygons to raster-scanning video signals could not be done rapidly enough for the generation of realistic images containing many polygons at the standard television rate of 30 frames per second. The new subsystem would divide the polygons into triangles, each of which would be processed rapidly in parallel, modular fashion and merged into the image. One proposed version, to consist of 127 integrated-circuit chips, could render 1,000 triangles in real time.

Figure 1 illustrates schematically a portion of the scan conversion of one triangle. The three control signals that define the raster are broadcast from a central controller to all such circuits. In synchronization with the raster video signal, this circuit would compute a color, the coordinate z (depth perpendicular to the image plane), or another linear function of the image coordinates x and y, using $z = ax + by + c$. The coefficients a, b, and c would be obtained from the computer specification of the image and would be used to compute the coefficients A, B, and C, which would be held in registers A, B, and C, respectively.

Seven such linear-function circuits would be combined into a module to produce a stream of data representative of one triangle. The seven functions would be z, red, green, blue, and three edge functions. Altogether, the data stream would be 49 bits wide: 24 bits for z, 8 bits for each color intensity, and a transparency bit that indicates whether the current picture element is inside or outside the triangle (if outside, then the other bits have no meaning and are to be ignored). The number of bits used in the internal computations of the linear-function circuit would be greater than the number of bits in the data streams.

A large number of these triangle modules would feed their 49-bit output data streams into the "leaves" of a binary tree at the standard video rate of about 10 MHz. At each branch point of the tree, a merging module would combine two of the data streams into one (see Figure 2). Of the two inputs to each merging module, one would be selected for output: If both picture elements were transparent, either could be selected. If one were opaque and the other transparent, the opaque one would be selected. If both were opaque, the one with the smallest value of z (the one in front) would be selected as in a standard z-buffer algorithm. The output of each merging module would serve as the input to a merging module at the next level of the tree.

As many triangle modules as possible would be put onto one integrated-circuit chip so that the chip would constitute a complete binary tree of merging modules with a triangle module at each "leaf." The chip would therefore have output pins for the 49-bit video-data stream emerging from the tree. The chip would also have address and data pins so that the "front-end" processor that performs the geometric transformations and calculates the coefficients for the triangles could write the coefficients into the chip.

Many such triangle chips could be built into a larger binary tree, connected by merging-module chips. Because it would contain only the merger logic, a merging-module chip would be relatively simple. However, it would require a total of 147 pins for the two 49-bit inputs and one 49-bit output. It might be possible to reduce the number of pins and, therefore, the cost, by time-multiplexing the data onto fewer pins at a higher bit rate.

An alternative design would be a linear pipeline of triangle chips, in which each triangle chip had a 49-bit input feeding into one leaf of its internal merge tree. The control signals would have to be staggered for the triangle chips in this linear pipeline. The merge chips would not be needed.

This work was done by Warren Robinett of **Ames Research Center**. *For further information, Circle 72 on the TSP Request Card.*

Inquiries concerning rights for the commercial use of this invention should be addressed to the Patent Counsel, Ames Research Center [see page 14]. Refer to ARC-11661.

Figure 1. A **Linear Function z of Image Coordinates x and y** is generated in synchronism with the video raster signal. Thus, $z(x,y)$ represents the function (depth or color) associated with the coordinates of the current picture element (x,y) in the video signal. The registers A, B, and C contain the coefficients of the function, which can change with time.

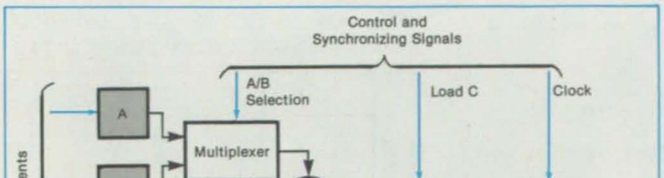

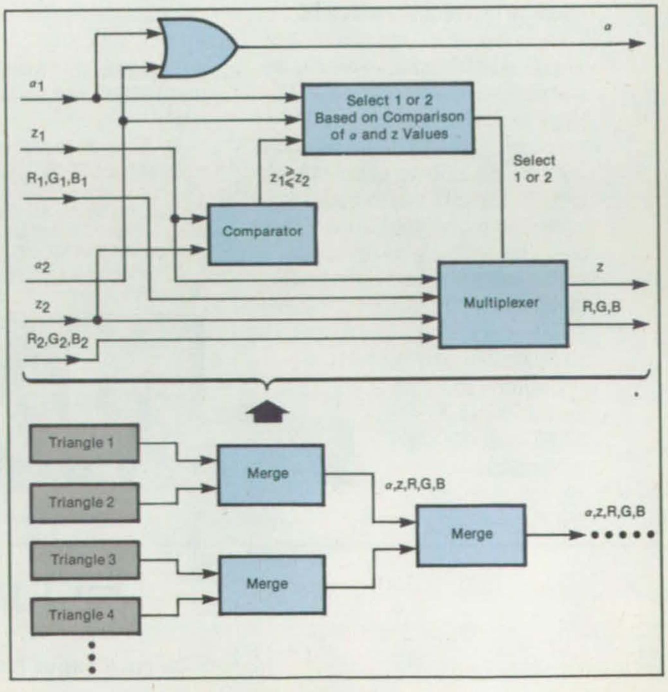

Figure 2. **Video Data From Triangle Modules Are Merged** in a binary tree by preferential selection according to transparency, opacity, and depth values. In the final merged video-data stream, the irrelevant data (representing hidden picture elements and the like) have all been suppressed, leaving only the scan-converted color and brightness signals for the visible portions of the polygons in the synthetic image. The symbols α, z, R, G, and B denote the transparency, depth coordinate, red, green, and blue signals, respectively.

Architecture for Intelligent Control of Robotic Tasks

An optimized data-abstracting hierarchy would plan, execute, and correct at acceptably high rates.

NASA's Jet Propulsion Laboratory, Pasadena, California

A proposed architecture for the control of such robotic devices as artificial hands calls for data-abstracting hierarchies of processing, controlling, and sensing equipment that would plan, execute, and correct the movements of the devices at acceptably high rates. The architecture combines features developed in research on artificial intelligence and control theory. It is characterized by causal connections between layers of the hierarchy, approximately equal complexities of the layers, and a directed focus of attention.

The hierarchical structure of this architecture is based partly on the analysis of human behavior during control actions. While other architectures developed previously are also hierarchical, they do not take full advantage of the possibilities offered by the hierarchical approach. In some of them, for example, the various layers represent various levels of abstraction of data, but the implementation of them with standard modules is not optimal for all levels of abstraction. Also, reflex control alone is insufficient to handle a large number of operating conditions, and expert systems are too slow for use with real-time processes.

Each level of the hierarchy would correspond to a different kind of mental process. The lowest level would interact directly with sensors and actuators, processing raw sensory feedback data and motor commands and immediately activating motor responses to important feedback signals. Middle levels could recognize typical patterns in feedback signals and command more-complicated reactions according to prescribed rules. The highest levels would be dedicated to such tasks as the recognition of sequences of patterns and general planning. In ascending the hierarchy, one would encounter increasingly symbolic types of logic, including the application of Boolean rules by artificial neural networks.

The figure illustrates a three-level hierarchy proposed for the control of a robotic hand. The intermediate level would be characterized by a response time and by an amount of knowledge intermediate between those of the planner (highest level) and the actuator controller (lowest level). The intermediate level would store expected relations among single feedback signals or subsets of them and would use the results to understand the evolution of a grasping task. This concept would provide for flexible reflex control in various grasping tasks and would enable the actuator controller to determine autonomously the best reaction to a given pattern of feedback signals. Both the planner and ac-

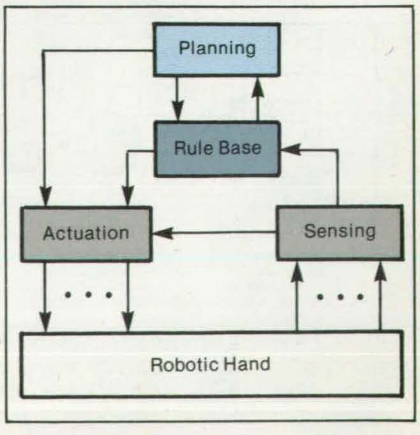

A **Three-Level Hierarchical Control System** would observe and direct the movements of an anthropomorphic artificial hand.

tuator controller would use feedback signals and outputs of rule-based reasoning processes to initiate modifications of actuator trajectories. When a new strategy was generated by the planner, the associated rules would be blended with the current rule base to assure a smooth transition between plans.

The use of such a hierarchical architecture to form an artificially intelligent controller has the potential for assuring immediate reactions to unexpected external conditions and for bypassing the longer processing time of the higher levels as much as possible. Such lower-level reactions would compensate for the different execution times of planning and control and fill in possible voids in the command stream. Each level would then be partly autonomous in that it could choose to continue tracking the trajectory specified by the most recently received plan or to activate a recovery procedure in case of error. Meanwhile, the error would signal the higher levels to adjust the plan.

This work was done by Paolo Fiorini and Jeffrey Chang of Caltech for **NASA's Jet Propulsion Laboratory**. *For further information, Circle 97 on the TSP Request Card. NPO-17871*

Monitoring Welding Images and Data Simultaneously

Data on process conditions are superimposed in real time on images of the process.

Marshall Space Flight Center, Alabama

A video/computer subsystem of a welding system produces an overlay, on a video image, containing numerical data on the parameters of the welding operation being viewed. The system was developed to assist a welding-machine operator in determining the width of the back bead of the weld.

The computer gathers data from sensors while a video camera observes the weld in progress. The computer sends the data to a vision processor in the computer, which superimposes the data on the image from the camera. The operator thus can watch the weld bead simultaneously with the instantaneous values of such data as elapsed time, welding current, and processed sensor measurements of the weld area, such as weld back-bead width and depth of penetration, pool temperature, or top bead dimensions.

The video image and superimposed data can be recorded on magnetic video tape. The welding operation can later be reviewed in slow motion or even frame by frame. The pertinent weld data will always be instantly available to the viewer and correlated in time with the image of the weld.

This work was done by Ray C. Delcher and Matthew A. Smith of Rockwell International Corp. for **Marshall Space Flight Center**. *No further documentation is available.*
MFS-29772

Books and Reports

These reports, studies, handbooks are available from NASA as Technical Support Packages (TSP's) when a Request Card number is cited; otherwise they are available from the National Technical Information Service.

Digital Control of a Telescope in an Airplane

Options for the design of an aim-stabilizing system are analyzed.

A report discusses the feasibility of a digital control system that would stabilize the aim of the 30-in. (76.2-cm) telescope aboard the NASA C141 airplane known as the Kuiper Atmospheric Observatory. The purpose of such a system is to keep the telescope aimed along the same direction once that direction has been set. To do this, it must reject both random disturbances like vibrations of the airplane and steady disturbances like imbalance of the telescope. The digital system would perform these functions, supplanting the analog stabilizing system that has been used since 1974.

The "brain" of the control system is the compensator. The transfer function of the present analog compensator is analyzed and shown to be mostly that of the well-known proportional/integral/derivative (PID) type; that is, the output of the compensator is mostly the sum of a component proportional to its input error signal and components proportional to the integral and to the derivative of its input error signal with respect to time. The transfer function is also found to include an additional filter pole in the derivative branch to suppress high-frequency noise, and to include several other filter functions as well. This transfer function is simplified, and the basic PID parameters are extracted from it to start the design of the digital compensator.

The proposed digital compensator would consist of an input analog-to-digital converter, a digital controller processor, and an output digital-to-analog converter. The digital processor would effect a discrete transfer function simpler than that of the analog controller, containing the PID components with the additional filter pole in the derivative branch, but not the other filter functions. The frequency responses of the present and proposed compensators are compared. The effects of sampling time, computational delay, and quantization errors in the digital system are taken into account.

The mathematical model of the compensator is combined with the mathematical models of the control amplifier, gyroscope and control actuators, and telescope. The combined models are used to perform computer simulations of the open-loop response of the proposed system in the time and frequency domains and of the effect of noise in the closed-loop response in the time domain. After some fine adjustments of the parameters of the digital compensator, the gain and phase margins and the response of the entire system containing the proposed digital compensator are found to exceed those obtained with the present analog compensator. In addition, the response is found to be well damped in comparison with that of the present system. The simulation shows that the digitally compensated telescope would respond with tracking errors peaking around 0.27 arcsec (a root-mean-square tracking error of less than 1 arcsec is acceptable).

Finally, the selection of equipment to implement the digital control system is discussed. Considerations include the ability of the controller processor to operate alone vs. the need for an additional computer, immunity to noise in transmission of signals to and from the compensator, packaging, and cost.

This work was done by Ann C. McCormack and Philip K. Snyder of **Ames Research Center**. *To obtain a copy of the report, "Digital Control of the Kuiper Atmospheric Observatory Telescope," Circle 40 on the TSP Request Card.*
ARC-12399

Behavior of Costas Loop in Reception of Telemetry

Effects of signal parameters and Doppler shift are computed.

A report presents a theoretical study of the behavior of a Costas loop in the reception of a radio carrier signal that is modulated in phase by a sinusoidal or square-wave subcarrier that is, itself, further modulated in phase by a nonreturn-to-zero binary data signal. The phase and frequency of the received signal may also be affected by a Doppler shift, and the instantaneous amplitude of the received signal is corrupted by additive white Gaussian noise. Signals of this type are ordinarily used in spacecraft telemetry, the sine-wave subcarrier being preferred for shorter signal paths and the square-wave subcarrier for longer signal paths.

The carrier component of the received signal is not completely suppressed, and the Costas loop reconstructs its carrier reference from this component. The residual-carrier modulation, Doppler shift, and noise degrade the ability of the Costas loop to lock onto the carrier signal. The study focuses on this degradation. As such, it extends a previous study of the performance of a Costas loop with a residual carrier but without phase-shift-keyed subcarrier modulation. In the previous study, it was assumed that the phase error of the Costas loop approaches zero at high signal-to-noise ratios. In this study, the phase error is assumed to remain small enough to keep the response of the loop within its approximately linear range, but it is not required to approach zero at high signal-to-noise ratios. This study also considers the maximum allowable telemetry rate for a specified tracking phase jitter and for a given combination of signal-to-noise ratio and bandwidth constraint.

It is shown both algebraically and by numerical examples that the Costas loop can be used to track the signals in the presence of the Doppler shift. The tracking performance is degraded in the sense that the mean-square phase jitter increases when a residual carrier is present. The tracking performance of a Costas loop is degraded further when the modulation index rises toward a critical value. At any signal-to-noise ratio, the loop ceases to lock onto the carrier when the critical value is reached. (The critical values for the square-wave- and sine-wave-subcarrier versions are different.) The performance can be optimized (in the sense that the mean-square tracking phase jitter can be minimized) by choosing the appropriate combination of (1) frequency of the subcarrier, (2) square or sinusoidal waveform of the subcarrier, (3) bit rate, and (4) noise bandwidth of the low-pass filters in the arms of the Costas loop.

This work was done by Tien M. Nguyen of Caltech for **NASA's Jet Propulsion Laboratory**. *To obtain a copy of the report, "The Behavior of a Costas Loop in the Presence of Space Telemetry Signals," Circle 129 on the TSP Request Card.*
NPO-18084

Digital Accumulators in Phase- and Frequency-Tracking Loops

Digital accumulators can degrade performances at low carrier-to-noise ratios.

A report describes an investigation of the deleterious effects of digital accumulators upon the performances of phase- and frequency-tracking electronic circuits. Digital accumulators are used extensively in these and other signal-processing circuits to compute averages and reduce processing rates. The report emphasizes problems encountered with respect to digital accumulators in the operation of receivers in the Global Positioning System (GPS). These receivers are required to track the phases and frequencies of the GPS carrier signals, which can be weak and are Doppler shifted by the high dynamics (high speeds, high accelerations, and sometimes high jerks) of the receiver with respect to the GPS spacecraft. Notwithstanding the emphasis on the GPS, the conclusions reached in this investigation are also applicable to more general receivers or other signal-processing systems that include digital accumulators.

The investigation focused on three different tracking loops: a digital phase-locked loop, a cross-product automatic frequency-control loop, and an extended Kalman filter. Algorithms that represent these loops were tested in a computer simulation. In addition, a hybrid analog/digital receiver was built to implement the algorithms, and the performances of the loops were measured to verify the simulations.

The report contains four sections. The first discusses the general problem and the questions that this investigation was intended to answer, reviews previous research on Doppler tracking in the presence of high dynamics, describes digital implementation of tracking loops, and introduces mathematical models that represent GPS signals under worst-case dynamics. The second chapter describes the hybrid analog digital receiver.

The third chapter describes the algorithms of the three loops. The results of the simulations and tests are presented in this chapter as various plots of frequency errors, amplitude losses, and probabilities of loss of lock vs. carrier-to-noise ratios, and as transient responses in terms of frequency errors and amplitude losses vs. time. The third chapter continues by comparing the performances of the three loops and ends by stating two conclusions: (1) simulations carried out without including the effects of digital accumulators can lead to erroneous predictions of performance, especially at low carrier-to-noise ratios, and (2) of the loops tested, the fourth-order version of the Extended Kalman filter performed the best.

The fourth chapter, which is very brief, summarizes the investigation, restating the first of the above-mentioned conclusions. It notes that at high carrier-to-noise ratios, the effects of digital accumulators are negligible, but that at low carrier-to-noise ratios, digital accumulators contribute substantial losses. It recommends that additional losses in threshold carrier-to-noise ratios should always be included in simulations to account for the digital accumulators. This could be done by including additional amplitude-suppression terms.

This work was done by Sami Hinedi and Joseph I. Statman of Caltech for **NASA's Jet Propulsion Laboratory.** *To obtain a copy of the report, "Digital Accumulators in Phase and Frequency Tracking Loops," Circle 83 on the TSP Request Card.*
NPO-17909

Experiences With the JPL Telerobot Testbed

Issues and insights are discussed.

A report identifies problems and technological gaps that exist in robotic systems integration. It focuses upon the problems that were experienced during the development of the Telerobot Testbed System at NASA's Jet Propulsion Laboratory (JPL): an integrated robotic testbed used to develop, implement, and evaluate the performance of advanced concepts in autonomous, teleautonomous, and teleoperated control of robotic manipulators. The objective of this report is to provide information that can be used to guide and expedite the development of future integrated robotic systems. Problems are identified in calibration and world modeling, process planning, and system architecture and software engineering.

- **Calibration**. Calibration issues in an integrated multisensory, multiactuated robotic system can have a profound impact upon the design, implementation, and performance of high-level-control and task-planning algorithms. As a prime example of this, the authors cite the difficulties involved in merging information from vision and touch sensors to estimate the location of an object in the workspace.

To merge information from disparate sensors, the information obtained by each must be transformed into a common representation to permit integration. In addition to providing a means for integration, the representation must also serve the informational needs of the rest of the system. In the Testbed, the common representation is a tree-topology connected data base describing the spatial relationships among all the objects.

The difficulty in integrating the various sensor information has arisen, in part, from the fact that several of the sensors (i.e., two force/torque sensors and two cameras) are mounted on independent platforms. Referencing sensors on a manipulator to a common coordinate system depends on the accurate calibration of manipulator kinematics, which is extremely difficult. Inherent physical constraints have also made it difficult to determine where each manipulator is with respect to another, as in the case of the system's vision arm.

These difficulties have had a significant impact upon several system functional components. For example, ad-hoc (i.e., engineered) methods have been employed to maintain the consistency of the system's data base.

The authors have concluded that the design of future large-scale robotic systems must include features that permit the system's calibration in a complete and coherent fashion. In particular, accommodations must be made to facilitate the accurate identification of device spatial relationships in terms of both hardware and software.

- **Planning**. The planning of telerobot processes (i.e., actions such as move, grasp, and rotate) presented special problems because of the complex and interacting nature of a very large number of problem constraints and characteristics. Among these were the usual constraints arising from the kinematic construction of the Puma 560 manipulators, which limited manipulability over large regions. Added to these were spatial constraints in the form of interarm collision avoidance for the three arms, arm/object collision avoidance, object/object interference avoidance during manipulation, and object occlusion during vision operations. Dynamic constraints included performance degradation and even instability of compliant motion operations near singular arm configurations, and poorly known gravity and friction effects.

The challenge in planning became that of trying to blend engineered solutions successfully with algorithmic approaches. Because a standard rule or logic-based planning system would have been very difficult to design, an alternative "generate and test" approach was used instead. This approach utilized action-selection rules and procedures based on a partial handling of the various constraints to generate candidate actions. Detailed world-model-driven simulation of the action was then used to accept or reject the candidate action.

- **Architecture**. In a well-established and -understood field, the construction of a system without first exploring its formulation and design in great detail is foolhardy. Unfortunately, this rigor is not feasible in a research environment where requirements fluctuate. In these situations, success is often determined by the ability to react rapidly to significant design changes.

First, it was observed that space telerobotics is not a highly structured task and that efforts should be placed on the reactive, feedback portion of the architecture that allows the robot to respond to the environment.

Second, interface "blindspots," whereby higher-level subsystems are unable to command all of the actions that the hardware devices can perform, must be avoided at all costs because they inevitably lie precisely in the regions that turn out to be crucial to the functioning of the overall system.

Third, the ability to shift functionality easily across subsystem interfaces is crucial as the development of new algorithms with improved functionality can force the shifting of large bodies of capability from higher-level subsystems to lower ones.

Fourth, the practice of inserting additional layers into implementations for the express purpose of decoupling external users from the internal details of a piece of software (i.e., abstraction) is essential during the development of subsystem interfaces because such practice prevents minor internal modifications from being propagated to other subsystems.

Finally, the most important issue in large systems' software development is human rather than technological. Frequent, detailed communication among all members of a development team is required to prevent minor choices on the part of subsystems from propagating disastrously to the system.

This work was done by Henry W. Stone, J. Balaram, and John J. Beahan of Caltech for **NASA's Jet Propulsion Laboratory**. *To obtain a copy of the report, "Experiences With the JPL Telerobot Testbed: Issues and Insights," Circle 143 on the TSP Request Card.*
NPO-17928

Electromagnetic Interference in New Aircraft

Updated standards will reflect a more severe environment and vulnerabilities of modern avionics.

A report reviews plans to develop tests and standards to ensure that digital avionics systems in new civil aircraft are immune to electromagnetic interference (EMI). The plans were prompted by trends that make new aircraft more susceptible to EMI than are older aircraft:

- New aircraft incorporate more electronic "fly-by-wire" controls.
- New electronic equipment uses highly integrated circuit chips, which are more easily affected by EMI.
- New aircraft structures are built from composite materials that afford less shielding than metals do.
- Future aircraft will be exposed to increased electromagnetic energy from broadcast, communication, and radar facilities of higher power.

Until now, avionic systems for transport aircraft have been required to meet radio-frequency susceptibility standards set forth in section 20 of the document *Environmental Conditions and Test Procedures for Airborne Equipment*, RTCA DO 160B, published by the Radio Technical Commission for Aeronautics. The document calls for protection against electromagnetic fields of 1 and 2 V/m, whereas a level of 100 V/m is more realistic for such equipment as electronic engine controllers.

Accordingly, the Federal Aviation Administration (FAA) has asked the commission to revise section 20 to reflect current information on the electromagnetic environment and to develop specifications for avionics equipment at the box and system levels. The FAA has also asked the Society of Automotive Engineers to draft an advisory circular and user's manual for certification of commercial aircraft operating in the electromagnetic environment created by incidental emitters. The FAA is coordinating its efforts with those of aviation regulatory authorities in other countries to ensure that the new standards will be internationally accepted.

This work was done by William E. Larsen of **Ames Research Center**. *To obtain a copy of the report, "Digital Avionics Susceptibility to High Energy Radio Frequency Fields," Circle 7 on the TSP Request Card.*
ARC-12161

Effects of Frame Rates in Video Displays

High rates are needed in rapidly changing images.

A report describes an experiment on the subjective effects of the rates at which a display on a cathode-ray tube in a flight simulator is updated and refreshed. The experiment was conducted to learn more about the jumping, blurring, flickering, and multiple lines that an observer perceives when a line moves at high speed across the screen of a calligraphic CRT.

A horizontal line on an oscilloscope display was moved vertically at various speeds and viewed by several observers. The 1-mm-thick line approximates the lines used on 19- to 21-in. (48-to 53-cm) cathode-ray tubes in flight-simulation visual displays. The line was refreshed at a rate of either once or twice per update. A line that is refreshed once per update is drawn on the screen once. Its position is then recomputed (updated), and it is redrawn. A line that is refreshed twice per update is drawn on the screen twice in one position, its position is recomputed, and it is then redrawn twice in the next position. Lines are frequently refreshed more often than they are updated to avoid flickering.

The report presents data from the observations on plots of rates of refreshing and updating as functions of speed. The speed above which the picture appears to deteriorate can be found from such a plot. This speed can be related by calculations to simulated angular and linear velocities of the aircraft in the flight simulator.

For example, a visual display updated at 30 hertz and refreshed at 60 hertz appears to deteriorate at angular and linear velocities considerably less than those of modern high-performance aircraft. However, the speed at which deterioration appears to set in can be increased significantly by increasing the update rate. Refreshing at twice the update rate produces only minor improvement. To display rapidly changing flight scenery without apparent deterioration of the image, it may be necessary to use an updating rate of at least several hundred hertz.

This work was done by Gary V. Kellogg and Charles A. Wagner of **Ames Research Center**. *Further information may be found in NASA TM-100415 [N88-22033], "Effects of Update and Refresh Rates on Flight Simulation Visual Displays."*

Copies may be purchased [prepayment required] from the National Technical Information Service, Springfield, Virginia 22161, Telephone No. (703) 487-4650. Rush orders may be placed for an extra fee by calling (800) 336-4700.
ARC-12358

Discover Tomorrow's Innovations Today

At Technology 2001
December 3-5, 1991
San Jose Convention Center

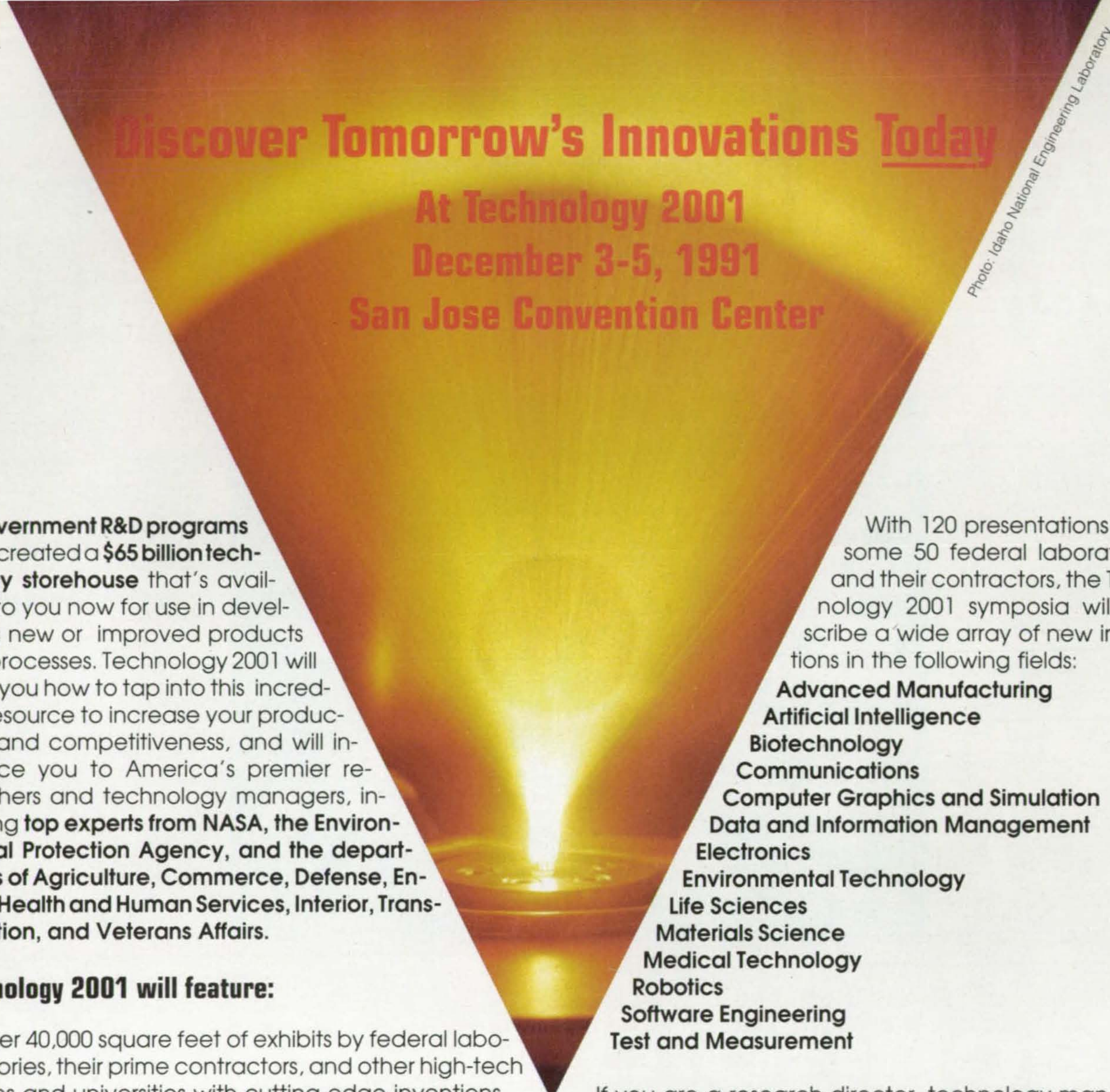

US government R&D programs have created a **$65 billion technology storehouse** that's available to you now for use in developing new or improved products and processes. Technology 2001 will show you how to tap into this incredible resource to increase your productivity and competitiveness, and will introduce you to America's premier researchers and technology managers, including **top experts from NASA, the Environmental Protection Agency, and the departments of Agriculture, Commerce, Defense, Energy, Health and Human Services, Interior, Transportation, and Veterans Affairs.**

Technology 2001 will feature:

- Over 40,000 square feet of exhibits by federal laboratories, their prime contractors, and other high-tech firms and universities with cutting-edge inventions available for license or sale;

- 120 symposia presentations spotlighting new advances with commercial promise in critical areas of technology;

- Government-Industry Workshops covering patent licensing, Cooperative Research and Development Agreements, and Small Business Innovation Research contracts.

Plus these special events:

- A Pre-Show Reception on Monday, Dec. 2 in the exhibit hall, offering attendees and the media the chance to preview the exhibits and meet the presenters in an informal atmosphere;

- The second annual Technology Transfer Awards Dinner, recognizing outstanding achievement in tech transfer to industry. This event offers a unique opportunity to network with government and industry executives in an elegant setting—the Imperial Ballroom of the San Jose Fairmont Hotel. (Seating is limited, so reserve tickets early!)

With 120 presentations from some 50 federal laboratories and their contractors, the Technology 2001 symposia will describe a wide array of new inventions in the following fields:

Advanced Manufacturing
Artificial Intelligence
Biotechnology
Communications
Computer Graphics and Simulation
Data and Information Management
Electronics
Environmental Technology
Life Sciences
Materials Science
Medical Technology
Robotics
Software Engineering
Test and Measurement

If you are a research director, technology manager, design engineer, scientist, or business owner/president, Technology 2001 is the most important event you will attend this year. Do not miss this opportunity to access a wealth of federally-developed technologies, meet the key players in government and high-tech industry, and discover tomorrow's innovations...today.

Show Schedule

Monday, Dec. 2	
6:00 pm - 8:00 pm	Opening Reception
Tuesday, Dec. 3	
9:00 am -10:30 am	Plenary Session
1:00 pm - 3:00 pm	Technical Sessions
4:30 pm - 6:00 pm	Govt./Industry Workshops
Wednesday, Dec. 4	
8:30 am -10:30 am	Technical Sessions
1:00 pm - 3:00 pm	Technical Sessions
4:30 pm - 6:00 pm	Govt./Industry Workshops
7:00 pm -10:00 pm	Awards Dinner
Thursday, Dec. 5	
8:30 am -10:30 am	Technical Sessions
1:00 pm - 3:00 pm	Technical Sessions
4:30 pm - 6:00 pm	Govt./Industry Workshops

Exhibit Hours

Dec. 3	10:00 am - 5:00 pm
Dec. 4	10:00 am - 5:00 pm
Dec. 5	10:00 am - 4:30 pm

Technology 2001 Exhibitors

Here are some of the more than 200 government R&D centers, universities, and high-tech firms exhibiting at Technology 2001:

AEROSPACE LUBRICANTS INC.
AEROSPATIALE
AGEMA INFRARED SYSTEMS
AIR FORCE MANUFACTURING TECHNOLOGY DIRECTORATE
AIR FORCE SYSTEMS COMMAND
AMBASSADOR MARKETING
AMERICAN CERAMIC SOCIETY
AMERICAN WELDING SOCIETY
AMES LABORATORY
AMES RESEARCH CENTER
AMPEX
ANALYTICAL GRAPHICS
ARMSTRONG LABORATORY
ARMY LABORATORY COMMAND
ARTHUR D. LITTLE
ASSOC. OF AMERICAN RAILROADS/US DEPARTMENT OF TRANSPORTATION
ASTRO-MED INC.
BIT 3 COMPUTER CORP.
BEND RESEARCH
BF GOODRICH AEROSPACE SUPER-TEMP
BROOKHAVEN NATIONAL LABORATORY
CALIFORNIA INSTITUTE OF TECHNOLOGY
CARNEGIE MELLON ROBOTICS INSTITUTE
CENTER FOR AEROSPACE INFORMATION
CORNING INC.
COSMIC
CYBERNET SYSTEMS
DATATAPE INC.
DEPARTMENT OF ENERGY
DESIGN & EVALUATION INC.
DIGIRAY CORP.
EARTH OBSERVATION SATELLITE CO.
EASTMAN KODAK COMPANY
EUROPEAN SPACE AGENCY
FERMI NATIONAL ACCELERATOR LAB
FLIR SYSTEMS INC.
GODDARD SPACE FLIGHT CENTER
HAMILTON TECHNOLOGIES INC.
HARDIGG INDUSTRIES
HEIMANN INFRARED DIVISION/ PYROMETRICS CORP.
HEMCO CORP.
HIGH-TECHNOLOGY SUPERCONNECTIONS
HITACHI DENSHI AMERICA INC.
HTS INC.
IDAHO NATIONAL ENGINEERING LAB
INDUSTRIAL MATERIALS TECHNOLOGY INC.
INFORMATION HANDLING SERVICES
INFRAMETRICS INC.
INTEGRATED ENGINEERING SOFTWARE
INTEGRATED SYSTEMS
IXYS CORP.
JAMES GRUNDER & ASSOCIATES
JET PROPULSION LABORATORY
JOHNSON SPACE CENTER
JP TECHNOLOGIES INC.
KEANE CONTROLS CORP.
KENNEDY SPACE CENTER
LANGLEY RESEARCH CENTER
LAWRENCE LIVERMORE NATIONAL LABORATORY
LEWIS RESEARCH CENTER
LOS ALAMOS NATIONAL LABORATORY
LUXTRON CORP., ACCUFIBER DIVISION
MAGNA ENGINEERING INC.
MARSHALL SPACE FLIGHT CENTER
MARTIN MARIETTA ENERGY SYSTEMS
McCLELLAN AIR FORCE BASE
MECHANICAL TECHNOLOGY INC.
METALWORKING TECHNOLOGY INC.
METRUM
MIKRON INSTRUMENT CO.
MORGANTOWN ENERGY TECHNOLOGY CENTER
NASA
NASA REGIONAL TECHNOLOGY TRANSFER CENTERS
NASA SMALL BUSINESS INNOVATION RESEARCH
NASA TECH BRIEFS
NATIONAL CENTER FOR MANUFACTURING SCIENCES
NATIONAL INSTITUTE OF ALLERGIES & INFECTIOUS DISEASES
NATIONAL INSTITUTE OF STANDARDS & TECHNOLOGY
NAVAL AIR WARFARE CENTER
NAVAL RESEARCH LABORATORY
NERAC INC.
NIAC
NOVESPACE
NUMERICAL ALGORITHMS GROUP
OLYMPUS CORP.
PACIFIC NORTHWEST LABORATORY
PATTON & PATTON SOFTWARE
PHILLIPS LABORATORY
PITTSBURGH ENERGY TECHNOLOGY CENTER
PMS ELECTRO-OPTICS
PRINCETON PLASMA PHYSICS LABORATORY
RAYTHEON COMPANY
RGB SPECTRUM
RG HANSEN & ASSOCIATES
RIBBON TECHNOLOGY CORP.
ROCKWELL INTERNATIONAL
ROME LABORATORY
SALCO CIRCUITS
SANDIA NATIONAL LABORATORIES
SIMMONDS PRECISION AIRCRAFT SYSTEMS
SOLAR ENERGY RESEARCH INSTITUTE
SORBILITE INC.
SOUTH CAROLINA UNIVERSITIES RESEARCH
SPECIALTY STEEL & FORGE
STANFORD RESEARCH INSTITUTE
STATISTICAL SCIENCES INC.
STENNIS SPACE CENTER
STEPHENS ANALYTICAL
STEREOGRAPHICS CORP.
STRATEGIC DEFENSE INITIATIVE ORG.
SUN MICROSYSTEMS
SUPERIOR PRODUCTS
SYMBOLICS
TECHNICAL INSIGHTS INC.
TECHNOLOGY CENTER OF SILICON VALLEY
TECHLAW GROUP
TECHNOLOGY TARGETING INC.
TECHNOLOGY TRANSFER SOCIETY
TENNESSEE TECHNOLOGY FOUNDATION
THIN FILM TECHNOLOGY INC.
TIODIZE INC.
ULTRAMET
UNITED MAGNET TECHNOLOGIES
UNIVERSITY OF DAYTON RESEARCH INSTITUTE
US GEOLOGICAL SURVEY
VA MEDICAL CENTER, REHAB R&D CENTER
VECTOR AEROMOTIVE CORP.
VIRGINIA CENTER FOR INNOVATIVE TECHNOLOGY
WOLFRAM RESEARCH
WRIGHT LABORATORY

See next page for a sample of the amazing inventions these high-tech leaders will demonstrate. For information on having your organization exhibit at Technology 2001, call Justina Cardillo or Evelyn Mars at (212) 490-3999.

See America's most advanced automobile — the Vector W8 TwinTurbo — in the Technology 2001 exhibit hall. Incorporating an array of aerospace technologies, this "supercar" goes from 0-60 mph in less than 3.8 seconds and reaches speeds of more than 200 mph.

Photo: Vector Aeromotive Corp.

Explore The Cutting Edge

The Technology 2001 exhibit hall will feature the best new inventions from federal laboratories, universities, and leading high-tech companies. Here's just a sample of the hundreds of innovations that await you.

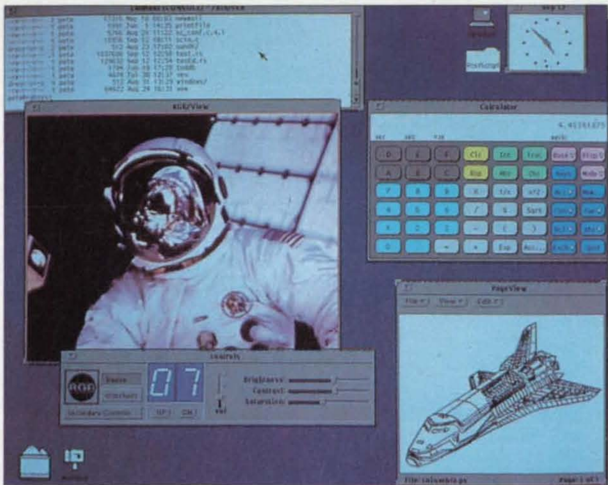

RGB Spectrum will demonstrate an advanced windowing system that displays live television or other real-time video on a workstation.

In one of the many innovative R&D projects it will exhibit, the Pittsburgh Energy Technology Center is using microbes to produce a clean form of coal.

The Ames Research Center exhibit will feature a "virtual" 3D sound system developed for artificial reality applications.

A patented recycling system to be displayed by Sorbilite Inc. converts paper, sawdust, and other waste products into high-quality, three-dimensional parts and products.

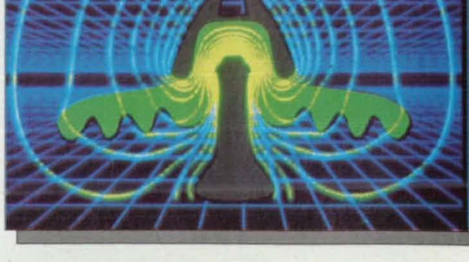

Integrated Engineering Software will exhibit new programs for design and analysis of electronic equipment, including ELECTRO, shown here simulating the electric field distribution around a pin-type insulator.

Meet Dexter, a computer-controlled mechanical finger-spelling hand, on display in the VA Rehabilitation R&D Center's booth. Dexter serves as a communication aid for the deaf and blind.

Ultramet will showcase an iridium/rhenium thrust chamber that has been called "the greatest advance in chemical rocket technology in three decades."

Among the inventions Pacific Northwest Laboratory will exhibit is a sensor for detecting soil contaminants (below) that is easier to use and more accurate than current detection devices.

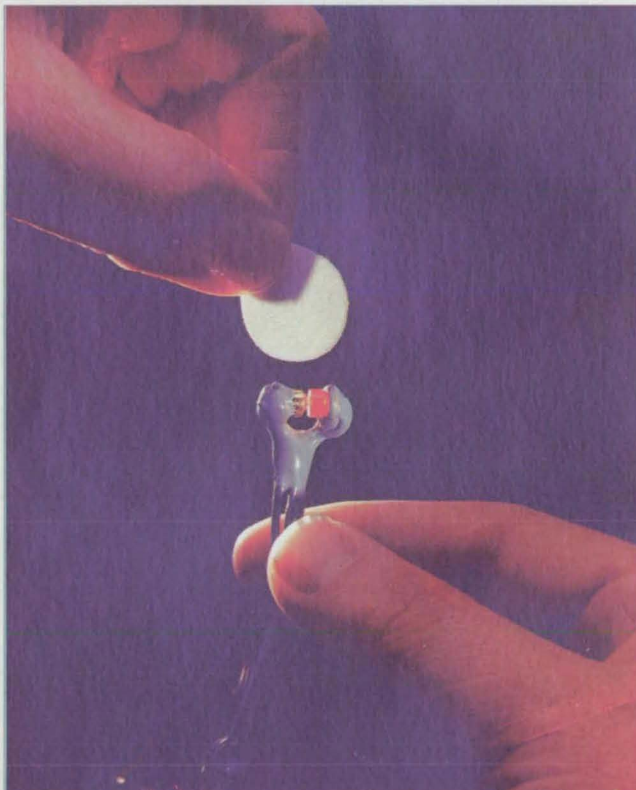

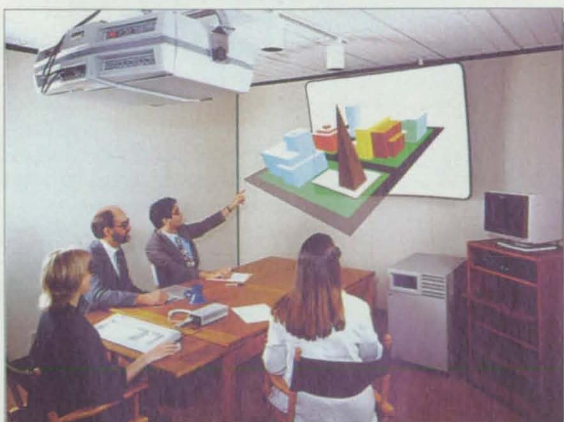

StereoGraphics Corp. will demonstrate CrystalEyes™, a computer graphics system that emulates human vision to create a vivid, flicker-free 3D depth effect.

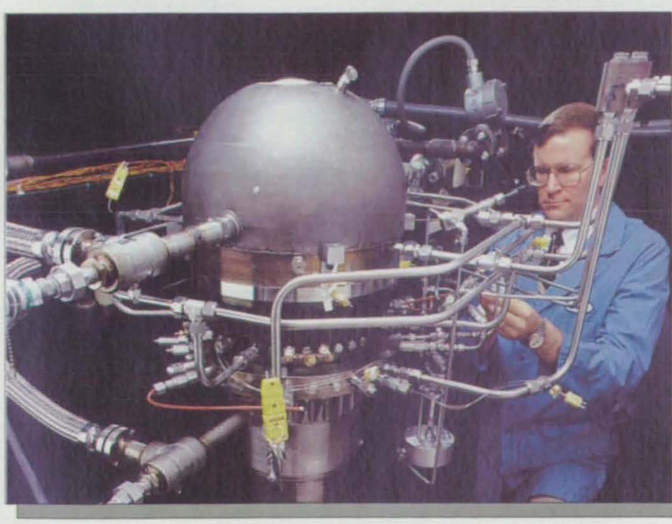

Mechanical Technology Inc. will display an external combustion Stirling engine designed to power space station Freedom. The high-tech engine has tremendous spinoff potential.

See state-of-the-art robotics technology, including vision equipment and force-reflecting hand controllers, in Cybernet Systems' booth.

Technology 2001 Program

Tuesday, December 3

Plenary Session
9:00 am—10:30 am

(Speakers to be announced)

9:00: Welcome
9:15: Conference Overview
9:30: Federal Initiatives In Technology Transfer
10:00: Technology 2001 Keynote Address

Concurrent Technical Sessions
1:00 pm—3:00 pm

Each presentation will last 30 minutes, including a question and answer period. Registrants may attend whole sessions (four presentations) or individual presentations from a number of different sessions. Meeting rooms are situated in close proximity for easy and quick movement during sessions. Room assignments will be listed in the final program distributed at the show.

(Session A1)

Advanced Manufacturing

Ceramic Susceptor for Induction Bonding of Metals, Ceramics, and Plastics
John D. Buckley, Senior Research Engineer, and Robert L. Fox, Electronics Technician, Langley Research Center

Langley researchers have developed a thin flexible carbon susceptor to join ceramics, plastics, metals, and combinations of these materials, using a unique induction heating process that dramatically reduces bonding times. The novel carbon susceptor allows application of heat directly and only to the bond line.

Applying NASA's Explosive Seam Welding
Laurence J. Bement, Senior Pyrotechnic Engineer, Langley Research Center

An explosive seam welding process created for aerospace use is finding a wide range of industrial applications. The process can be used to join aluminum and steel alloys, copper, brass, titanium, and other metals in thicknesses from 0.25 to 4.7 mm, and to remotely plug tubes.

Laser-Based Weld Joint Tracking System
Alan Looney, Welding Engineer, Marshall Space Flight Center

A laser-based system developed to control and monitor welding operations on space vehicles has been modified to provide a weld joint tracking system for industrial applications. The weld beam profiler features a precision laser-based vision sensor, automated two-axis machine motion, and an industrial PC controller. It eliminates weld repairs caused by joint tracking errors, reducing manufacturing costs.

Precision Joining Center
J.W. Powell, Joining Technology, EG&G Rocky Flats

Mr. Powell will describe a new center designed to provide a training ground for precision joining techniques. The center will transfer this advanced technology from the Department of Energy weapons complex and joining equipment manufacturers to US industries, through the training of technologists and engineers in such areas as process control, data acquisition, and joining.

(Session A2)

Biotechnology

Cooperative Research and Development Opportunities with the National Cancer Institute
Dr. Kathleen Sybert, Deputy Director, Office of Technology Development, National Cancer Institute

The National Cancer Institute's Office of Technology Development negotiates Cooperative Research and Development Agreements with university and industry investigators for the development of new products to diagnose and treat cancer and AIDS. Drug screening, preclinical testing, clinical trials, and AIDS program capabilities form the basis for this new technology transfer vehicle.

Technologies for the Marketplace from the Centers for Disease Control
Frances L. Reid-Sanden and R. Eric Greene, Technology Transfer Office, Centers for Disease Control

The Centers for Disease Control develops and transfers technologies designed to prevent and control disease and injury. Recent innovations include a vaccine against hepatitis A, a recombinant rabies vaccine, monoclonal antibodies for the detection of legionellae, a rapid method to diagnose human cysticercosis, and a variety of devices to ensure worker safety.

Enhancement of Biological Control Agents for Use Against Forest Insect Pests and Diseases
Dr. James M. Slavicek, Project Leader, US Forest Service Northeastern Forest Experiment Station

Dr. Slavicek will describe new biological control agents for use against forest pests such as the gypsy moth and diseases such as tree vascular fungal wilts.

Use of T7 Polymerase to Direct Expression of Outer Surface Protein A (OspA) from the Lyme Disease Spirochete, *Borrelia burgdorferi*
John J. Dunn, Senior Scientist, Brookhaven National Laboratory

Brookhaven researchers have cloned the ospA gene of *Borrelia burgdorferi*, the spirochete that causes Lyme disease. They are testing the resultant truncated protein for use as an immunogen in a vaccine against Lyme disease.

(Session A3)

Communications

Commercial Applications of ACTS Mobil Terminal Millimeter-Wave Antennas
Arthur C. Densmore, Antenna System Manager, and Rick A. Crist, Microwave Processor Subtask Manager, Jet Propulsion Laboratory

A JPL research team is developing low-profile, high-gain millimeter-wave antennas for future communication systems. Commercial opportunities include advanced land-mobile satellite communications, hybrid satellite/cellular systems, remote satellite news gathering, aeronautical and maritime satcom, and handheld personal satellite communications.

Antennas for Mobile Satellite Communications
John Huang, Jet Propulsion Laboratory

The NASA-sponsored Mobile Satellite Experiment program has generated several innovative microstrip antennas at L-band frequencies. Due to their thin profile, surface conformability, light weight, and low manufacturing cost, microstrip antennas are finding increasing applications in land-mobile satellite communications.

MMIC Linear-Phase and Digital Modulators for Space Communications Applications
Narayan R. Mysoor, Jet Propulsion Laboratory, and Fazal Ali, Pacific Monolithics

This presentation will review the design concepts, analyses, and development of monolithic microwave integrated circuit (MMIC) modulators for the next generation of space-borne communication systems. Commercial applications include phased arrays, satellite systems, and microwave systems that require continuous phase control in trimming multiple channels.

Phased-Array Antenna Beamforming Using an Optical Processor
Louis P. Anderson, Hughes Aircraft Company, and Richard Kunath, Lewis Research Center

Phased-array antennas are playing an increasingly important role in radar and communications applications, and will soon become the preferred way to achieve fixed spot, scanning spot, multiple spot, and other multi-functional beams for satellite communications. The presenters will discuss how a lightweight optical-processor-based beamformer can provide the required aperture excitations using a single lightweight network.

(Session A4)
Computer Graphics and Simulation

Global Positioning System Supported Pilot's Display
Marshall Scott, Systems Engineer, Kennedy Space Center

A new cockpit display for pilots of test aircraft uses the Global Positioning System to calculate aircraft position. This data is displayed graphically along with the runway, the desired flight path, and "fly-by" alignment needles.

Application of Technology Developed for Flight Simulation
Jeff I. Cleveland, Aerospace Technologist, Langley Research Center

Langley researchers are employing supercomputers for mathematical model computation to support real-time flight simulation. Mr. Cleveland will discuss commercial spinoff of these techniques in fields such as nuclear process control, power grid analysis, process monitoring, and chemical processing.

FAST: A Multi-Processed Environment for Visualization of Computational Fluid Dynamics
Gordon V. Bancroft, Fergus J. Merritt, Todd C. Plessel, Paul G. Kelaita, R. Kevin McCabe, and Al Globus, Research Scientists, Sterling Zero One Inc.

This presentation will focus on the Flow Analysis Software Toolkit (FAST), a software system for visualization and analysis of complex fluid flows. FAST is extensible and able to handle a wide range of problems. It can be adapted to new software and hardware configurations through modular structured programming methods, a graphics library standard, and common network communication protocols.

A Full-Parallax Holographic Display for Remote Operations
Helene P. Iavecchia, CSC/Analytics Inc.; Lloyd Huff, University of Dayton Research Institute; and Neville I. Marzwell, Jet Propulsion Laboratory

A near-real-time, full-parallax holographic display system developed for Jet Propulsion Laboratory could provide a 3D display for remote handling operations in hazardous environments on Earth and in Space.

(Session A5)
Electronics

Nonvolatile, High-Density, High-Speed, Magnet-Hall Effect Random Access Memory
Jiin-Chuan Wu, Romney R. Katti, and Henry L. Stadler, Flight Command and Data Management Systems, Jet Propulsion Laboratory

A radiation-hard, nonvolatile random access memory cell (MHRAM) with a density of 1 Mbit/cm^2 and an access time of less than 100 nsec is being developed using a magnet-Hall effect element. Such a memory will have a very competitive performance/price ratio to replace current commercial nonvolatile memory technologies, including ROM, EPROM, EEPROM, and Flash EEPROM, and will be competitive with static RAM for many applications.

Analog VLSI Neural Network Integrated Circuits
Francis Kub, Head, Microelectronic Device Physics Section, Naval Research Laboratory

Using a standard CMOS foundry process, Navy researchers have fabricated analog VLSI vector-matrix multiplier integrated circuit chips that perform vector-matrix multiplication operations at speeds up to 3 billion multiplications per second. Such high-speed operations are required for artificial neural networks and many signal processing applications, including image processing.

Monolithic Microwave Integrated Circuit Water Vapor Radiometer
L.M. Sukamto, Spacecraft Telecommunications Equipment Section, Jet Propulsion Laboratory

Mr. Sukamto will discuss efforts to design and fabricate a 31.4 GHz monolithic microwave integrated circuit (MMIC) radiometer as one channel of a thermally-stable water vapor radiometer (WVR). With improved thermal stability and signal accuracy, the WVR will have far-ranging commercial applications. It can be used, for example, in weather pattern prediction, calibration of polar-orbiting and geostationary satellites, and monitoring of aircraft icing conditions.

A Noncontacting Waveguide Backshort for Millimeter and Submillimeter Wave Frequencies
William R. McGrath, Technical Group Leader, Jet Propulsion Laboratory

A new backshort design employs a metallic bar with rectangular or circular holes to provide a periodic variation of guide impedance. The size, shape, and spacing of the holes can be adjusted to provide a large reflection of rf power over a useful frequency bandwidth. Mechanically rugged and easy to fabricate for frequencies up to 1000 GHz, the backshort offers applications in radar and communication systems, microwave test instruments, and remote-sensing radiometers, and will help extend waveguide technology into the submillimeter wave band.

(Session A6)
Materials Science

Novel Applications for TAZ-8A
William J. Waters, Sverdrup Technology Inc., and Stephen M. Riddlebaugh, Lewis Research Center

Alloy research for jet engine applications has produced a commercially promising nickel-based alloy called TAZ-8A. The alloy's unique combination of properties includes high temperature strength, oxidation resistance, abrasion resistance, and exceptional thermal shock resistance. Using a plasma vapor deposition technique, TAZ-8A can be applied as a coating with high reflectivity and extreme hardness.

Test Methods for Determining the Suitability of Metal Alloys for Use in Oxygen-Enriched Environments
Joel Stoltzfus, Projects Manager, White Sands Test Facility

Mr. Stoltzfus will describe test methods developed by NASA to study the ignition and combustion of metal alloys, including high- and low-speed particle impact tests, frictional heating and coefficient-of-friction tests, and the promoted combustion test. Test data and the resultant rankings of metal alloys will be discussed, along with licensing opportunities.

A Major Advance in Powder Metallurgy
B.E. Williams, J.J. Stiglich, R.B. Kaplan, and R.H. Tuffias, Ultramet

Under SBIR funding from the Army, Ultramet has developed a process that promises to significantly increase the mechanical properties of powder metallurgy (PM) parts. Conventional PM fabrication processes typically result in nonuniform distribution of the matrix, flaw generation due to particle-particle contact, and grain growth caused by high-temperature, long-duration compaction processes. In Ultramet's process, each particle is coated with the matrix material, and compaction is performed by solid-state processing, improving the part's homogeneity.

Permanent Magnet Design Methodology

Dr. Herbert A. Leupold, Research Physicist, US Army Electronics Technology and Devices Laboratory

The high remanences and coercivities of rare earth permanent magnets have made possible magnet structures of unusual form and performance, including permanent magnet solenoids, cylindrical transverse field sources, and high-field permanent magnet field sources. Dr. Leupold will describe military and commercial applications such as MR imagers, traveling wave tubes, gyrotrons, free electron lasers, Faraday rotators, and ultraviolet/x-ray telescopes.

Concurrent Government-Industry Workshops 4:30 pm—6:00 pm

(Presenters to be announced)

In these highly-interactive sessions, federal agencies will brief attendees on their present and planned R&D initiatives and technology transfer mechanisms, spotlighting opportunities for industry to work with the government to develop and commercialize technology. Cooperative Research and Development Agreements, Small Business Innovation Research, and patent licensing will be discussed. The objective of these workshops is to begin a dialog that will lead to increased use of federally-sponsored technologies by industry, and better utilization of private sector resources by the government. Agencies holding workshops during this time period will include:

- Department of Defense
- Department of Energy
- Department of Health and Human Services
- Environmental Protection Agency

Wednesday, December 4

Concurrent Technical Sessions 8:30 am—10:30 am

(Session B1)

Advanced Manufacturing

Concentrating Solar Systems: Manufacturing with the Sun

Lawrence M. Murphy, Division Director, Bimleshwar P. Gupta, Program Manager, and Steven G. Hauser, Industry Liaison, Solar Energy Research Institute

Recent advances in concentrating solar systems have produced solar flux densities in excess of 20,000 suns, creating unique process conditions of very high temperatures and heating rates. These conditions enable applications in manufacturing, materials processing, surface engineering, and toxic waste destruction.

Ultra-Precision Processes for Optics Manufacturing

William R. Martin, Associate Director, Engineering Technology Division, Oak Ridge National Laboratory

The Optics MODIL (Manufacturing Operations Development and Integration Laboratory) is developing advanced manufacturing technologies for fabrication of ultra-precision optical components, aiming for a ten-fold improvement in precision and a shortening of the schedule lead time. Discussion will focus on diamond single point turning, ductile grinding, ion milling, and in/on process metrology.

Integrated Automation for Manufacturing of Electronic Assemblies

T. Joseph Sampite, CIM Program Manager, Naval Ocean Systems Center

Mr. Sampite will describe how a standardized file transfer format developed with the National Institute of Standards and Technology will be used to create generic, open architecture computer-aided engineering tools for the automatic exchange of data between design and manufacturing.

Air Force Manufacturing Technology (MANTECH) Technology Transfer

Tracy J. Houpt, MTX Program Manager, and Margaret M. Ridgely, Technology Transfer Center Director, Wright Patterson Air Force Base

This presentation will illustrate the techniques and concepts employed in Air Force MANTECH's new comprehensive, proactive technology transfer program, using as an example the successful transfer of transmit/receive modules to industry.

(Session B2)

Electronics

Gallium Arsenide Quantum-Well-Based Far Infrared Array Imaging Radiometer

Kathrine A. Forrest and Murzy D. Jhabvala, Electronics Engineers, Goddard Space Flight Center

A new imaging radiometer developed for the thermal infrared (8 to 12 microns) employs a staring 128 x 128 GaAs quantum well detector array for stability, uniformity, high yield, and radiation-hardness. It is suited for thermal imaging in forestry, electronics processing, and medicine. Potential applications include aerial detection of small forest fires and location of hot spots in integrated circuits.

A Video Event Trigger for High-Frame-Rate, High-Resolution Video Technology

Glenn L. Williams, Electrical Engineer, Lewis Research Center

Mr. Williams will describe a highly-parallel digital state machine that generates a trigger signal at the onset of a video event. Random access memory storage coupled with fuzzy comparator logic devices permit monitoring a video stream for long- or short-term changes caused by spatial translation, dilation, or color change. Pretrigger and post-trigger storage techniques allow researchers to archive only significant images, alleviating costly data storage problems.

Camera Orientation of Pan, Tilt, and Zoom with No Moving Parts

Dr. H. Lee Martin, President, and Steven D. Zimmermann, Design Engineer, TeleRobotics International Inc.

Under contract to NASA Langley, TeleRobotics has developed a remote viewing system that provides pan, tilt, zoom, and rotational capabilities with no moving parts. The system features a fisheye lens for complete hemispherical field-of-view imaging and high-speed image transformation to correct peripheral distortion. Applications include remote viewing, inspection, and surveillance.

Fiber Optic TV Camera Direct

John Edward Kassak, Electronics Engineer, Kennedy Space Center

The Kennedy Center is developing a multiple color camera system for installations where video, synchronization, control camera data, and status data are transmitted via a single fiber cable at distances exceeding five miles. Expected benefits include improved video performance, immunity from EMI and RFI, and more broadcast flexibility.

(Session B3)

Environmental Technology

Waste Management Technology Development and Demonstration Programs

Paul D. Kalb, Research Engineer, Brookhaven National Laboratory

Brookhaven researchers have developed two new thermoplastic processes for the disposal of hazardous wastes: polyethylene encapsulation of nitrate salt wastes and modified sulfur cement encapsulation of incinerator fly ash wastes. Both systems provide significant improvements over conventional solidification techniques and result in durable waste forms that meet regulatory criteria.

Regulated Bioluminescence as a Tool for Bioremediation Process Monitoring and Control of Bacterial Cultures
Robert S. Burlage, Environmental Sciences Division, Oak Ridge National Laboratory; Armin Heitzer and Philip Digrazia, Center for Environmental Biotechnology, University of Tennessee

A new technique for monitoring biodegradation in toxic waste sites employs bioluminescence in a recombinant bacterial strain to detect contaminant levels. The process is rapid, often completed in minutes, and is sensitive in the part-per-billion range.

Fiber-Optic-Based Biosensor
Joel M. Schnur, Head, Molecular Science and Engineering Center, Naval Research Laboratory

Mr. Schnur will illustrate a new fiber-optic-based biosensor for environmental monitoring, pollution control, and clinical diagnostics. The device integrates a novel array of components, long fused silica fibers, and proteins for detection.

Ambient Temperature CO Oxidation Catalysts
Billy T. Upchurch, Senior Research Scientist, Langley Research Center

Langley researchers have produced ambient temperature oxidation catalysts for the recombination of CO and CO_2 dissociation products formed during CO_2 laser operation. The catalysts allow continuous operation of CO_2 lasers in a closed-cycle mode, and offer applications in other closed environments where the removal or control of CO is required, such as in catalytic converters for control of auto emissions.

(Session B4)

Materials Science

High-Temperature Adhesives
Terry L. St. Clair, Head, Polymeric Materials Branch, Langley Research Center

LARC-TPI, a high-temperature linear polymer adhesive developed to bond titanium, offers application as a hot-melt adhesive. Mr. St. Clair will describe the chemical structure and physio-mechanical properties of LARC-TPI and other important new polyimides with commercial potential.

Fluorinated Epoxy Resins with High Glass Transition Temperatures
James R. Griffith, Research Chemist, Naval Research Laboratory

The Navy has developed a new class of easily-processed liquid resins with low dielectric constants and high glass transition temperatures. These materials are useful for the manufacture of composite electronic boards.

Polyimides Containing Pendent Siloxane Groups
John W. Connell, Polymer Scientist, Langley Research Center

Incorporation of siloxane units into the backbone of aromatic polyimides imparts enhanced solubility, lower moisture adsorption, lower dielectric constant, improved toughness, and protection against atomic oxygen erosion. Mr. Connell will describe the physical and mechanical properties of these materials, as well as potential electronics and aerospace applications.

Corrosion-Protective Coatings from Electrically-Conducting Polymers
Karen Thompson, Kennedy Space Center; Brian Benicewicz and Debra Wrobleski, Los Alamos National Laboratory

Researchers are investigating the use of processible conductive organic polymers as corrosion-protective coatings on metal surfaces. Recent tests in saline and acidic oxidizing environments have demonstrated greatly improved corrosion resistance of mild steel with these coatings as compared to steel coated solely with epoxy.

(Session B5)

Medical Advances:

Computers in Medicine

Computation of Incompressible Viscous Flows through Artificial Heart Devices
Stuart Rogers and Dochan Kwak, Research Scientists, Ames Research Center

Ames researchers are applying computational fluid dynamics (CFD) techniques to simulate the blood flow through artificial hearts. Computer modeling will help pinpoint regions subject to clotting and lead to safer, more durable mechanical hearts and valves.

Computer Interfaces for the Visually Impaired
Gerry Higgins, Computer Systems Engineer, Marshall Space Flight Center

Mr. Higgins will address current research efforts to provide computer technology for people with vision-related handicaps. One such effort, the Mercator Project, looks to create a prototype system for audible access to graphics-based interfaces.

Extended Attention Span Training System
Dr. Alan Pope, Leader, Human Engineering Methods Group, Langley Research Center

A biocybernetic system developed to assess the degree to which automated flight management systems maintain pilot engagement is being adapted for treatment of youngsters with attention disorders. The Extended Attention Span Training (EAST) system increases the difficulty of a video game as the player's brain waves indicate attention is waning. The player can only succeed at the game by maintaining an adequate attention level.

Man/Machine Interaction Dynamics and Performance Analysis Capability
Harold P. Frisch, Head, Robotic Applied Research, Goddard Space Flight Center

As part of its flight telerobotics program, NASA is developing the ability to study the consequences of machine design alternatives as they relate to machine and machine operator performance. This capability will have far-reaching medical applications, such as enabling orthopedic surgeons to study the consequences of surgical options from the perspective of post-operative human performance predictions.

(Session B6)

Software Engineering

Hybrid Automated Reliability Predictor Integrated Workstation (HiREL)
Salvatore J. Bavuso, Aerospace Technologist, Langley Research Center

The HiREL system marks a major step toward producing a totally integrated CAD workstation design capability. HiREL uses a graphical input description language to increase productivity and reduce error. It enables reliability engineers to quickly analyze huge amounts of reliability/availability data to observe trends due to exploratory design changes.

Using Ada and the Rapid Development Lifecycle
Lloyd DeForrest, Technical Group Supervisor, Jet Propulsion Laboratory

Under contract to the US Army, JPL is developing a multifaceted computerized command center using an accelerated software development approach called the Rapid Development Lifecycle. Through the use of Ada and the X-Window/Motif Graphical User Interface, software developed under this program can be reused in similar projects requiring non-computer-literate users with little or no training to operate advanced command center tools and applications.

Advances in Knowledge-Based Software Engineering
Walt Truszkowski, Head, Automation Technology Section, Goddard Space Flight Center

The Knowledge-Based Software Engineering Environment (KBSEE) is designed to demonstrate that a rigorous and comprehensive software reuse methodology can enable more efficient utilization of resources in the development of large-scale software systems. Designed for use by both government and industry, KBSEE could aid in improving the reliability of future software systems.

Reducing the Complexity of Software Development through Object-Oriented Design
Mary Pat Schuler, Aerospace Technologist, Langley Research Center

Ms. Schuler will illustrate how Object-Oriented Design (OOD), coupled with formalized documentation and tailored object diagramming techniques, can simplify the software design process. The OOD methodology uses a hierarchical decomposition approach in which parent objects are decomposed into layers of lower-level child objects, with the relationships between design layers represented pictorially. This approach makes the resulting code more portable, reusable, and maintainable.

Concurrent Technical Sessions 1:00 pm—3:00 pm

(Session C1)

Data and Information Management

Techniques for Efficient Data Storage, Access, and Transfer
Robert F. Rice, Jet Propulsion Laboratory, and Warner Miller, Goddard Space Flight Center

Advanced techniques for efficient data representation have been placed in practical hardware and software form though the joint effort of three NASA centers. The techniques, which involve the use of high-speed coding and decoding modules as well as machine-transferable software routines, adapt to local statistical variations to continually provide optimum code efficiency when representing data without error.

A Vector-Product Information Retrieval System Adapted to Heterogeneous, Distributed Computing Environments
Dr. Mark E. Rorvig, Library Scientist, Johnson Space Center

The Automated Online Library Management System (AutoLib) provides a ranked list of the most likely relevant objects in collections, in response to a natural language query. AutoLib is constructed with standards and tools such as UNIX and X-Windows, which permit its use in organizations that have many different hosts, workstations, and platforms. Applications include information-intensive corporate management environments, such as finance, manufacturing, and biotechnology.

AutoClass: An Automatic Classification System
Peter Cheeseman, Research Scientist, Ames Research Center

A useful tool for exploratory data analysis, AutoClass enumerates and describes the natural classes in a data set. The program automatically determines the optimal number of classes.

Silvabase: A Flexible Data File Management System
Steven J. Lambing, Marshall Space Flight Center, and Steven T. Harris, Boeing Computer Support Services

Developed for mission planning at the Marshall Center, Silvabase enables efficient forward and backward sequential reads, random searches, and appends to large amounts of data. The system, designed to run on VAX/VMS computers, has unique features applicable to management of data involving time histories and intervals such as in operations research.

(Session C2)

Electro-Optics

Nonlinear Optical Polymers for Electro-Optic Signal Processing
Geoffrey A. Lindsay, Polymer Science Branch Head, Naval Weapons Center

Mr. Lindsay will discuss several new classes of nonlinear optical polymers for use in optical signal processing (photonics). These materials offer large electro-optics figures of merit, high temperature performance, ease of processing into films and fibers, ruggedness, and low cost. They can be applied in electro-optic switches, optical frequency doublers, sensors, spatial light modulators, and optical data storage systems.

High-Resolution Optical Data Storage on Polymers
C.M. Roland, Supervisory Chemist, Naval Research Laboratory

A new thermal method for lithography on amorphous polymer films yields remarkably high resolution images with excellent edge acuity. Images imparted to the films can be made electrically conductive via a single-step process, without using extraneous reagents.

Laser Discrimination by Stimulated Emission of a Phosphor
Dr. V.K. Mathur, Research Physicist, Naval Surface Warfare Center

Dr. Mathur will describe a new method for discriminating near infrared and far infrared laser light sources, based on the use of a magnesium sulfide phosphor which is thermally/optically stimulated to generate a color correlatable to the incident laser radiation. The technology offers potential for discrimination between even smaller bandwidths within the infrared spectrum—a possible aid to communication or wavemixing devices that need to rapidly identify and process optical signals.

Pulsed Laser Prelasing Detection Circuit
George Eugene Lockard, Engineering Technician, Langley Research Center

Langley researchers have developed a circuit to detect prelasing—the premature leakage of energy from a laser rod—in pulsed laser systems. The circuit, which is small, economical, and easily incorporated into virtually any pulsed laser system, shuts off the laser before the prelasing energy can cause costly optical damage.

(Session C3)

Life Sciences

Application of CELSS Technology to Controlled Environment Agriculture
Dr. Maynard E Bates, Bionetics Corporation, and Dr. David L. Bubenheim, Ames Research Center

Controlled Ecological Life Support Systems (CELSS) expand the concept of Controlled Environment Agriculture (CEA)—the use of environment manipulation for the commercial production of organisms—to create miniature ecosystems in which food, oxygen, and water in closed habitats are provided by regeneration of waste streams through systems containing microorganisms, plants, and animals. The development of CELSS will provide information needed to improve the efficiency, reliability, and cost-effectiveness of CEA, while reducing its environmental impact to negligible levels.

Advanced Forms of Spectrometry for Space and Commercial Application
Dr. Kenneth J. Schlager, Chief Technical Officer, Biotronics Technologies Inc.

Biotronics has discovered wide commercial application for two spectrometric technologies developed under the Kennedy Space Center's sponsorship. Ultraviolet absorption spectrometry, originally investigated for on-line measurement of hydroponic plant nutrient solutions, is finding utility in a new line of ultraviolet process analyzers for the water treatment market. A second technology, liquid atomic emission spectrometry, holds even greater commercial promise, representing the first application of atomic emission to direct on-line measurements of liquids.

Ion-Selective Electrode for Ionic Calcium Measurements
John W. Hines and Sara Arnaud, Research Scientists, Ames Research Center

NASA has developed a coated wire ion-selective electrode that noninvasively measures ionic calcium. It can be used to monitor bone calcium changes during extended exposure to microgravity or during prolonged hospital or fracture immobilization, and to conduct osteoporosis research.

A 99% Purity Molecular Sieve Oxygen Generator

Major George W. Miller, Research Chemical Engineer, Air Force Systems Command

A molecular sieve oxygen generator employing a new pressure swing adsorption process produces oxygen concentrations of up to 99.7% directly from air, exceeding the present oxygen purity limitations of 93-95%. The device may find use in aircraft and medical breathing systems, and industrial air separation systems.

(Session C4)

Materials Science

Advanced Composite Materials and Processes

Robert M. Baucom, Group Leader, Composite Materials, Langley Research Center

Mr. Baucom will report on techniques for combining high-performance graphite fibers and resin matrix systems into composite prepregs, innovative tooling concepts, and fabrication procedures for complex structures. The plastics and aerospace industries could benefit greatly by adopting these materials and processing procedures.

RTM: Cost-Effective Processing of Composite Structures

Greg Hasko and H. Benson Dexter, Materials Research Engineers, Langley Research Center

Resin transfer molding (RTM), a method of making high-strength, lightweight composite structures, is used extensively in the automotive, recreation, and aerospace industries. The presenters will compare the material requirements of various industries, methods of orienting and distributing fibers, mold configurations, and processing and material parameters such as resin viscosity, preform compaction, and permeability.

A Low-Cost Method of Testing Compression-After-Impact Strength of Composite Laminates

Alan Nettles, Marshall Space Flight Center

Marshall researchers have developed a new method to test the compression strength of composite laminate specimens as thin as .04 inches and up to 3 inches wide. This method is easier and less costly than the current compression-after-impact standard, and yields more meaningful results.

Resonant Acoustic Determination of Complex Elastic Moduli

Steven L. Garrett, Professor of Physics, and David A. Brown, Electronics Engineer, Naval Postgraduate School

The presenters will describe a new technique for measuring and tracking the complex shear and Young's moduli of nonmagnetic samples using the resonance frequency of an unconstrained bar sample. The same inexpensive electrodynamic transducers are used to excite and detect the sample's longitudinal, flexural, and torsional resonances. Sample data for composites, metals, plastics, and viscoelastic materials will be presented.

(Session C5)

Robotics

A Unique Cable Robot for Space and Earth

James Kerley, Design Engineer, Goddard Space Flight Center

A novel cable robot bends like a worm, moving up and down, back and forth, and even upside down. With magnets on its feet, the robot can climb or adhere to tall structures. It can be used to clean or paint towers, tanks, bridges, and ships, and, with an attached video camera, to inspect structures for damage or rust.

A Lightweight, High-Strength Dexterous Manipulator Arm

Neville I. Marzwell, Jet Propulsion Laboratory; Bruce M. Schena and Steve M. Cohan, Odetics Inc.

The presenters will describe the design and features of a lightweight, high-strength, modular manipulator arm developed for space and commercial applications. Fully operational in 1 g, the arm has seven degrees of freedom, a reach of 55 inches, and can lift 50 pounds. Bilateral teleoperator control can be added to the current robotically operated system.

Real-Time, Interactive Simulator System for Telepresence

Neville I. Marzwell, Jet Propulsion Laboratory; A.H. Chiu, P.G. Gottschalk, F.S. Schebor, and J.L. Turney, KMS Fusion Inc.

The Global-Local Environment Telerobotics Simulator (GLETS) immerses an operator in a real-time, interactive, visually-updated simulation of the remote telerobotic site. Stereo graphics are shown on a computer screen and fused together by the operator's special glasses to form stereoscopic views of the simulated world. The operator, interacting with the GLETS through voice and gesture commands, can form a gestalt of the virtual "local site" that matches his/her normal interactions with the real remote site.

A Hazard Control System for Robot Manipulators

Ruth Chaing Carter, FTS System Safety Manager, Goddard Space Flight Center

Ms. Carter will review system safety management and engineering techniques developed for telerobotic operations in space, focusing on a precise hazard control system for test flight of NASA's Flight Telerobotic Servicer. The same software monitoring and control approach could ensure the safe operation of a slave manipulator under teleoperated or autonomous control in undersea, nuclear, or manufacturing applications.

(Session C6)

Test and Measurement

Knowledge-Based Autonomous Test Engineer (KATE)

Dr. Carrie Belton and Barbara Brown, Computer Engineers, Kennedy Space Center

Developed for ground launch operations at the Kennedy Center, KATE employs concepts of sensor-based and model-driven monitoring and fault-location, and performs control and redundancy management of process control systems. KATE is designed as a generic, model-based expert system shell for autonomous control, monitoring, fault recognition, and diagnostics in the electrical, mechanical, and fluid system domains.

Advanced Computed Tomography Inspection System (ACTIS)

Lisa H. Hediger, Materials Engineer, Marshall Space Flight Center

ACTIS, developed at the Marshall Center to support its solid propulsion test programs, is being applied to inspection problems in the aerospace, lumber, automotive, and nuclear waste disposal industries. Ms. Hediger will discuss the unique capabilities of ACTIS and present a broad overview of computed tomography technology.

High-Resolution Ultrasonic Spectroscopy System for Nondestructive Evaluation

Dr. C.H. Chen, Information Research Laboratory Inc.

Under SBIR funding from the Army, IRL researchers are developing a high-resolution ultrasonic inspection system supported by modern signal processing, pattern recognition, and neural network technologies. This presentation will review the details of the system and its software package.

Force Limited Vibration Testing

Terry D. Scharton, Jet Propulsion Laboratory

An improved method of controlling vibration tests used to verify equipment design and manufacturing workmanship closely simulates field conditions. Offering commercial application throughout the aerospace, electronics, and automotive industries, the new test method eliminates costly failures associated with overtesting in the laboratory.

Concurrent Government-Industry Workshops 4:30 pm—6:00 pm

(Presenters to be announced)

Agencies holding workshops during this period will include:

- Department of Energy
- Department of Veterans Affairs
- Environmental Protection Agency
- National Aeronautics and Space Administration

Thursday, December 5

Concurrent Technical Sessions 8:30 am—10:30 am

(Session D1)

Advanced Manufacturing

Development of a Rotary Joint Fluid Coupling for Space Station Freedom

John A. Costulis, Technical Project Engineer, Langley Research Center

Langley researchers have developed and tested a 360-degree rotary joint fluid coupling for the Freedom station's thermal control system. The mechanism can be applied commercially to transfer fluid across rotating interfaces, such as in gun turrets, coal slurries, and farming machinery.

Spline Screw Comprehensive Fastening Strategy

John M. Vranish, Electronics Engineer, Goddard Space Flight Center

A fastener developed for assembly, maintenance, and equipment replacement operations in space also has down-to-Earth manufacturing applications. Use of the "spline screw" fastener in prime subassemblies would enable machines to disconnect and replace parts with ease, reducing product life cycle costs and enhancing the quality, timeliness, and consistency of repairs and upgrades.

Commercial Application of an Innovative Nut Design

Jay Wright, Materials Research Engineer, Johnson Space Center

A nut developed for space station use allows a fastener to be inserted or removed from either side by simply sliding the fastener in or out of the nut. Detentes on either face of the nut ensure positive engagement of the threads. The nut has applications wherever a fastener needs to be taken on and off quickly or used on a threaded part which could become so damaged that a conventional nut could not be removed.

Inflatable Traversing Probe Seal

Paul A. Trimarchi, Mechanical Engineer, Lewis Research Center

Mr. Trimarchi will describe an inflatable seal that acts as a pressure-tight zipper to provide traversing capability for instrumentation rakes and probes. The seal can replace sliding face-plate/O-ring systems in applications where lengthwise space is limited.

(Session D2)

Artificial Intelligence

CLIPS: An Expert System Building Tool

Gary Riley, Computer Engineer, Software Technology Branch, Johnson Space Center

The C Language Integrated Production System (CLIPS) provides a complete environment for the development and delivery of rule- and/or object-based expert systems. CLIPS offers a low-cost option for developing and deploying expert system applications across a wide range of hardware platforms.

Fuzzy Logic Applications to Expert Systems and Control

Dr. Robert N. Lea, Aerospace Engineer, Johnson Space Center

Commercial use of fuzzy technology in Japan and China indicate that it should be exploited by government and private industry to save energy and reduce human involvement in industrial processes. Johnson Center researchers have applied fuzzy logic in guidance control systems for space vehicles, control of data processing during rendezvous navigation, collision avoidance algorithms, and camera tracking controllers. The technology may also find use in diagnostic systems, control of robotic arms, pattern recognition, and image processing.

Neural Network Technologies

James A. Villarreal, Computer Engineer, Johnson Space Center

Mr. Villarreal will describe the Neural Execution and Training System (NETS), a software tool designed to facilitate and expedite the use of neural network technology in industry, government, and academia. Neural networks have been successfully applied to modeling and data fusion problems, robotics, structural design, speech synthesis, financial forecasting, spectrographic analysis, and many other areas. This presentation will highlight various commercial projects under development with NETS.

From Biological Neural Networks to Thinking Machines

Dr. Muriel D. Ross, Research Scientist, Ames Research Center

Dr. Ross is studying the three-dimensional organization of a simple biological neural network found in inner ear organs of balance to uncover basic principles of neural organization and function. This effort will result in new applications of biological attributes to artificial systems, and could lead to the development of highly-intelligent parallel-processing computers.

(Session D3)

Biotechnology

The Microassay on a Card—A Rugged, Portable Immunoassay

Dr. David Kidwell, Research Scientist, Naval Research Laboratory

The Microassay on a Card (MAC), a portable, handheld immunoassay, can test for a wide variety of substances in the environment. Intended for use as an on-site screen for drugs of abuse in urine or saliva, the MAC may also be applied to test for intoxication, to identify seized materials, and to test for environmental pollutants.

Flow Immunosensor for Drug Detection

Joel M. Schnur, Head, Molecular Science and Engineering Center, Naval Research Laboratory

Dr. Schnur will describe an antibody-based sensor designed to detect drugs of abuse. The biosensor is faster, less expensive, and as sensitive as any current method for cocaine detection. It can be operated outside the laboratory by personnel with no scientific training. Opportunities exist for Cooperative Research and Development Agreements.

Nucleic Acid Probes in Diagnostic Medicine

Phillip A. O'Berry, National Technology Transfer Coordinator for Animal Science, US Department of Agriculture

Mr. O'Berry will discuss the application of nucleic acid probe technology to the diagnosis of disease in humans and animals, and will present examples of commercially-promising probes.

The Rotating Spectrometer: New Biotechnology for Cell Separations

David A. Noever, Universities Space Research Association, and Helen C. Matsos, Marshall Space Flight Center

A new rotating spectrometer, able to separate previously inseparable cell cultures, is intended for use in pharmacological studies requiring fractional splitting of heterogeneous cell cultures based on cell morphology and swimming behavior. Unlike standard separation and concentrating techniques such as filtration or centrifugation, the instrument can separate motile from immotile fractions.

(Session D4)
Electronics

Method for Producing High-Quality Oxide Films on Surfaces
Mark W. Ruckman, Associate Physicist, Brookhaven National Laboratory

Mr. Ruckman will describe a new method for the reactive deposition of metal oxide and other inorganic compound thin films for use in microelectronic devices fabricated on compound semiconductors and high-temperature superconducting oxides. The technology can be integrated with ion, electron, or photon beam methods used to accelerate or selectively promote deposition and etching.

Advanced Silicon on Insulator Technology
Francis J. Kub, Senior Research Engineer, and David J. Godbey, Research Chemist, Naval Research Laboratory

Navy researchers have developed bonding, thinning, and selective etching techniques for producing ultra-thin silicon on insulator materials. These techniques can be used to fabricate silicon membranes, balometers, and other devices requiring free-standing thin-film silicon. Other applications include high-voltage/high-temperature power devices, backside-illuminated thinned CCD imagers, and x-ray masks.

High-Temperature Superconducting Stripline Filter
J.J. Bautista, Technical Group Supervisor, Jet Propulsion Laboratory

Mr. Bautista will describe the fabrication of a five-pole interdigital stripline filter made of the 93K superconductor $Y_1Ba_2Cu_3O_y$ coated on a silver substrate. The filter features a center frequency of 8.5 GHz and an extremely high rejection ratio of 80 dB.

An Adjustable rf Tuning Element for Microwave, Millimeter Wave, and Submillimeter Wave Circuits
William R. McGrath, Technical Group Leader, Jet Propulsion Laboratory; Victor Lubecke and David B. Rutledge, Dept. of Electrical Engineering, California Institute of Technology

The presenters have developed an adjustable rf tuning element consisting of a series of thin plates that can slide in unison along a coplanar strip transmission line to allow active tuning. The structure can be fabricated for frequencies as high as 1000 GHz using existing micromachining techniques. By easing constraints on circuit design, it will aid in extending microwave integrated circuit technology into the high millimeter wave and submillimeter wave bands.

(Session D5)
Materials Science

Passive Chlorophyll Detector
Leonard A. Haslim, Research Scientist, Ames Research Center

Using a low-cost, uniquely-dyed optical filter plastic sheet, the Passive Chlorophyll Detector enhances the visual discrimination of vegetation and trees in varying states of health. The invention's far-reaching applications include enabling farmers to identify and nurse or replant unhealthy sections of their fields to achieve higher crop yields, and serving as an early warning device for environmental scientists monitoring the health of forests and wetlands exposed to acid rain or contaminated groundwater.

Commercial Application of Thermal Protection System Technology
Gordon L. Dyer, Technology Transfer Officer, Martin Marietta Manned Space Systems

Thermal protection system materials and processes developed for the space shuttle's external tank have been reapplied in a new type of children's lunch box—a microwavable urethane foam insulation container that keeps a prepackaged meal warm for four to five hours. Two major food manufacturers are currently considering licensing the high-tech foam container.

Oxynitride Glass Fibers
Donald R. Messier, Research Ceramic Engineer, Materials Technology Laboratory, US Army Laboratory Command

Oxynitride glasses offer exciting opportunities for making high-modulus, high-strength glass fibers. Mr. Messier will describe processes for fabricating oxynitride glasses and fibers in compositions similar to commercial oxide glasses, but with significantly enhanced properties.

Commercial Applications of Advanced Photovoltaic Technologies
R.D. McConnell, Technology Transfer Manager, Solar Energy Research Institute

Mr. McConnell will describe research into high-tech photovoltaic materials including III-V, II-VI, amorphous silicon, and crystalline silicon, and will highlight possible spinoff applications such as optoelectronics and space power systems.

(Session D6)
Software Engineering

Software Reengineering
Ernest M. Fridge, Deputy Chief, Software Technology Branch, Johnson Space Center

During space shuttle development, Johnson Center engineers created a set of tools to develop and maintain FORTRAN and C code. This tool set forms the basis for an integrated environment to reengineer existing code into modern software engineering structures which are easier and less costly to maintain and which allow straightforward translation into other target languages.

COSTMODL: An Automated Software Development Cost Estimation Tool
George B. Roush, Software Engineer, Johnson Space Center

One of the most widely used software cost estimation tools, COSTMODL can help reduce the risk of cost overruns and failed projects. COSTMODL has an intuitive user interface and extensive on-line help system, and can be customized to a particular user environment. It can be used for in-house cost management, cost analysis consulting, or for research.

Increasing Productivity through Total Reuse Management
Mary Pat Schuler, Aerospace Technologist, Langley Research Center

NASA Langley is promoting total reuse management (TRM) as a way to lower software development costs, reduce risk, and increase code reliability. Ms. Schuler will describe methods used to adopt TRM, and will discuss the reuse of products from all phases of the software life cycle.

How Hypermedia Can Increase the Productivity of Software Development Teams
L. Stephen Coles, Group Chief Technologist, Institutional Data Systems, Jet Propulsion Laboratory

Mr. Coles will describe how the productivity of software developers can be dramatically improved through the use of hypermedia, the seamless integration of disparate data structures—including text, graphics, animation, voice, and full-motion video—in a graphical user interface. The presentation will cover basic machine architecture, special-purpose video boards, video equipment, optical memory, software for animation, voice I/O, and networking and integration issues.

Concurrent Technical Sessions 1:00 pm—3:00 pm

(Session E1)
Advanced Manufacturing

Intelligent Robotic System with Dual-Arm Dexterous Coordination and Real-Time Vision
Neville I. Marzwell, Jet Propulsion Laboratory, and Alexander Chen, Scientific Research Associates

The presenters will demonstrate a prototype robot with built-in intelligence. It features 18 degrees of freedom, comprised of two articulated arms, a movable robot head, two CCD cameras for producing stereoscopic views, an articulated cylindrical lower body, and an optional mobile base. The robotic system addresses a broad spectrum of manufacturing demands, including both complex and labor-intensive jobs.

Neural Network Software for Distortion-Invariant Object Recognition
Max B. Reid and Lilly Spirkovska, Research Scientists, Ames Research Center

Ames has created neural network software that performs the complete feature extraction/pattern classification paradigm required for automatic pattern recognition. The software is being used in an autonomous robotic vision system which could have extensive application in robotic manufacturing.

Constraint-Based Scheduling
Monte Zweben, Assistant Chief, Artificial Intelligence Research Branch, Ames Research Center

Mr. Zweben will describe the Space Shuttle Ground Processing Scheduling system, which uses artificial intelligence search methods to solve large-scale scheduling problems. The system can be applied to a variety of scheduling problems. In the manufacturing domain, it can help to minimize set-up time or tardiness.

COMPASS: A General-Purpose Computer-Aided Scheduling Tool
Dr. Barry R. Fox, Project Leader, McDonnell Douglas Space Services Co; and Christopher Culbert, Technical Monitor, Software Technology Branch, Johnson Space Center

COMPASS is an powerful, interactive planning and scheduling system with a mouse-driven, X-Windows user interface. It can be used to manage activities subject to timing constraints, ordering constraints, Boolean conditions, and resource availability, and to manage a wide range of resources including tools, electricity, and water.

(Session E2)

Data and Information Management

ELAS: Powerful General-Purpose Image Processing Software
David Walters, Electronics Engineer, Information Systems Division, Stennis Space Center

Originally developed to process Landsat images, the ELAS software package has evolved to handle a vast range of data types including MRI, soil maps, topographic and rainfall data, and sonar images. Mr. Walters will describe applications in such fields as agriculture, forestry, and geology, and will highlight important new enhancements to the software.

TAE Plus: A NASA Tool for Building and Managing Graphical User Interfaces
Martha R. Szczur, TAE Project Manager, Goddard Space Flight Center

Transportable Applications Environment Plus is a WYSIWYG tool for designing, building, and tailoring an application's graphical user interface. Its main component is the WorkBench, which allows the application developer (who need not be a programmer) to interactively construct an application screen's layout and manipulate graphical objects such as menus, buttons, icons, and dials. TAE Plus is used in such disciplines as image processing, simulation, network management, real-time command and control, database management, and office automation.

Instrumentation, Performance Visualization, and Debugging Tools for Multiprocessors
Jerry C. Yan and Charles E. Fineman, Sterling Federal Systems; Philip J. Hontalas, Ames Research Center

As part of a major effort to advance multiprocessor parallel computing performance, NASA Ames is developing techniques to efficiently monitor and visualize parallel program execution. Such techniques will help simplify the debugging and tuning of parallel programs. The presenters will describe various prototype software tools and their incorporation into the run-time environments of hardware testbeds.

The Data Egg: One-Handed Text Entry Without Positional Constraints
Gary L. Friedman, Technical Group Leader, Jet Propulsion Laboratory

JPL researchers have devised a small, handheld unit that allows text entry with only one hand. Dubbed the Data Egg, it can be operated in any position, either autonomously or tethered to a personal computer. This invention will benefit the handicapped and those normally barred from using a computer on the job, such as astronauts and journalists.

(Session E3)

Electronics

Thermoacoustic Refrigeration
Steven L. Garrett and Thomas Hofler, Naval Postgraduate School

The presenters will demonstrate the first practical, autonomous thermoacoustic refrigerator, which employs high-amplitude sound in inert gas to pump heat. Scheduled for flight on the space shuttle, the acoustically-resonant refrigerator has only one moving part, no sliding seals, and uses inexpensive components. Since thermoacoustic refrigerators use no CFCs and have coefficients of performance comparable with vapor compression cycle refrigerators, they are good candidates for food refrigeration and commercial/residential air conditioning applications.

Ambient Temperature Recorder
Larry D. Russell, Electronics Engineer, Ames Research Center

The ATR-4 ambient temperature recorder is a small battery-powered device that records 32 kilobytes of temperature data from four channels, over a range of -40° to +60°C at sampling intervals from 1.88 to 15 minutes. Data is stored in its internal memory for subsequent readout by a personal computer. Developed for use on the space shuttle, the ATR-4 can answer a variety of needs for a small, remote, unattended temperature recorder, such as in transportation of perishables and recording life system or process temperatures over time.

Fiber-Optic Push-Pull Sensor Systems
Steven L. Garrett and David A. Brown, Naval Postgraduate School

The Navy has created fiber optic "push-pull" sensors that greatly enhance the optical fiber's response to the measurand of interest while providing common-mode rejection of spurious environmental effects such as pressure or temperature changes. The presenters will describe several new fiber optic, interferometric accelerometers and acoustic pressure sensors which generate such large optical phase modulations that their signals can be demodulated with inexpensive lasers similar to those used in CD players.

Commercial Capaciflector
John M. Vranish, Electronics Engineer, Goddard Space Flight Center

Goddard researchers are developing a capacitative proximity/tactile sensor with unique performance capabilities for use on space robots and payloads. The simple, robust sensor will enable robots to avoid collisions with humans in orbit and to dock payloads in a cluttered environment. Mr. Vranish will report on NASA's efforts to "spin" this technology off into the private sector.

(Session E4)

Environmental Technology

Water Quality Monitor
Warren C. Kelliher, Langley Research Center

A portable x-ray fluorescence spectrometer developed for the Viking mission to Mars has been adapted for terrestrial use. Called EMPAX (Environment Monitoring with Portable Analysis of X-ray), the unit answers a critical need for on-site, real-time analysis of toxic metal contamination. The government is seeking a commercial manufacturer for EMPAX.

Remote Semi-Continuous Flowrate Logging Seepage Meter
William M. Reay, Virginia Polytechnic Institute and State University, and Harry Walthall, Langley Research Center

The presenters have created a remote semi-continuous flowrate logging seepage meter that enables direct assessment of ground water discharge and associated solute fluxes. It is designed to replace current manually-operated meters.

Calcification Prevention Tablets
G.A. Lindsay, Naval Weapons Center

The subject invention is a slow-release tablet for preventing or removing calcium crust and build-up in pipes and containers that process hard water and other calcium-containing fluids. Extremely effective in sea water, the tablet is biodegradable and nontoxic. It can be used in urinals, commodes, drain., and holding tanks.

Automated Carbon Dioxide Cleaning System
David T. Hoppe, Marshall Space Flight Center

An environmentally-safe cleaning system jointly developed by NASA, the Air Force, and Martin Marietta uses solidified carbon dioxide pellets to blast the surface to be cleaned. The process can be automated using a programmable robot. Results from cleaning a variety of substrate materials has shown the system to be capable of reducing the amount of chlorofluorocarbon-based cleaning fluids and in some cases totally eliminating their use.

(Session E5)
Materials Science

Applications of Biologically-Derived Microstructures
Joel M. Schnur, Head, Molecular Science and Engineering Center, Naval Research Laboratory

Navy scientists have fabricated hollow 0.5 micron diameter cylindrical-shaped microstructures using modified lipids and the self-assembly provided by nature. Potential applications for the microstructures include controlled release of biocide for antifouling paint, composites for electronic and magnetic uses, and high-power microwave cathodes.

Structural Modification of Polysaccharides: A Biochemical/Genetic Approach
Roger Kern and Gene Peterson, Space Biological Sciences Group, Jet Propulsion Laboratory

This presentation will describe the development of unique biological techniques for adapting polysaccharides for use in electronic and optical devices. The ability to manipulate polysaccharides genetically and chemically will have an immediate impact on current commercial applications based on rheological properties, such as materials coatings, pharmaceutical delivery systems, and food additives.

Cryogenic Focusing, Ohmically Heated On-Column Trap
Stephen R. Springston, Department of Applied Science, Brookhaven National Laboratory

Mr. Springston will present a new method for thermally desorbing volatile solutes that have been cryogenically trapped within a capillary. Advantages of this trap for gas chromatographic analyses include fast response, simplicity, and elimination of connections. Other applications include physico-chemical studies, sample modulation chromatography, and restrictors for supercritical fluid chromatography.

Study of the Effect of Hydrocarbon Contamination on PFTE Exposed to Atomic Oxygen
Morton A. Golub and Theodore Wydeven, Research Scientists, Ames Research Center

As part of an effort to improve the surface properties of PFTE (commonly known as Teflon™), Ames researchers are using x-ray photoelectron spectroscopy analysis to study the effect of hydrocarbon contamination on PFTE exposed to an oxygen plasma. Their work will lead to the development of better surface-modified PFTE products for the medical and industrial markets.

(Session E6)
Medical Advances

Applications of the Strategic Defense Initiative's Compact Accelerator Technology
Nick Montanarelli, Deputy Direct, Office of Technology Applications, Strategic Defense Initiative Organization

The Strategic Defense Initiative's investment in particle accelerator technology for its energy weapons program has produced small and powerful accelerations with a variety of "spinoff" medical applications. These include a radio frequency quadropole linear accelerator for a cancer therapy unit, a compact induction linear accelerator to sterilize medical products, and accelerators to produce the radioactive isotopes used as radiopharmaceuticals for positron emission tomography.

Acoustically-Based Fetal Heart Rate Monitor
Allan J. Zuckerwar, Langley Research Center, and Dr. Donald A Baker, Baker Guardian Medical Labs

A new fetal heart rate monitor, using piezopolymer pressure sensors on a belt worn by the mother, can identify the fetal heart tone from among competing background signals and, through signal processing, yield a real-time evaluation of the fetal heart rate. The monitor is inexpensive and lends itself to an ambulatory mode of operation, whereby the mother can conduct fetal non-stress tests in her home.

Surgical Force Detection Probe
Ping Tcheng, Charles Scott, and Paul Roberts, Research Engineers, Langley Research Center

A precision electromechanical instrument detects and documents the forces and moment applied to human tissue during surgery. The pen-shaped probe measures just 6 inches long and features a tip with an interchangeable scalpel. A PC-based data system provides signal conditioning, data acquisition, and graphics display.

Correcting Night Myopia with Biofeedback and a Simple Pocket Optometer
Dr. William B. Cushman, Research Physiologist, Naval Aerospace Medical Research Laboratory

Navy researchers are using a pocket optometer to implement biofeedback training to correct night myopia. Although developed to improve pilots' night vision, the lightweight, handheld optometer could benefit others, including children with "student myopia."

Concurrent Government-Industry Workshops 4:30 pm—6:00 pm

(Presenters to be announced)
Agencies holding workshops during this period will include:
- Department of Defense
- Department of Health and Human Services
- Department of Veterans Affairs
- National Aeronautics and Space Administration

SEE NEXT PAGE FOR REGISTRATION INFORMATION

Reserve Your Place At Technology 2001 Today

Save time and money: Preregister for Technology 2001 using the convenient form below. Mail the completed form with check payable to the Technology Utilization Foundation, or fax it with credit card information to (212) 986-7864 (VISA and Mastercard accepted). To register by phone, call (212) 490-3999. Government organizations may register using a purchase order. **Deadline for preregistration is November 8.**

Choose from four types of registrations:

- Complete Registration—includes technical sessions, workshops, and exhibits for all three show days; tickets to the opening reception on Monday, Dec. 2 and the Technology Transfer Awards Dinner on Wednesday, Dec. 4; and a copy of the Technology 2001 proceedings.
- Symposia/Exhibits Registration—covers technical sessions, workshops, and exhibits for all three days.
- One-Day Symposia/Exhibits Registration
- One-Day Exhibits Only Registration

	By 11/8	On-Site
Complete Registration	$300	$325
Symposia/Exhibits Reg.	$200	$225
One-Day Symposia/Exhibits Reg.	$100	$125
One-Day Exhibits Only Reg.	$25	$30

Federal government employees are entitled to a 50 percent discount on above prices. Discounts are also available to groups of ten or more; call (212) 490-3999 for details.

Tickets to the Technology Transfer Awards Dinner may be purchased separately for $150 each using the preregistration form or by calling (212) 966-3100. Preregistrants can pick up their badges and reception/dinner tickets at the San Jose Convention Center, 150 West San Carlos St., during the hours listed below. Registration confirmations will be sent via mail.

On-Site Registration Hours

Monday, December 2	8:00 am - 5:00 pm
Tuesday, December 3	7:00 am - 4:00 pm
Wednesday, December 4	7:00 am - 4:00 pm
Thursday, December 5	7:00 am - 3:00 pm

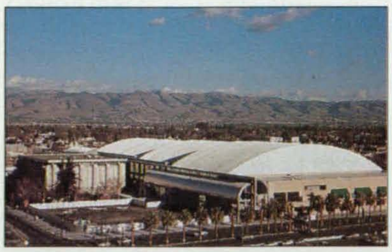

The new San Jose Convention Center is situated in the heart of Silicon Valley.

Special Hotel Rates

Hotel space is limited, so act early to secure these special conference rates:

	Single	Double
Fairmont Hotel (headquarters hotel) (800) 527-4727	$105	$105
Hyatt San Jose (408) 993-1234	$85	$105
Red Lion (408) 453-4000	$80	$80
Hotel De Anza (800) 843-3700	$115	$130

The Fairmont and Hotel De Anza are within walking distance of the Convention Center; the Hyatt and Red Lion are approx. ten minutes away by Light Rail—San Jose's modern, efficient public transit system. When making reservations, you must mention Technology 2001 to obtain the special rates.

Transportation Discounts

Ground: Hertz Corp. is offering special discounted car rental rates with unlimited mileage. For reservations, call Hertz Meeting Services at (800) 654-2240 and identify yourself as an attendee of Technology 2001, meeting #9208.

Air: Discounted air fares are available to Technology 2001 attendees through American Airlines. Call American Airlines' Meeting Service Desk at (800) 433-1790 and ask them to display Star File #S01N1BG. Make reservations as the lowest applicable fare from your departure city and give your mailing address. Nepal Travel Bureau—the official travel agency for Technology 2001—will mail you the tickets. For follow-up inquiries about your tickets, call Nepal Travel at (800) 666-4519.

An Ideal Location

The Convention Center is located just three miles from San Jose International Airport, and offers plenty of indoor parking. At the heart of the downtown cultural center, the Convention Center is within easy walking distance of restaurants, shops, and entertainment. For information on cultural activities, attractions, and tours, call the San Jose Convention and Visitors Bureau at (408) 295-9600.

Questions? Call Joseph Pramberger or Justina Cardillo at (212) 490-3999.

Technology 2001 Preregistration Form

Use a separate form or photocopy for each registrant. Type or print clearly.

Name ____________________

Title ____________________

Company ____________________

Address ____________________

City/St/Zip ____________________

Phone ____________________

❐ check enclosed charge my: ❐ VISA ❐ Mastercard

Account No.____________________

Expiration: Mo.______ Yr.______

Signature____________________

Registration Fees:

Complete Registration	$300	$ _____
Symposia/Exhibits Reg.	$200	$ _____
One-Day Symposia/Exhibits *(circle day: Tues. Wed. Thurs.)*	$100	$ _____
One-Day Exhibits Only *(circle day: Tues. Wed. Thurs.)*	$25	$ _____
Awards Dinner Only	$150	$ _____
Total: (Fed. govt. employees deduct 50%)		$ _____

Registrations and awards dinner reservations are transferable, and may be cancelled until Nov. 8, 1991 subject to a $50 cancellation fee. After that date no cancellations will be accepted and no money refunded.

Return with payment to: Technology Utilization Foundation, 41 East 42nd St., Suite 921, New York, NY 10017

Physical Sciences

Mathematical Model for Deposition of Soot

This model is expected to be more generally applicable than prior experimental correlations have been.

Marshall Space Flight Center, Alabama

A semiempirical mathematical model predicts the deposition of soot in a tubular gas generator in which hydrocarbon fuel is burned in a very-fuel-rich mixture (equivalence ratio of the order of 10) with pure oxygen. The model was developed in response to concern over the deposition of soot in the gas generators and turbomachinery of rocket engines. The model may also be of interest in terrestrial applications that involve fuel-rich combustion or analogous processes; e.g., the purposeful deposition of soot to manufacture carbon black pigments.

Previously, the deposition of soot in rocket gas generators was studied by making crude empirical correlations between measurements of differential pressures and inferred measurements of soot. In contrast, this model is based on the physics of aerosols and is meant to be calibrated by correlation with direct measurements of the formation and deposition of soot, including measurements of the scattering of laser light from soot and laser measurements of flow fields. Once so calibrated, the model is expected to be generally applicable to gas generators of various configurations.

The principal mechanisms in the model are (1) inception of the solid soot particles from gaseous products of combustion, (2) the increase in the sizes and masses of soot particles that results from surface reactions with gas-phase hydrocarbons, and (3) deposition via thermophoresis (the transfer of mass down a gradient of temperature). The first and most important equation of the model is the one that accounts for the volume fraction of soot (the volume of soot per unit volume of flow) as a function of time. The right side of this equation consists of a term that accounts for inception and a term that accounts for growth. This equation can be used to calculate the volume fraction of soot as a function of position along the axis of a gas generator by assuming that the flow is one-dimensional and converting the time variable to the equivalent axial position.

The two critical variables in the equation are the rate of inception of particles (which is a function of injector mixing) and the rate of growth of soot on the surfaces of the particles. These variables were chosen because they can be quantified empirically via laser measurements of the soot and flow field.

The second major equation of the model is the one that accounts for the gross deposition of soot particles from the flow onto the wall. This equation uses well-defined correlations among local coefficients for the transfer of heat and mass to determine the local coefficients for the deposition of soot. One factor in this equation is the volume fraction of soot calculated in the first equation. The coefficient for the transfer of mass in the deposition of soot is found by using the conventional analogy between the transfers of heat and mass and accounting for thermophoresis. The thermophoretic influence on deposition is characterized by the ratio between the temperature of the wall and the temperature of the free-stream part of the flow.

The amount of soot ultimately deposited on the wall is calculated as the difference between the gross amount deposited (calculated as described above) and the amount of previously deposited soot that is sheared off the wall by the flow. The equation for the fraction sheared off is based on a semiempirical soot-layer-adhesion-strength criterion that has been found to be accurate in studies of the adhesion of dust and includes an assumed log-normal distribution of the force required to remove a particle of soot from the surface. The force that causes the removal of soot is assumed to correspond to the wall shear stress.

This work was done by Darby B. Makel of Aerojet TechSystems for **Marshall Space Flight Center**. *For further information, Circle 145 on the TSP Request Card.*

Inquiries concerning rights for the commercial use of this invention should be addressed to the Patent Counsel, Marshall Space Flight Center [see page 14]. Refer to MFS-28506.

Improved Gas-Gap Heat Switch

Residual conductance in the "off" state is reduced.

NASA's Jet Propulsion Laboratory, Pasadena, California

Four modifications in the design of a gas-gap heat switch decrease its residual thermal conductance in the "off" state, thereby making it act more nearly like a true on/off switch. Gas-gap heat switches are used in cryogenic systems; for example, to connect and disconnect redundant coolers with a single load. Gas-gap heat switches have no moving parts and, therefore, offer reliability and long operating life.

In a gas-gap heat switch of the type described here (see figure), the gap is the space between interdigitating fins and slots machined into lengthwise-mating copper cylinders. The copper cylinders are sealed in a supporting stainless-steel tube, and the gap is made much less thermally conductive (the switch is turned "off") by evacuating it. The gap is made more thermally conductive (the switch is turned "on") by filling the evacuated gap with neon, nitrogen, hydrogen, helium, or other suitable gas from a gas-adsorption pump. The gas-adsorption pump could be, for example, a bed of charcoal that is heated to fill, and cooled to evacuate, the gap.

In many actual and potential applications, the "hot" side of the heat switch can be considerably hotter (e.g., at 300 K) than the cold side is (e.g., at 80 K). At such large differences in temperature, the residual conductance in the "off" state caused by parasitic radiation across the gap and conductance in the supporting cylinder can result in unacceptably high transfer of heat across the nominally "off" switch. In addition, differences among the thermal expansions of the hot and cold copper cylinders and the stainless-steel supporting cylinder can result in contact between the tips of fins and the bottoms of slots, with

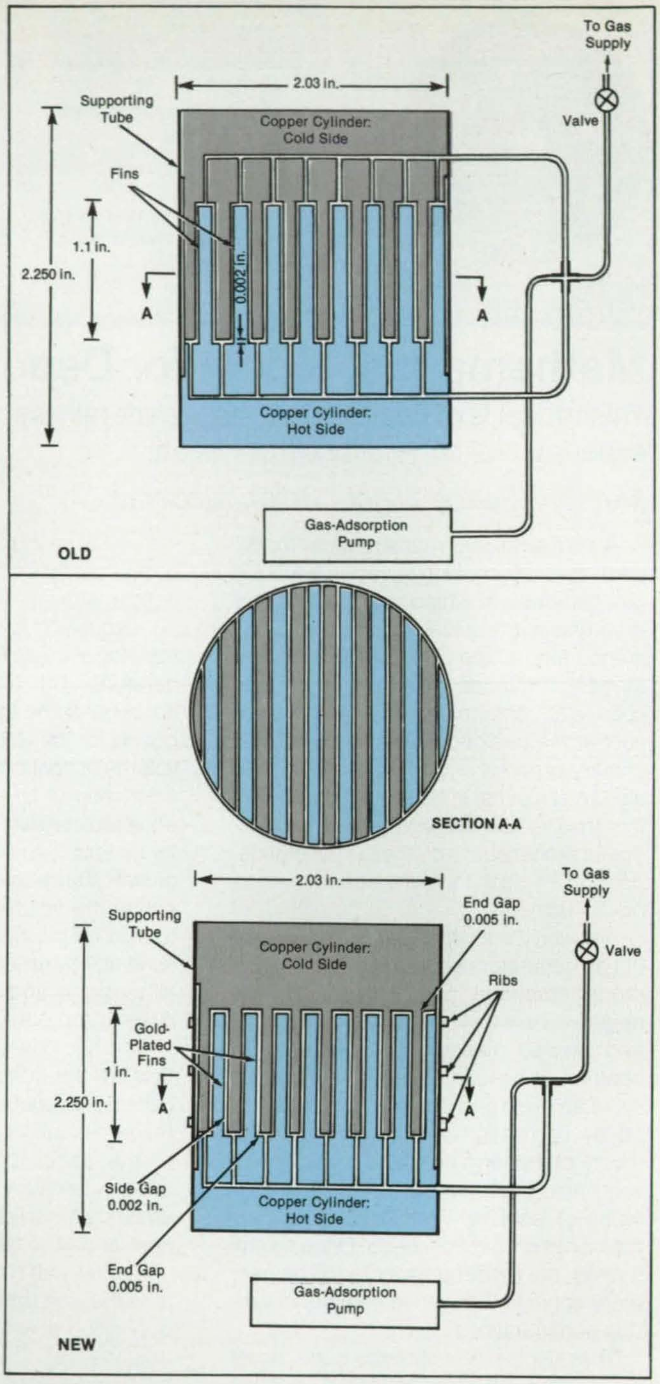

The **Old and New Versions** of the gas-gap heat switch differ in the surface finish of the fins, the thickness of the stainless steel supporting cylinder, the size of the gaps at the ends of the fins, and the plumbing for the gas.

a consequent large increase in thermal conduction.

The four modifications reduce these undesired contributions to the "off"-state conduction. They are as follows:

1. Whereas previously the fins were made by electrical-discharge machining, in the improved version they were made by a carbide circular saw, then lapped by hand to the precise 0.002 in. (0.05 mm) gap dimension, then polished by hand, then electroplated with low-emissivity gold to reduce the radiative transfer of heat from the hot side to the cold side.
2. To reduce parasitic conductance along the supporting stainless-steel tube, the thickness of the wall of this tube was reduced from 0.004 in. (0.1 mm) to 0.002 in. (0.05 mm). Three circumferential stiffening ribs were added to prevent collapse under high differential pressures.

3. To prevent contact caused by differential thermal expansion, the clearance between the tips of the fins and the bottoms of the slots was increased from the previous value of 0.002 in. (0.05 mm) to 0.005 in. (0.13 mm).
4. Whereas the gas flowed in and out through passages in both the hot and cold sides in the previous version, the modified version includes passages on the hot side only. This feature both minimizes the parasitic transfer of heat through the gas and simplifies construction.

This work was done by Chung K. Chan of Caltech for **NASA's Jet Propulsion Laboratory.** *For further information, Circle 125 on the TSP Request Card. NPO-18136*

Compact Apparatus for Growth of Protein Crystals

Growth can be initiated and terminated automatically.

Marshall Space Flight Center, Alabama

A compact apparatus proposed specifically for the growth of protein crystals in microgravity could also be used in terrestrial laboratories in which it is desired to initiate and terminate growth at prescribed times automatically. The apparatus would have few moving parts. It would also contain no syringes, which are difficult to clean, load, and unload and which can introduce contaminant silicone grease into the crystallization solution. After the growth of the crystals was terminated, the specimens could be retrieved and transported simply.

The apparatus (see figure) would be a 12- by 8- by 2-cm transparent, polycarbonate tray assembly that would contain 24 crystal-growth chambers, each 15 mm in diameter and 16 mm deep. Centered within each chamber would be a movable pedestal (piston), a guide sleeve, and an O-ring seal. At the tip of each pedestal (piston), there would be a depression, 3 mm deep and 5 mm in diameter, that would serve as a crystal-growth compartment. Each such depression could contain up to 0.1 mL of the protein/precipitant mixture.

The sleeves and O-rings would allow the pedestals to move vertically approximately 3 mm while maintaining the seals among the chambers. The 4-mm annulus formed by the walls of the chambers and the pedestal would serve as the reservoir for the precipitant solution. A doughnut-shaped wick of high-molecular-weight polyethylene or other porous material would fit into the annulus to contain the precipitant solution and to provide adequate surface area for the vapor-equilibration crystal-growth process to occur.

Under normal conditions, a protein/precipitant solution would be placed in the crystal-growth compartment in each pedestal while the precipitant solution was added to the annulus containing the porous wick. The solutions in the tray assembly would then rapidly be frozen to a temperature of −150 °C or lower and remain frozen until the experiment was activated. Upon activation, the solutions would be allowed to thaw — initiating the growth process — and then maintained at a constant temperature.

To terminate growth, a ganging mechanism under the tray would simultaneously seal the 24 crystal-growth compartments by pushing the pedestals in them up against a 12- by 8-cm strip of polypropylene tape supported under a 12- by 8- by 2-cm polycarbonate tray cover. The cover would provide additional containment for the experiment and reinforce the tape. The specimen in each chamber could be removed by simply cutting through the tape seal over the desired chamber and removing the crystals, leaving the other experiments undisturbed.

In cases in which freezing would negatively affect crystallization, the tray cover could be modified to provide an O-ring seal for each crystal-growth compartment. In this configuration, growth would be initiated when the ganging mechanism moved the pedestals away from the cover, thus allowing communication between the crystal-growth compartments and the precipitants. Growth would be terminated by using the ganging mechanism to move the pedestals back into the original sealed position. In a variant of this concept, tape would be used to seal the crystal-growth compartments both before activation and at the time of termination of growth.

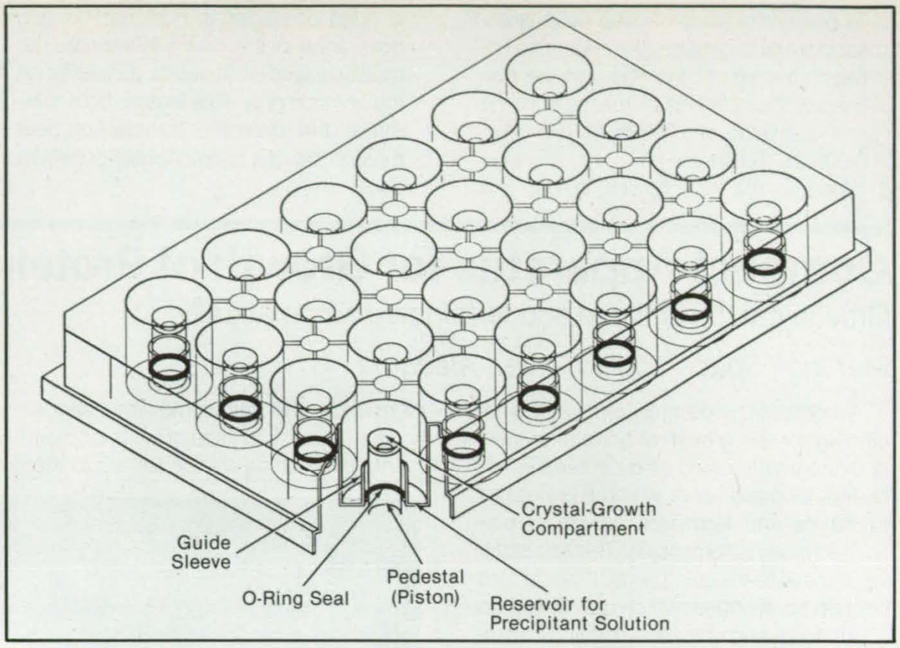

This **Compact Vapor-Diffusion Apparatus** for the growth of protein crystals would enable experimenters to initiate and terminate growth by remote or automatic control at prescribed times.

This work was done by Daniel C. Carter and Teresa Y. Miller of **Marshall Space Flight Center**. *For further information, Circle 152 on the TSP Request Card.*

Inquiries concerning rights for the commercial use of this invention should be addressed to the Patent Counsel, Marshall Space Flight Center [see page 14]. Refer to MFS-28507.

Scanning X-Ray or Extreme-Ultraviolet Monochromator

The angle of incidence would be varied to change the wavelength of Bragg reflection.

Marshall Space Flight Center, Alabama

The wavelength of peak transmission of a proposed high-throughput, narrow-band-pass x-ray or extreme-ultraviolet monochromator would be continuously adjustable. The essential filtering and reflecting components of the monochromator would be designed according to the principles described in the preceding article, "Compact X-Ray and Extreme-Ultraviolet Monochromator" (MFS-28499). However, in this case, the angle of the mirrors and, therefore, the wavelength of peak transmission (via Bragg reflection from the mirrors) would be made adjustable.

The scanning monochromator (see figure) could include one or more pairs of parallel mirrors on two or more substrates. The facing surfaces of the substrates in each pair would be coated with identical Bragg-reflecting multilayers. Each mirror would pivot about an axis parallel to its reflecting faces and would be part of a parallelogram linkage that would also include spacer bars. A motor would turn a lead screw in a threaded way on the housing of the monochromator. As the lead screw advanced, it would slide in a grooved way on one of the mirrors and would push or pull on the sides of the grooves, changing the angle of all the mirrors.

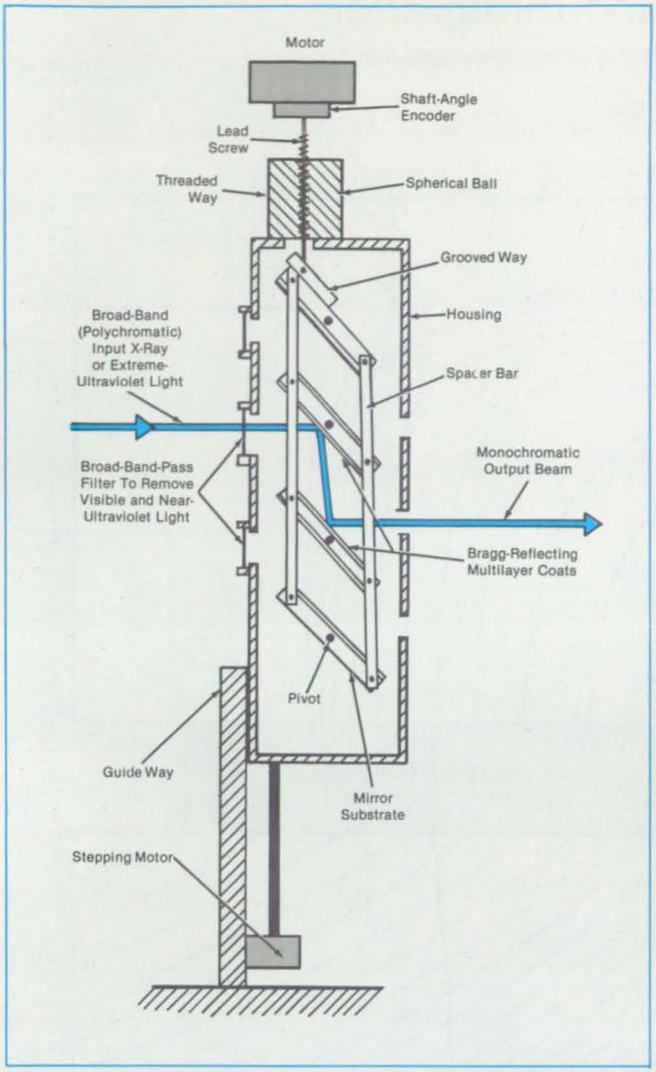

The **Scanning X-Ray or Extreme-Ultraviolet Monochromator** would feature parallel Bragg reflectors on an adjustable parallelogram linkage.

A shaft-angle encoder on the motor would send signals indicating the angle of the lead screw to monitoring and controlling equipment outside the vacuum system in which the monochromator would be operated. The external equipment would compute the angle of the mirrors and the associated peak-transmission wavelength from the encoder outputs and would use these computed values as feedback control signals during a wavelength scan.

Preferably, the mirrors would be scanned through the range of grazing-incidence angles from 30° to 60°, thereby scanning from the shortest wavelength to $\sqrt{3}$ times the shortest wavelength in the range. Because each facing pair of mirror surface could be coated with a different Bragg-reflecting multilayer, each pair of mirrors could cover a different range of wavelengths. The wavelength range would be selected by using a stepping motor to move the monochromator housing vertically along a guideway to the position in which the pair of mirrors for that range would be exposed to the input beam.

This work was done by Richard Hoover of **Marshall Space Flight Center.** *For further information, Circle 139 on the TSP Request Card.*

Inquiries concerning rights for the commercial use of this invention should be addressed to the Patent Counsel, Marshall Space Flight Center [see page 14]. Refer to MFS-28492.

Designing Accelerated Tests of Electromigration

Error analysis helps in the selection of currents, temperatures, and durations.

NASA's Jet Propulsion Laboratory, Pasadena, California

A method for the design of accelerated tests of electromigration (as in microscopic conductors in integrated circuits) is based partly on a simplified mathematical model of electromigration and partly on error analysis. As in other accelerated-aging methods, the objective is to determine quickly what the operating life of tested components would be under normal operating conditions by extrapolation from lifetime measurements at operating stresses greater than normal. The design of an accelerated test involves a compromise between (1) reducing the testing time by increasing the stresses and (2) reducing the uncertainty in the extrapolated lifetime by decreasing the stresses.

In the case of electromigration, the stresses are the applied electrical current and the temperature. The median time to failure, t, is used as the measure of operating life and is assumed to be approximated by

$$t = AI^{-n}\exp(E_a/kT)$$

where A and n are constants, I is current, E_a is an activation energy, k is Boltzmann's constant, and T is the absolute temperature. This equation is first linearized by taking the natural logarithm of both sides, then applied to tests at different currents and temperatures. A minimum of three different combinations of current and temperature are necessary for the determination of n, E_a, and the value of t extrapolated to normal operating current and temperature.

The selection of currents and temperatures for these tests is guided by linear-regression and propagation-of-errors analyses of the linearized equation. The figure illustrates such a selection based on the results of such an analysis. In the upper part of the figure, each curve is a contour of constant normalized error $\delta\ln t$ (at normal operating current and temperature)/$\delta\ln t$ (at the test current and temperature). The upper right corner of this plot represents the point of maximum stress (maximum current I_{max} and maximum temperature T_{max}), which is determined by the capabilities of the testing equipment and the boundary of the electromigration-failure regime. The contours were generated by use of the stress points labeled 1 through 4, with all contours referred to point 3.

In the lower part of the figure, each curve is a contour of constant normalized testing time, S, which is t (at the test current and voltage)/t (at I_{max} and T_{max}). These contours are computed for the stress points shown in the upper part of the figure. Once a total test time is chosen, other stress points are determined from the intersections of the constant-time and constant-error contours. These intersections can be seen by superimposing the upper and lower parts of the figure.

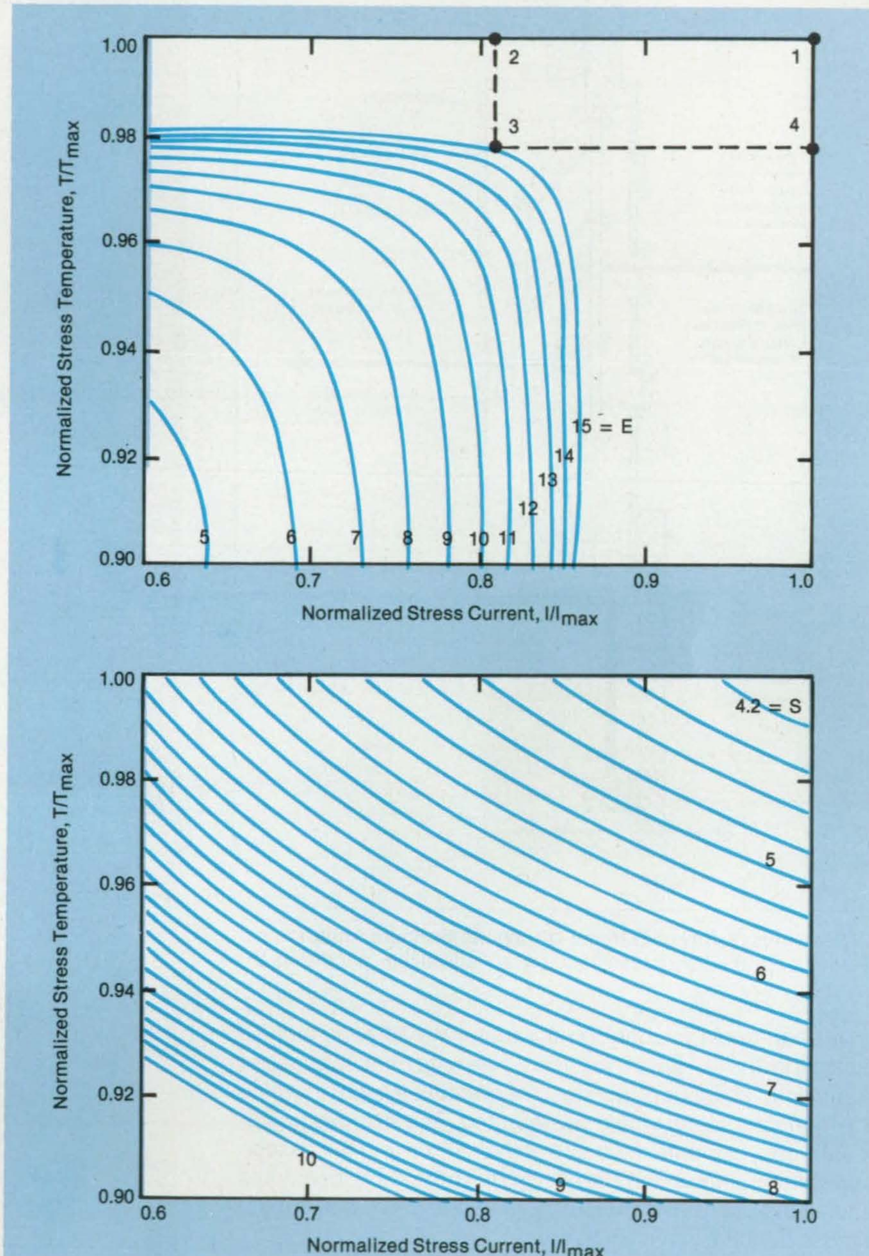

Error and Testing-Time Contours are used to select test currents and temperatures different from those represented by points 1 through 4. The contours of constant normalized error (E) were computed by using $I_{max}/I_{operating}$ = 10 and $T_{max}/T_{operating}$ = 1.25. The contours of constant normalized testing time (S) were calculated by using n = 1.5 and E_a/kT_{max} = 10.

This work was done by Martin G. Buehler of Caltech for **NASA's Jet Propulsion Laboratory**. *For further information, Circle 55 on the TSP Request Card. NPO-18012*

Modification of Catadioptric Telescope for Laser Velocimetry

A commercially available unit can be made to work well.

Ames Research Center, Moffett Field, California

Computations and an experiment have shown that a Schmidt–Cassegrain catadioptric (including both reflective and refractive optics) telescope can be modified for use in dual-beam laser Doppler velocimetry. The issues involved in the modification are not trivial, because the imaging tasks in the two applications are different. The telescope in a laser Doppler velocimeter must focus two Gaussian-profile laser beams at an intersection that defines the probe volume and collect the light backscattered from the probe volume for final focusing into a photodetector. The distance from the telescope to the probe volume is typically of the order of ten times the focal length. On the other hand, a typical commercial telescope is designed for viewing objects at a distance between 50 times the focal length and infinity and is not optimized for the simultaneous beam-focusing and backscatter-collecting functions.

The modification process for a given telescope is subject to the following issues:

1. Can good performance be obtained by simply repositioning the optical components of the catadioptric telescope?
2. What are the required modifications as a function of the f-ratio? (The f-ratio is the distance between the probe volume and the corrector plate of the telescope, divided by the diameter of that corrector plate.)
3. What is the aberration limit of the modified telescope as a function of the f-ratio?
4. What is the resulting collection solid angle as a function of f-ratio?
5. How well do the modified catadioptric optics perform in comparison to a lens of similar design?

The analytical approach taken to obtain answers to these questions emphasized the use of a simple ray-tracing computer program to analyze modified optical configurations. The ray-tracing software also incorporated a Gauss–Newton optimization algorithm, which systematically varied tagged parameters until successive iterations provided less than a 10^{-6} improvement in a target value, typically a point-focus specification. This feature was quite useful in the optimization of the collector system. The root-mean-square blur of ray bundles originating at the axis vertex in the object plane and converging to a best focus in the image plane was used as an indication of the imaging performance of the optical system. Both point-focus and confocal backscatter zoom configurations were considered. Finally, a paraxial Gaussian beam-propagation calculation was made to evaluate the beam-focusing function.

This analytical procedure was first applied to a generic, aperture-normalized Schmidt–Cassegrain telescope that was based on an average of the specifications of several commercial units. The results of the computation showed that very good performance could be obtained for f-ratios as low as 4.0. Two relatively simple alternative modification procedures were found to maintain diffraction-limited imaging performance:

1. The three active elements (primary mirror, secondary mirror, and corrector plate) may be independently repositioned (see figure). This requires a lengthening of the telescope tube and modification of the secondary mirror mount.
2. The primary mirror may be relocated, and the secondary mirror may be replaced. This again requires a lengthening of the tube and replacement of the secondary mirror with a stock convex mirror or with a reflectively coated lens of the correct curvature.

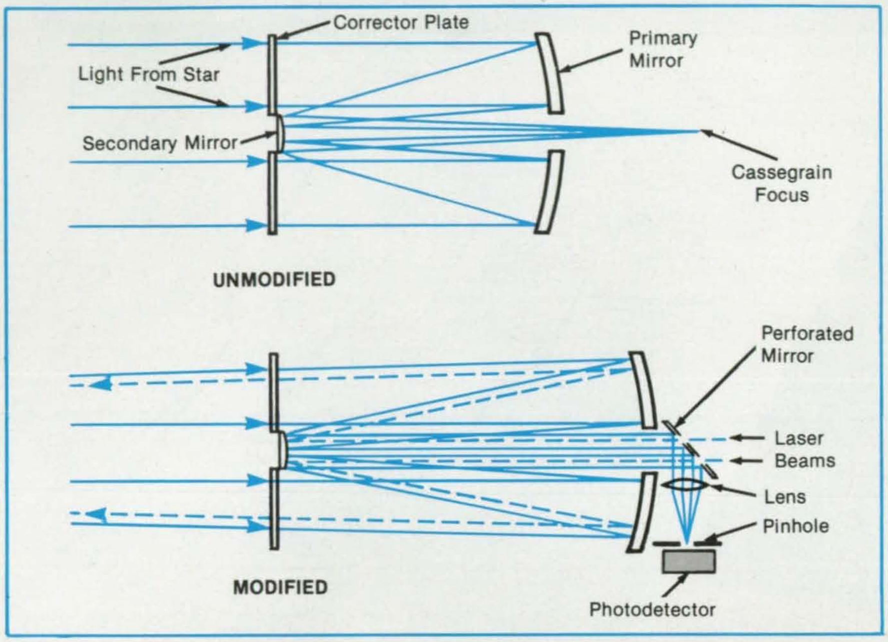

A **Schmidt-Cassegrain Astronomical Telescope** can be optimized by repositioning of its components to focus two laser beams on a nearby probe volume and confocally collect light backscattered from the probe volume.

The predicted performance of these modified telescope systems was compared with the predicted performance of large-aperture commercial lenses. The probe-volume imaging capability of the modified telescopes was found to be superior to that of the lenses for both monochromatic and dichromatic operation. Because of the central obstruction of the secondary mirror and the separation of the primary mirror from the corrector plate, the collection solid angle of the modified telescopes was considerably less than that of a lens of equivalent aperture, particularly at low f-ratio. However, the excellent imaging capabilities and large apertures of the modified telescopes offset this limitation.

The modified telescope (see figure) was also predicted to focus laser beams quite well. The negative-secondary-mirror/positive-primary-mirror combination provided a very small (high-energy-density) beam waist near the probe volume. The beam-waist and beam-intersection points were predicted not to coincide (as is generally the case in dual-beam laser velocimetry). However, this deficiency may be treated with additional optics upbeam of the beam splitter to adjust the beam-waist location.

These promising predictions were tested in a laboratory. A 200-mm-aperture telescope was purchased and modified to the predicted optimum configuration for both point collection and dual-beam focusing. Measurements of the imaging resolution and of the diameter and location of the beam waist agreed well with the predictions.

This work was done by Stephen E. Dunagan of **Ames Research Center**. *For further information, Circle 128 on the TSP Request Card.*

This invention is owned by NASA, and a patent application has been filed. Inquiries concerning nonexclusive or exclusive license for its commercial development should be addressed to the Patent Counsel, Ames Research Center [see page 14]. Refer to ARC-12610.

Books and Reports

These reports, studies, handbooks are available from NASA as Technical Support Packages (TSP's) when a Request Card number is cited; otherwise they are available from the National Technical Information Service.

Aiming Schedule for Orbiting Astrometric Telescope

Many requirements and limitations are balanced to obtain adequate measurements.

A report discusses the schedule of observation times and aiming directions of the proposed astrometric telescope facility to be mounted on the Space Station in orbit around the Earth. This facility would primarily make repeated observations of the apparent positions of each of 127 selected stars with respect to distant reference stars in the same field of view known to have unperturbed proper motions. The purpose of these observations is to detect motions of the selected stars about centers of mass and to analyze the harmonic content of the motions to infer the existence, number, masses, and orbital radii of planets.

The preliminary concept of the system and the associated aiming-schedule algorithm must reflect both observational requirements based on the need to gather sufficient scientific data and restrictions on the observations posed by the instrument itself, the other equipment on the Space Station, and the motions of natural celestial bodies. To achieve scientifically meaningful results, it will be necessary to make 20 to 50 complete observations of each star during 20 years. Each complete observation will be synthesized from all the data (representing about 10^8 collected photons) on each selected star and its reference stars to produce one measurement of position and may require tens of hours of viewing the same selected star in nonperiodic intervals of about 13 min each.

Some of the complicating factors are the following:

- To reduce contamination of the telescope optics by impinging particles, the telescope must not be aimed within 90° of the orbital velocity.
- Observations cannot be made during orbital-reboost and Space-Shuttle-docking maneuvers.
- The telescope must avoid the Sun and reflections of Sunlight from the Earth, Moon, and parts of the Space Station. The telescope also cannot view stars that are temporarily obscured by these bodies.
- The viewing time must be allocated fairly among all targets, taking account of such factors as the viewing time already allocated to each star, the need to observe fainter stars during longer intervals, and the statistical decrease in brightnesses of stars with increasing galactic latitude.
- The available viewing time is reduced by the time required to turn the telescope from one target to another, plus a 15-second settling time after each change of target.

To obtain a preliminary indication of capabilities of the system, computer simulations were conducted, taking into account the constraints on the telescope, the science requirements, the orbital mechanics of the Space Station, and the telescope-aiming maneuvers during 20 years. The simulations included a "baseline" system concept and modified versions obtained by imposing the various constraints as parameters.

The simulations showed that the facility should be able to provide each of the 127 stars with a viewing time (normalized with respect to the dependence of brightness on celestial latitude to an equivalent time for a star seen at the celestial equator) of about 24 hours per year. Because stars at large galactic latitudes require inordinate viewing times, longer normalized viewing times might be obtained by selecting targets closer to the galactic equator.

Under the "baseline" constraints, the facility should be able to view all regions of the sky during its lifetime, spending about 79 percent of its time viewing stars. The imposition of more severe constraints decreases this performance figure only slightly. Thus, it appears that the efficiency of the facility can be high and that there may be time available for other astrophysical investigations.

This work was done by Alfred C. Mascy and Charlie Sobeck of **Ames Research Center** *and Helen Jorgensen of Sterling Software Co. To obtain a copy of the report, "Space Station Astrometric Telescope Tracking for the Detection of Planetary Systems," Circle 2 on the TSP Request Card. ARC-12103*

Transpiration Cooling of Hypersonic Blunt Body

Results of an analytical approximation and a numerical simulation are compared.

A report presents a theoretical study of the degree to which transpiration can block the heating of a blunt, axisymmetric body by use of injected air. Transpiration cooling has been proposed to reduce operating temperatures on the nose cones of proposed hypersonic aerospace vehicles. Analyses of the type presented here will be important in the design of thermal protection for such vehicles.

On the basis of previous studies of the proposed hypersonic flight regime, the dominant mechanisms of transfer of heat to the surface are known to be conduction and convection (radiation is neglected). In addition, when dissociated atoms from hot boundary-layer gases reach the relatively cool surface, they can recombine and release their energy of formation directly to the surface. Therefore, the chemical reactivity or catalyticity of the surface material can affect heating, and these chemical effects are taken into account in this study.

The study involves the use and comparison of two methods of analysis: approximate equations based on similarity theory, and a numerical simulation via the nonsimilar, reactive-boundary-layer mathematical model embodied in the BLIMPK computer program. The governing equations are presented as conservation laws in a two-dimensional axisymmetric coordinate system fixed to the body with the origin at the stagnation point. These equations are supplemented by mechanical and calorical equations of state and by boundary conditions. The Levy–Lees transformation is applied to the equations, grouping dominant effects into specific terms and putting the equations into forms more suitable for both algebraic approximation and numerical integration.

Both methods of analysis are applied to the stagnation region of a sphere/cone blunt body under the operating conditions that are expected to result in the maximum heating of a representative aerospace vehicle during ascent. The heat fluxes computed by the two methods are compared. The effects of injection of pure nitrogen, helium, and argon on the heat flux and the distributions of molecular species in the boundary layer are also presented. It is shown how the numerical results from BLIMPK can be used to develop a correlation between the coefficients for the transfer of heat in the presence of transpiration and the coefficients for the transfer of heat obtained from similarity theory. This provides both a test of the validity of the similarity theory and a means of using it rapidly and easily to approximate flows that deviate only slightly from the similarity theory.

This work was done by William D. Henline of **Ames Research Center**. *Further information may be found in NASA CR-177516 [N89-24580], "Transpiration Cooling of Hypersonic Blunt Bodies with Finite Rate Surface Reactions."*

Copies may be purchased [prepayment required] from the National Technical Information Service, Springfield, Virginia 22161, Telephone No. (703) 487-4650. Rush orders may be placed for an extra fee by calling (800) 336-4700. ARC-12383

Materials

Hardware, Techniques, and Processes

Grease Inhibits Stress-Corrosion Cracking in Bearing Race

Operating life is extended at low cost.

Marshall Space Flight Center, Alabama

Coating with a suitable grease has been found to inhibit stress-corrosion cracking in the bore of the inner race of a ball-bearing assembly that operates in liquid oxygen. The grease apparently protects the bore and its corner radii from corrosion-initiating and -accelerating substances like moisture and contaminants, which can enter during assembly. Previously, stress-corrosion cracking in the bore has been prevented by either (1) maintaining the bore clean and extensively purging and drying it, all requiring 72 hours of assembly time, or (2) shot-peening and nickel-plating the bore, at a cost of $658 per bearing (1989 prices). The principal advantages of coating with the special grease are that unlike the previous methods, it is relatively inexpensive (about $5 per bearing) and involves very little extra assembly time.

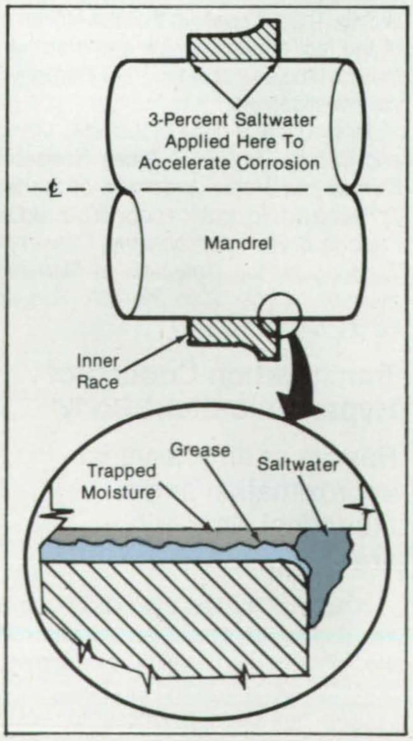

Inner Races of ball-bearing assemblies were tested for resistance to stress-corrosion cracking by shrink-fitting them onto a mandrel, applying saltwater, and exposing them to a humid environment.

The efficacy of the grease-coating method was demonstrated in a simple experiment. Three inner races of 440C stainless steel were prepared. One race was left uncoated, the bore and corner radii of the second race were coated with Braycote 640 AC-MS grease, and the bore and corner radii of the third race were coated with Krytox grease with a strontium nitrate additive. The races were installed on a molybdenum-coated mandrel (see figure) with an interference fit at a hoop stress of 45 kpsi (310 MPa) by initially shrinking the mandrel in liquid nitrogen, then sliding the races onto the mandrel while it was still cold.

During the brief interval between removal from the liquid-nitrogen bath and the installation of the races, moisture condensed from the atmosphere onto the mandrel. When the mandrel warmed up and expanded into contact with the bores of the races, the moisture was trapped between the bores and the mandrel. Any pitting (caused, for example, by corrosion initiated by the trapped moisture) near the corner radii would concentrate the already high hoop stress and might thereby cause the ring to fracture.

The shaft and races were placed in a humid environment and a 3-percent saltwater solution was applied to accelerate corrosion. The uncoated race failed in 7 hours. The greased races lasted more than a month and had not yet failed when the results of the experiment were recorded.

This work was done by Robert F. Beatty and Scott E. McVey of Rockwell International Corp. for **Marshall Space Flight Center**. *For further information, Circle 162 on the TSP Request Card.*
MFS-29664

Computer Programs

COSMIC: Transferring NASA Software

COSMIC, NASA's Computer Software Management and Information Center, distributes software developed with NASA funding to industry, other government agencies and academia.

COSMIC's inventory is updated regularly; new programs are reported in *Tech Briefs*. For additional information on any of the programs described here, circle the appropriate TSP number.

If you don't find a program in this issue that meets your needs, call COSMIC directly for a free review of programs in your area of interest. You can also purchase the annual *COSMIC Software Catalog*, containing descriptions and ordering information for available software.

COSMIC is part of NASA's Technology Utilization Network

COSMIC® — *John A. Gibson, Director,*
(404) 542-3265
The University of Georgia, 382 East Broad Street, Athens, Georgia 30602

Computer Programs

These programs may be obtained at a very reasonable cost from COSMIC, a facility sponsored by NASA to make computer programs available to the public. For information on program price, size, and availability, circle the reference number on the TSP and COSMIC Request Card in this issue.

Electronic Systems

Design and Analysis of Linear Control Systems

Programs implement root-locus and frequency-response methods.

A package of five computer programs was developed by the Kennedy Space Center Robotics Laboratory to assist in the design and analysis of linear control systems by the use of root-locus and frequency-response methods. The BODE program calculates magnitude and phase as a function of frequency. The Laplace transform is expressed as a ratio of factors and their reciprocals. Factors may be first- or second-order polynomial terms. The transport-lag factor and minimum- and non-minimum-phase factors are taken into account. BODE can be used to determine the general shape of the magnitude-versus-frequency curve, with options to investigate peaks of interest more closely.

The LOCUS program calculates the roots of a closed-loop characteristic equation for positive or negative gain. KTUNE, a modified version of LOCUS, allows small gain variations to establish break-in or breakaway positions and the gain corresponding to a specified damping ratio. TPEAK calculates the approximate time to peak overshoot of a closed-loop system. The program assumes that a pair of dominant complex poles characterize the system. The POLYROOT program determines the roots of polynomials. POLYROOT output aids in formulating the factored input to BODE and LOCUS. All programs require the user to set parameter switches inside the source code and alter DATA statements to specify the input.

The package is written in FORTRAN (BODE, TPEAK) and BASIC (LOCUS, KTUNE, and POLYROOT) for batch execution. The programs have been implemented on a DEC VAX computer operating under VMS with a central-memory requirement of approximately 8K of 8-bit bytes. The program was developed in 1986.

This program was written by John W. Jamison of **Kennedy Space Center**. *For further information, Circle 43 on the TSP Request Card.*
KSC-11376

Mechanics

Program for Elastoplastic Analyses of Plane Frames

Nonlinear collapse phenomena are simulated by iterative linear analyses.

PLAN2D is a FORTRAN computer program for the plastic analysis of planar frame structures. Given a structure and loading pattern as input, PLAN2D calculates the ultimate load that the structure can sustain before collapse. Element moments and plastic hinge rotations are calculated for the ultimate load. The locations of hinges required for collapse mechanisms to form are also determined.

The program proceeds in an iterative series of linear elastic analyses. After each iteration, the resulting elastic moments in each member are compared to the reserve plastic moment capacity of that member. The member or members in which moments are closest to their reserve capacities determine the minimum load factor and the site where the next hinge(s) is(are) to be inserted. Next, hinges are inserted and the structural-stiffness matrix is reformulated. This cycle is repeated until the structure becomes unstable. At this point, the ultimate collapse load is calculated by accumulating the minimum load factor from each previous iteration and multiplying these factors by the original input loads.

PLAN2D is based on the program STAN, originally written by Dr. E. L. Wilson at U. C. Berkeley. PLAN2D has several limitations: (1) although PLAN2D detects the unloading of hinges, it cannot remove hinges; (2) PLAN2D does not allow the user to put in different positive and negative moment capacities; and (3) PLAN2D does not consider the interaction between axial and plastic moment capacity. Axial yielding and buckling are ignored, as is the reduction in moment capacity due to axial load.

PLAN2D is written in FORTRAN and is machine-independent. It has been tested on an IBM PC and on a DEC MicroVAX computer. The program was developed in 1988.

This program was written by C. Lawrence, and A. A. Huckelbridge of **Lewis Research Center**. *For further information, Circle 26 on the TSP Request Card.*
LEW-14889

Mathematics and Information Sciences

Computer Language for Optimization of Design

Nonlinear methods are incorporated at the language level.

SOL is a computer language geared to the solution of design problems. SOL includes the mathematical modeling and logical capabilities of a computer language like FORTRAN but also includes the additional power of nonlinear mathematical programming methods (i.e., numerical optimization) at the language level (as opposed to the subroutine level).

The language-level use of optimization has several advantages over the traditional, subroutine-calling method of using an optimizer: first, the optimization problem is described in a concise and clear manner that closely parallels the manner of the mathematical description of the optimization; second, a seamless interface is automatically established between the optimizer subroutines and the mathematical model of the system being optimized; third, the results of an optimization (objective, design variables, constraints, termination criteria, and some or all of the optimization history) are put out in a form directly related to the description of the optimization; and finally, automatic checking for errors and recovery from an ill-defined model of the system or description of the optimization are facilitated by the language-level specification of the optimization problem. Thus, SOL enables rapid generation of models and solutions for optimum design problems with greater confidence that the problem is posed correctly.

The SOL compiler takes SOL-language statements and generates the equivalent FORTRAN code and system calls. Because of this approach, the modeling capabilities of SOL are extended by the ability to incorporate existing FORTRAN code into a SOL program. In addition, SOL has a powerful MACRO capability. The MACRO capability of the SOL compiler effectively gives the user the ability to extend the SOL language and can be used to develop easy-to-use shorthand methods of generating complex models and solution strategies. The SOL compiler provides syntactic and semantic checking for recovery from errors and provides detailed reports containing cross-references to show where each variable was used. The lists summarize all optimizations and include the objective functions, design variables, and constraints. The compiler checks for errors specific to optimization problems, so that simple mistakes will not cost hours of debugging time.

The optimization engine used by and included with the SOL compiler is a version of Vanderplatt's ADS system (Version 1.1) modified specifically to work with the SOL compiler. SOL allows the use of the more than 100 ADS optimization choices; for example, sequential quadratic programming, modified feasible directions, interior- and exterior-penalty-function methods, and variable-metric methods. Default choices of the many control parameters of ADS are made for the user, but the user can override any of the ADS control parameters for each individual optimization.

The SOL language and compiler were developed with an advanced compiler-generation system to ensure correctness and simplify the maintenance of programs. Thus, the syntax of SOL was defined precisely by a LALR(1) grammar, and the parser of the SOL compiler was generated automatically from the LALR(1) grammar with a parser generator. Hence, unlike in ad-hoc, manually coded interfaces, the lexical analysis of the SOL compiler ensures that the SOL compiler recognizes all legal SOL programs, can recover from and correct for many errors, and can report the location of errors to the user.

This version of the SOL compiler has been implemented on VAX/VMS computer systems and requires 204 KB of virtual memory to execute. Inasmuch as the SOL compiler produces FORTRAN code, it requires the VAX FORTRAN compiler to produce an executable program. The SOL compiler consists of 13,000 lines of Pascal code. It was developed in 1986 and last updated in 1988. The ADS and other utility subroutines amount to 14,000 lines of FORTRAN code and were also updated in 1988.

This program was written by Stephen J. Scotti of **Langley Research Center** *and Stephen H. Lucas of Vigyan Research Associates, Inc. For further information, Circle 155 on the TSP Request Card. LAR-14280*

Graphical Planning of Spacecraft Missions

Maps, overlays, and other graphical displays are available.

The Mission Planning Graphical Tool (MPGT) computer program provides analysts with graphical representations of the spacecraft and environmental data used in planning missions. Developed by the Flight Dynamics Division at NASA's Goddard Space Flight Center, MPGT is designed to be a generic software tool that can be configured to analyze any specified Earth-orbiting spacecraft mission. The data are presented as a series of overlays on top of a two-dimensional or three-dimensional projection of the Earth. Included are spacecraft-orbit tracks, ground-station-antenna masks, solar and lunar ephemerides, and coverage by the Tracking Data and Relay Satellite System (TDRSS). From these graphical representations, an analyst can determine such spacecraft-related constraints as communication coverage, infringement upon zones of interference, availability of sunlight, and visibility of targets to instruments.

The presentation of time and geometric data as graphical overlays on a world map makes possible quick analyses of trends and time-oriented parameters. With the three-dimensional display, the user specifies a vector that represents the position in the universe from which the user wishes to view the Earth. From these "viewpoint" parameters the user can zoom in on or rotate around the Earth. The zoom feature is also available with the two-dimensional map image. The program contains data files of world-map continent coordinates, contour information, antenna-mask coordinates, and a sample star catalog.

Inasmuch as the overlays are designed to be independent of any particular mission, no software modifications are required to satisfy the different requirements of various spacecraft. All overlays are generic, with the contours of communication zones and spacecraft terminators generated analytically based on data on the altitude of the spacecraft. Contours of zones of interference are specified by the user through text-edited data files. Spacecraft-orbit tracks are specified via Keplerian or Cartesian orbit vectors. Finally, all time-related overlays are based on an epoch supplied by the user.

A user-interface subsystem of the software system enables the user to alter any parameter of the system that affects a mission or that affects the graphics through a series of pull-down menus and pop-up data-entry panels. The user can specify and load mission-data files, control graphical-presentation formats, and terminate the system. The interface automatically checks for errors in, and validates, all data put into the system from either a file or the keyboard. A help software facility is provided.

MPGT also includes a software utility called ShowMPGT, which displays screen images that were generated and saved with the MPGT system. Specific sequences of images can be recalled without having to reset parameters related to the graphics and the mission. The MPGT system does not provide for printout. To obtain printed graphical output, the computer must be configured with a color printer that captures the video signal and copies it onto a hard-copy medium.

The program was implemented on an IBM PC/AT-compatible computer that was configured with an EGA board (but will run with any board supported by the HALO '88 Graphics Package) and running MS-DOS version 3.3. MPGT was written in MicroSoft FORTRAN, version 4.1 (99 percent) and MicroSoft Macro Assembler, version 4.0 (1 percent). Because of copyright and licensing restrictions on commercial software incorporated in this program, executable codes are not distributed. To compile and link the source code, the following commercial programs are required: The Screen Generator, The Linkable Screen Manager, and The Screen Manager FORTRAN Compiler Interface from West Chester Group; HALO '88 Graphics Subroutine Package from Media Cybernetics; and the FORTRAN 4.1 Optimizing Compiler and Macro Assembler from Microsoft Corp. An 80X87 math coprocessor is recommended. MPGT was developed in 1989 and has a memory requirement of 400 KB.

This program was written by J. F. Jeletic and L. T. Ruley of **Goddard Space Flight Center**. *For further information, Circle 160 on the TSP Request Card.*
GSC-13318

Helicity-Density and Normalized-Helicity Maps of Flows

These maps clearly indicate vortexes and other important features.

Ames Research Center, Moffett Field, California

Maps of helicity density and normalized helicity have been shown to be useful as graphical representations of important features of three-dimensional flow fields that contain vortexes. The more conventional pressure, density, and velocity-vector maps often do not adequately represent the vortical features of interest and sometimes give ambiguous indication of swirl direction. In contrast, the helicity-density and normalized-helicity representations emphasize the complicated and, therefore, important parts of a flow field, identify the vortexes, differentiate between primary and secondary vortexes, indicate the sense of the swirling motion, locate the free singular points (those not attached to surfaces), and trace the vortex-core streamlines that emanate from these points.

The helicity density is defined as the scalar product of the velocity and vorticity vectors at a given location in the flow field. The normalized helicity is defined as the inner product of the unit vectors along the velocity and vorticity directions; that is, the normalized helicity is the cosine of the angle between the velocity and the vorticity. One of the great advantages of the helicity density and the normalized helicity is that both their magnitudes and their senses are meaningful. A large helicity density reflects a large velocity and a large vorticity when the angle between them is small. The sign of the helicity density indicates the direction of swirl of the vortex relative to the velocity. Both the relative size of the helicity density and the changing of swirl direction, emphasized by graduation in color for magnitude and by different colors for positive or negative values, facilitate the distinction between primary and secondary vortexes in a graphical representation (see Figure 1).

The effectiveness of the helicity density as an indicator of vortexes is even much greater for low-subsonic flows, for which the conventional density mapping is not sufficiently sensitive because the variations in density are almost negligible. The sensitivity of the helicity-density representation remains high because in the core regions of the vortexes, both the velocity and vorticity always reach relatively high values and the angle between them is small. All these contribute to high values of the helicity density and to a clear representation of the vortexes.

Figure 2 shows the components of the vorticity vectors relative to a local streamline. One component is parallel to the local velocity vector, and the other two are perpendicular to it. The component parallel to the velocity, which is the only component that contributes to the helicity density, vanishes everywhere in a two-dimensional flow. It also vanishes wherever the flow is locally two dimensional, as on planes of symmetry. Therefore, the normalized helicity must be zero in two-dimensional flows and must vanish locally on planes of symmetry, thus emphasizing them in the graphical representation.

Each of the two components of vorticity perpendicular to the velocity is responsible for the curvature of the streamline in the plane that is perpendicular to it and includes the velocity vector. When these two perpendicular components decrease relative to a constant parallel component, the

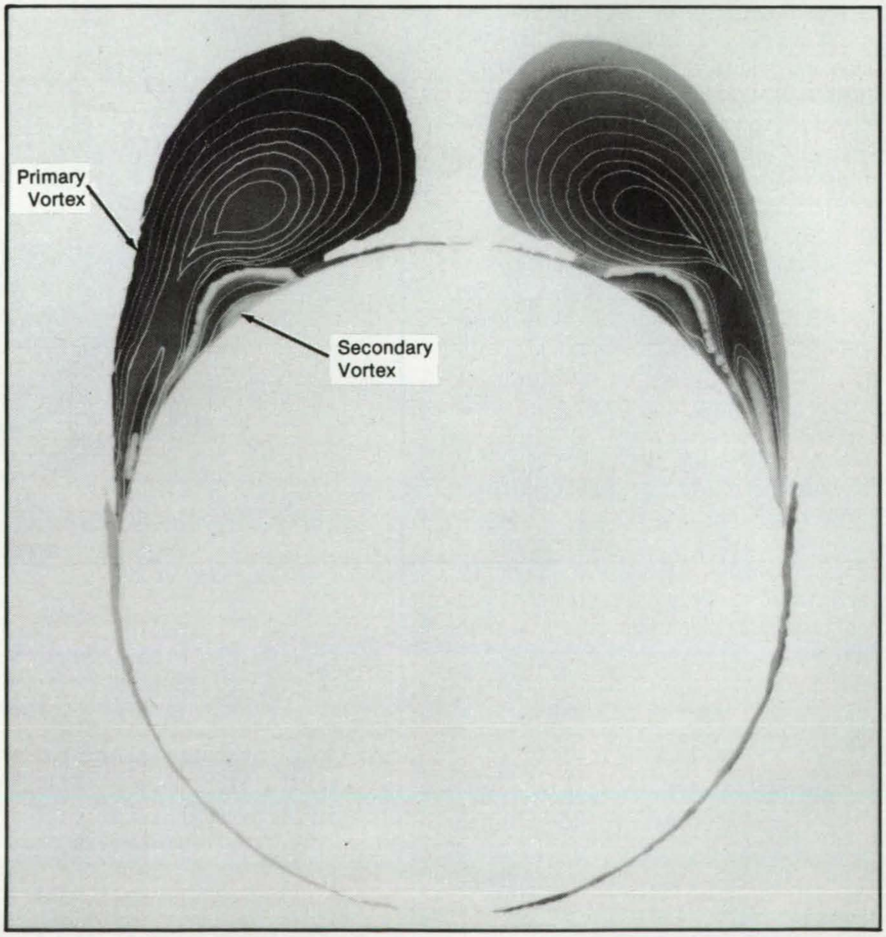

Figure 1. A **Primary and a Secondary Vortex** can be seen clearly in this plot of helicity-density contours in a cross section of the computed flow field about an ogive/cylinder body. The parameters of the flow field are free-stream mach number 0.2, angle of attack 40°, and Reynolds number 200,000.

local curvature of the streamline decreases, the angle between the vorticity and velocity vectors vanishes, and the normalized helicity tends toward unity.

The magnitude of the normalized helicity thus indicates the local curvature of the streamlines. In the limiting case, where the velocity and vorticity vectors are parallel, the normalized helicity is exactly equal to unity, and the streamline is locally straight. However, the flow is far from being two dimensional, because adjacent streamlines spiral around this streamline. The fact that the normalized helicity goes to its maximum value on a streamline of minimum curvature can be used to locate a vortex-core axis, which is such a streamline.

This work was done by David Degani of **Ames Research Center** *and Yuval Levy and Arnan Seginer of Israel Institute of Technology. Further information may be found in AIAA paper 88A-40769, "Graphical Representation of Three-Dimensional Vortical Flows By Means of Helicity Density and Normalized Helicity."*

Copies may be purchased [prepayment required] from AIAA Technical Information Service Library, 555 West 57th Street, New York, New York 10019, Telephone No. (212) 247-6500. ARC-12464

Figure 2. The **Components of Vorticity** parallel and perpendicular to the streamline play an important role in the helicity-density and normalized-helicity graphical representation and are related to the local curvature of the streamline.

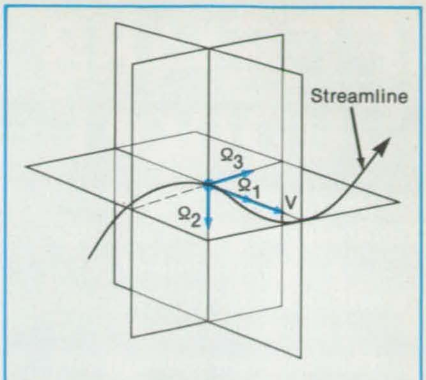

Notes:
1. V = speed.
2. Ω_1 = parallel component of vorticity.
3. Ω_2 and Ω_3 are perpendicular components of vorticity.

Algebraic Model of Turbulence for Internal Flow

An enhanced eddy-viscosity approximation simplifies calculations.

Ames Research Center, Moffett Field, California

An algebraic approximation has been developed for use in calculating turbulent flow in a duct with a sharp 180° turn. Sharp curvatures of the surfaces at the turn increase the complexity of the flow and the equations that describe it, and previous studies of the effect of curvature on turbulence have been limited to mild curvatures. The approximation is expected to simplify the mathematical modeling of complicated turbulent flows, particularly those in air-breathing engines.

The effects of turbulence are summarized in a composite eddy viscosity ν_t. For this purpose, it is first necessary to define an effective mixing length via

$$\ell = k^2\left[1-\exp\left(-\frac{y}{k\delta_\omega}\right)\right]\delta_\omega$$

for fully turbulent internal flow, and

The **Flow in an Axisymmetric Turnaround Duct** model was measured and compared with the flow predicted by a computer program that includes the algebraic eddy viscosity described in the text. (The experimental duct model represents a design concept for a compact turbine engine.)

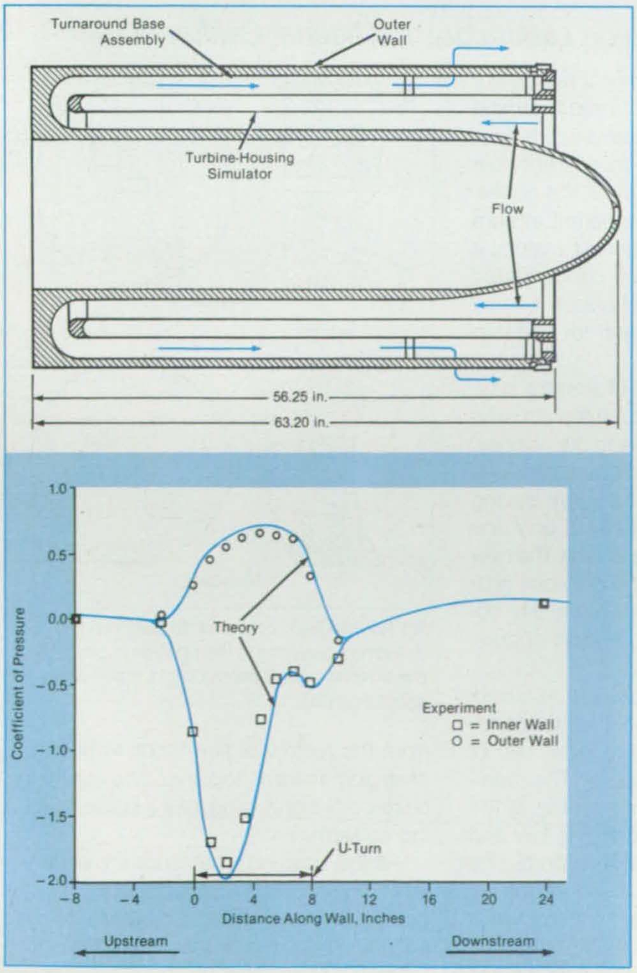

$$\ell = ck\left[1-\exp\left(-\frac{y}{c\delta_\omega}\right)\right]\delta_\omega$$

for partially developed turbulent flow, where y is the distance from the wall, δ_ω is the distance from the point of maximum vorticity to the point where vorticity vanishes, and c and k are adjustable parameters with typical values of 0.25 and 0.4, respectively. Next, it is necessary to define an effective vorticity length near the wall as

$$\Lambda = \frac{u_{\mathrm{ref}}}{|\boldsymbol{\omega}|_{\max}}$$

where u_{ref} is the average velocity at the inlet boundary and $|\boldsymbol{\omega}|$ is the magnitude of vorticity. Then, using the concept of laminar viscous spreading, an effective thickness of the viscous region is defined as

$$\delta^+ = \sqrt{\frac{\nu\Lambda}{u_{\mathrm{ref}}}} = \sqrt{\frac{\nu}{|\boldsymbol{\omega}|_{\max}}}$$

The scale length y^+ of the inner sublayer is then given by

$$y^+ = \frac{y}{\delta^+}$$

where y is the distance from the wall.

Finally, one must define a factor γ, which represents the intermittency of turbulence in the outer layer:

$$\gamma = \frac{1}{2}\left\{1-\mathrm{erf}\,\left[5\left(\frac{y-y_{\omega\max}}{\delta_\omega}-0.8\right)\right]\right\}$$

where $y_{\omega\max}$ is the distance of the maximum vorticity from the wall. Then the composite eddy viscosity is given by

$$\nu_t = \gamma\left[\ell\left(1-e^{-y^+/A^+}\right)\right]^2|\boldsymbol{\omega}|$$

This algebraic model of viscosity was inserted in a computer program that uses the Navier–Stokes equations to simulate three-dimensional, incompressible, steady flow. The results of the simulation agreed fairly well with the results of experiments in an axisymmetric turnaround-duct model (see figure).

This work was done by Dochan Kwak of **Ames Research Center** *and James L. C. Chang of Rockwell International Corp. Further information may be found in AIAA paper 88A-22446, "A Numerical Study of Turbulent Internal Shear Layer Flow in an Axisymmetric U-Duct".*

Copies may be purchased [prepayment required] from AIAA Technical Information Services Library, 555 West 57th Street, New York, New York 10019, Telephone No. (212) 247-6500. ARC-12544

Self-Adjusting Choke for Nozzle

The issuing stream remains coherent for greater distances despite fluctuations in pressure and/or rate of flow.

NASA's Jet Propulsion Laboratory, Pasadena, California

A self-adjusting choke for a nozzle enables the issuing stream of liquid to remain coherent, despite fluctuations in the flow, along a greater distance than is possible with the same nozzle without the choke. The resulting extended coherent stream is advantageous for firefighting, making it possible to direct a more concentrated flow of water at a flame or hotspot. It could also be used in mining and for transferring liquids.

The natural instabilities of streams leaving nozzles frequently cause the streams to disperse relatively close to the nozzles. Although a previously developed advanced nozzle produces a more-coherent issuing stream, it functions optimally at only one upstream pressure or rate of flow. The new choke, based partly on the previous nozzle concept, helps to maintain the coherence of the flow over a range of pressures and rates of flow.

The self-adjusting choke is a relatively thick, flexible membrane that contains, typically, three orifices, the outer two of which are slanted (see figure). The membrane is inserted into the opening of the nozzle. When the rate of flow is low and the membrane is not much distorted by the upstream pressure of the fluid, the liquid issuing from the outer orifices tends to separate into two diverging streams. Simultaneously, the web of fluid issuing from the middle orifice tends to pull the diverging streams together. The resulting balance of forces produces a stable spiraling stream.

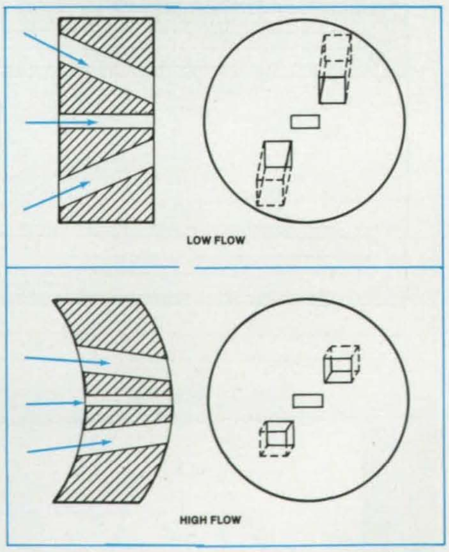

A **Flexible Membrane With Slanted Orifices** deforms according to the upstream pressure in the flowing liquid, producing a more-coherent spiraling stream.

As the upstream pressure (or, equivalently, the rate of flow) increases, the membrane flexes, redirecting the outer streams so that they have a lesser tendency to diverge. Thus, although the greater flow tends to cause the outer streams to separate more than under the unloaded condition, the smaller angle between the outer streams still enables the web to counterbalance the tendency toward divergence, and a stabler stream results.

This work was done by Andrew D. Morrison of Caltech for **NASA's Jet Propulsion Laboratory**. *For further information, Circle 96 on the TSP Request Card.*

This invention is owned by NASA, and a patent application has been filed. Inquiries concerning nonexclusive or exclusive license for its commercial development should be addressed to the Patent Counsel, NASA Resident Office-JPL [see page 14]. Refer to NPO-17625.

Liquid-Crystal Coats Help Make Flows Visible

Changes of color are rapid and reversible.

Langley Research Center, Hampton, Virginia

The visible indication of the transition of a boundary layer from laminar to turbulent flow plays an important role in aerodynamic tests in wind tunnels and in flight. The most popular methods for making boundary layers visible in such tests have included the sublimating-chemical technique and the oil-flow technique. However, each method has limitations that constrain its applicability. In a newly developed method, liquid-crystal coats are used to make visible such features of boundary-layer flows as transitions, separations, and the locations of shocks.

Typically, temperature and shear stress are the primary stimuli in response to which liquid-crystal coats selectively reflect discrete wavelengths (colors) of light. Because the fundamental chemical structure is unaffected by these changes, a liquid-crystal coat can respond repeatably to the same physical changes. Thus, the color changes can be reversible.

Liquid-crystal coats can respond very rapidly to changes in shear stresses or temperature distributions; characteristic response times as small as 0.2 second have been observed. The particular color observed depends on the viewing angle and on the local shear and temperature to which the liquid crystals are subjected. The vividness and brilliance of the reflected colors also depend on the amount and angle of incident light.

One flight evaluation of the liquid-crystal technique was conducted on a Lear Model 28/29 business jet airplane operated by NASA at its Langley Research Center in research on the reduction of viscous drag. The airplane provides, for research, an extensive combination of ranges of flight operating conditions, including mach numbers up to 0.805, maximum unit Reynolds numbers up to 2.65×10^6 ft^{-1} (8.69×10^6 m^{-1}), and altitudes up to 51,000 ft (15.6 km). The right winglet of the airplane was prepared for testing by coating it with a liquid-crystal mixture.

Correlations between transitions measured by hot films and by liquid crystals showed that the change in the color of the liquid-crystal coat corresponded to the first appearance of turbulent spots in the hot films. This response differs from that of sublimating chemicals, which show the end of the transition region.

The time-dependent response of a liquid-crystal coat was also evaluated. The transition on the winglet was changed by conducting sideslip oscillations with a period of about 2 cycles per second. The observed movement of the transition was in phase with the sideslip oscillation, indicating that the coat responded rapidly.

Another flight experiment involving liquid crystals was conducted with a Grumman OV-1B Mohawk airplane operated by NASA. In addition, a test of both liquid-crystal and sublimating-chemical indications of transitions was conducted in the Langley 14-by-22-ft (4.3- by-6.7-m) wind tunnel on a fuselage forebody. Comparison of the results showed good agreement between the two methods.

The use of liquid-crystal coats in the measurement of transitions provides data that can be very difficult to acquire by other visualization techniques. For flight applications, liquid crystals provide the capability for making transitions visible throughout almost the entire altitude and speed ranges of subsonic aircraft. The use of liquid crystals is not known to expose humans to any hazard of toxicity. Because liquid crystals are derived from the fatty acids of animals, they tend to be less hazardous than many other chemicals are. The liquid-crystal method is also applicable to the visible indication of supersonic flows and is suitable for general use in high- and low-speed wind-tunnel and water-tunnel testing.

This work was done by Bruce J. Holmes of **Langley Research Center** *and Clifford J. Obara of PRC-Kentron. For further information, Circle 147 on the TSP Request Card.*

LAR-14342

Adaptive Grids for Computations of Three-Dimensional Flows

A spring-system analogy is extended from two to three dimensions.

Ames Research Center, Moffett Field, California

A self-adaptive-grid method has been devised and enhanced for the efficient computation of complicated three-dimensional flows. An extension of a method developed previously for two-dimensional flows, this method is based in part on the analogy of a fictitious system of tension and torsion springs that connect the grid points (see Figure 1).

The stiffnesses of the springs can be specified in terms of some measures of the flow-field characteristics (density, mach number, and the like) or in terms of parameters computed on the grid itself. By specifying minimum and maximum permissible spacings, the grid can be said to be "self-adaptive" or "solution-adaptive" (see Figure 2), and iterative adaptions/solutions can be performed in the effort to achieve a desired convergence.

An adaptation involves the use of variational principles to minimize the potential energy stored in the springs. For the adaptation along one coordinate line (e.g., the $\xi_{j,k}$ line in Figure 1), that line is held fixed while each grid point on the line is allowed to move freely along it in response to the tugs of the tension springs that connect it to the two adjacent grid points on the same line and to the twists of the torsion springs that connect it to the adjacent grid points on the adjacent lines that represent the same (e.g., ξ) coordinate. For a three-dimensional adaptation, the procedure is split into a sequence of adaptations, each along one coordinate axis at a time.

A user-friendly computer research code has been written to implement the adaptive-grid algorithm. In response to the maximum and minimum grid spacings specified by the user, the code automatically calculates most of the incorporated grid parameters, which affect orthogonality and smoothness. The user selects the direction of initial adaptation along a curvilinear grid line in the physical space. Grid points are then redistributed to optimal positions along a family of such lines, the collection of which sweeps a curved grid surface specified by the user. The procedure crosses, in a given marching direction, the entire physical space filled by these surfaces.

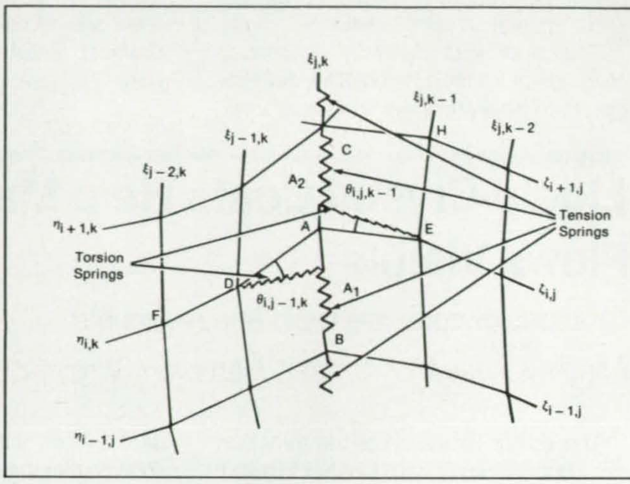

Figure 1. **Fictitious Springs** connecting the points of the computational grid are used to determine an optimum grid spacing. Each point (e.g., A) is connected to neighboring points (B through E) by tension and torsion springs. The stiffnesses of the tension springs are related to flow-field quantities. The stiffnesses of the torsion springs resist the departure of the grid from orthogonality.

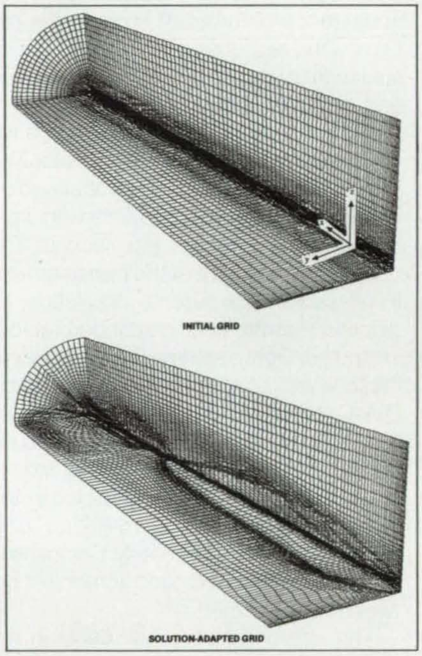

Figure 2. This **Initial Grid and Resulting Solution-Adapted Grid** were used to calculate the three-dimensional supersonic flow about a two-nozzle afterbody. In this case, the grid is adapted to the solution of mach numbers. In the adapted grid, points are clustered across the shocks and mixing layers, depicting all the features of the flow.

This work was done by M. Jahed Djomehri and George S. Deiwert of **Ames Research Center**. *Further information may be found in NASA TM-101027 [N89-11718], "Three-Dimensional Self-Adaptive Grid Method for Complex Flows."*

Copies may be purchased [prepayment required] from the National Technical Information Service, Springfield, Virginia 22161, Telephone No. (703) 487-4650. Rush orders may be placed for an extra fee by calling (800) 336-4700.
ARC-12479

Accounting for Compressibility in Viscous Flow in Pipes

Variations of density and velocity across the flow cross section are included in calculations.

Ames Research Center, Moffett Field, California

A method has been developed to account for the effects of compressibility in viscous flows through long, circular pipes of uniform diameter. The method is based on the approximation of variations in density and velocity across the pipe cross section by profile equations previously developed for boundary-layer flow between flat plates.

The concept of "fully developed" flow was originally defined for an incompressible flow in which the velocity at any given

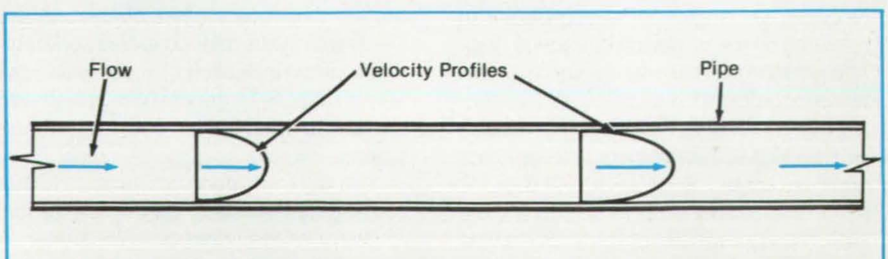

The **Velocity of Flow** varies along the pipe, but the power-law shape of the velocity profiles is assumed to be invariant along the pipe.

point on the cross section does not vary with position along the pipe. This concept is extended here to compressible flow in which the ratio of the velocity at any given point to the velocity at the centerline point does not vary with position along the pipe. Measurements have confirmed that subsonic flows tend to be "fully developed" in this extended sense (see figure).

The cross-sectional velocity profile is assumed to be similar to a flat-plate boundary-layer profile:

$$u/u_c = (2y/d)^n$$

where u = the velocity at radial distance y from the wall, u_c = the velocity at the centerline, and d = the diameter of the pipe. The cross-sectional distribution of temperature is constructed in a manner similar to the procedure normally used in flat-plate boundary-layer flows. The wall of the pipe is assumed to be adiabatic. In this way, the temperature at any point in the flow can be expressed in terms of the ratio of specific heats of the flow medium, the mach number at the centerline, the velocity profile, and a "recovery factor" (which is 0.88 for turbulent flows).

The governing equations of flow (conservation of mass, momentum, and energy) are reduced to convenient forms by introducing dimensionless variables and defining special profile integrals of velocity and temperature profiles. A method is developed to solve the equations and obtain solutions for values of flow friction in terms of measured gradients of wall static pressure.

The method was used to analyze the detailed pressure measurements made in a long pipe for flow of air at a wide range of flow speeds. Values of flow friction derived from these measurements were compared with data in the literature on incompressible flow in pipes. The effect of the mach number on flow friction was then extracted from these data by applying a special procedure that isolated the effects of the Reynolds number and the roughness of the surface. The results show that the effect of the mach number in pipe flow follows the trend previously established for flows over flat plates.

This work was done by Frank W. Steinle of **Ames Research Center**, *Ken Gee of the California Polytechnic State University, and Sreedhara V. Murthy of CALSPAN. Further information may be found in AIAA paper 88A-48888, "Compressibility Effects on Flow Friction in a Fully Developed Pipe Flow."*

Copies may be purchased [prepayment required] from AIAA Technical Information Service Library, 555 West 57th Street, New York, New York 10019, Telephone No. (212) 247-6500.
ARC-12249

Docking System Would Accommodate Misalignments

The system would also absorb kinetic energy.

Lyndon B. Johnson Space Center, Houston, Texas

A conceptual docking system would absorb kinetic energy along each of three orthogonal directions. It would accommodate large misalignments between the docking objects. Conceived for docking the Space Shuttle in the Space Station, the system may be useful in other applications in which a large moving object must be aligned with and joined to another — for example, cranes, robots, and fuel or material-loading lines.

The lightweight system would consist of a probe on one of the two docking objects and a drogue on the other object. The probe would contain a latching mechanism; pitch, roll, and yaw dampers; and centering and rigidizing mechanisms (see figure). The latching mechanism would ride on a y-axis track, which would ride on an x-axis track, which, in turn, would ride on a z-axis track. The probe could therefore translate in the x and y directions to accept misalignment with the drogue and in the z direction to enter the drogue. Three eddy-current dampers would absorb the energy of motion along the orthogonal directions, bringing the docking objects to a smooth stop.

According to the concept, as the docking objects approached, the z track would extend the probe by 9 in. (22.9 cm). At the first contact of the probe with the drogue, the x and y drives would allow such lateral translation as would be necessary to accommodate misalignment between the probe and the drogue, and the z drive would rapidly extend the probe deep into the drogue. Latches on the probe would engage the drogue.

Meanwhile, the dampers would absorb kinetic energy. The probe could rotate ±10° with respect to the x and y axes and ±11° with respect to a gimbal. When motion had been stopped, a collet on the probe would retract to lock against pitching and yawing. Actuator-driven plungers would lock the probe latches against movement in the x, y, and z directions. The z-track drive would slowly retract the probe to its storage position.

For release, the probe collet would be extended, relieving the preload between the probe and the drogue. The latch-locking piston would then be retracted, releasing the spring-loaded latches. The probe would then be disconnected from the drogue.

This work was done by Rasmik Ajemian, Earl V. Holman, and Siamak Ghofranian of Rockwell International Corp. for **Johnson Space Center**. *For further information, Circle 100 on the TSP Request Card. MSC-21596*

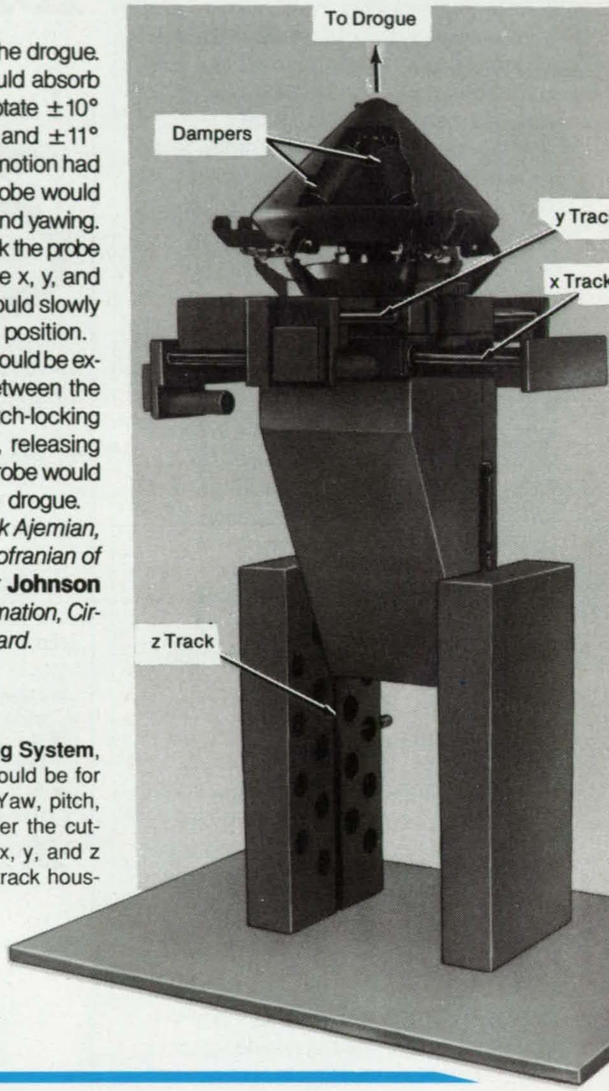

In this **Mockup of the Docking System**, the probe is extended as it would be for initial contact with a drogue. Yaw, pitch, and roll dampers appear under the cutaway shell of the probe. The x, y, and z dampers are hidden in the z-track housing.

Strain Center for Analysis of Forces

After yielding, forces are perpendicular to radii from the strain center.

NASA's Jet Propulsion Laboratory, Pasadena, California

The concept of a strain center has been introduced to facilitate the analysis of forces resulting from an eccentric load after the elastic limit has been exceeded. The concept is especially useful where the loads are known and the directions of the forces are being analyzed; e.g., the limiting frictional force between a wheel and the ground.

Conventional force analysis superimposes direct forces upon separately computed torsional forces when an object is eccentrically loaded. The conventional torsional forces are perpendicular to and proportional to their radii from the center of gravity of the force pattern. This superposition gives rise to a centroid from which the vector sums are also perpendicular to and proportional to their radii from this centroid.

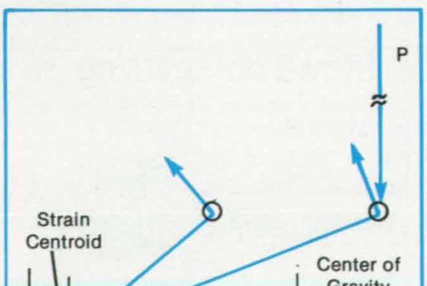

Strain Centroid has equal resisting forces.

The centroid lies on a line through the center of gravity and perpendicular to the direction of the eccentrically applied load.

After the elastic limit is exceeded (the wheels slip on the ground), the forces redistribute until each is at its maximum value. The forces are no longer perpendicular to radii from the centroid. They shift to being perpendicular to radii from the strain center. The strain center also lies on the line through the center of gravity and perpendicular to the direction of the eccentrically applied load.

This work was done by Donald B. Bickler of Caltech for **NASA's Jet Propulsion Laboratory**. *For further information, Circle 99 on the TSP Request Card. NPO-17966*

Zero-Spring-Rate Mechanism/Air Suspension Cart

A compact mechanism suspends articulating flexible structures with minimal constraints.

Langley Research Center, Hampton, Virginia

New suspension techniques will be necessary for ground-testing of the flexible spacecraft anticipated in NASA's future space activity. The most complex spacecraft involve nonlinear maneuvering (i.e., large-angle slewing) with such articulating substructures as remote manipulating systems. Ultimately, the goal of research in advanced suspension systems is to simulate flight boundary conditions (weightlessness) when testing flexible space structures on the ground. To achieve such a goal, a suspension system must counteract gravitational loads while allowing a structure to move without constraint. Because vibratory motion results from the elasticity of a flexible spacecraft, the suspension problem involves the development of methods of suspending spacecraft that have vibratory motions superimposed on large rigid-body motions. Any suspension device must be considered as an integral part of the structure. However, it should be designed so that the dynamics of the device interact minimally with the dynamics of the structure.

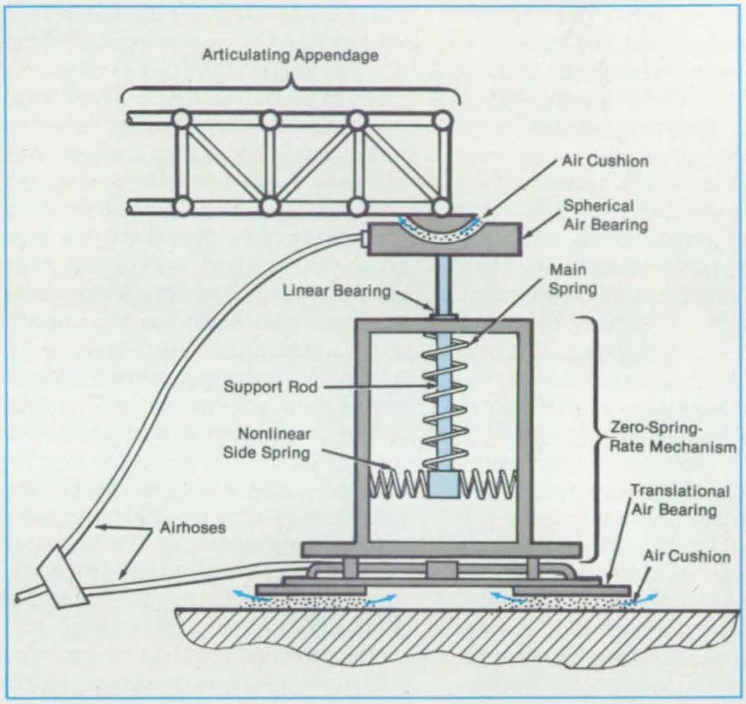

An **Articulating Appendage** is suspended from underneath by a ZSRM/air suspension cart.

A zero-spring-rate mechanism (ZSRM)/air suspension cart is being developed by NASA Langley Research Center. It is to be used to suspend flexible, "mass-critical" articles like lightweight spacecraft undergoing such large motions as slewing, translation, and telescoping/retraction. The novelty of the method and equipment is the ability to suspend a flexible article undergoing large rigid-body motion concurrent with vibratory motion, with minimal interaction between the suspended article and the suspending hardware. Previous suspension devices include cable suspensions, airbags, air bearings, and cables with ZSRM's. These devices are not designed for structures that undergo concurrent rigid-body and vibratory motions. The ZSRM/air suspension cart is very adaptive to active control, which would reduce undesirable effects caused by friction, nonlinearity, and mass coupling. The ZSRM/air suspension cart (see figure) is very small compared to a test article and is easily adapted to most test facilities. Because no cables are needed, minimal overhead clearance is needed. Because this device is built easily, it is practical for most suspension applications.

The design of this device evolves from the premise that as the dynamic properties of the suspension device are diminished, the dynamic properties of the test structure dominate the structure/suspension system. By combining a translational air bearing, a ZSRM, and a spherical air bearing, the design goal can be met. An air bearing carries a load in translation with very low friction. This air bearing allows the structure to have any horizontal motion. The ZSRM, which is placed atop the air bearing, supports the weight of structure with minimal vertical stiffness. A ZSRM is a negative nonlinear spring in parallel with a positive spring such as a prestressed coil spring. The negative spring can be any prestressed member that provides a component of prestressed stiffness in the vertical direction.

The weight of a structure is supported by the main spring. A compressive side load is applied to the structure-attachment point. When the article under test is displaced vertically from the equilibrium position of the main spring, a vertical component of the side load acts in a direction opposite to that of the load produced by the main spring. Because the vertical component of the side force acts in a sense opposite to that of the main spring, it behaves effectively like a negative spring. This negative spring reduces the overall stiffness in suspending a structure. By reducing the vertical stiffness, one decreases the constraint on the motion of the structure; that is, there is very little resistance to the vibratory motion of the structure. The spherical air bearing atop the ZSRM leaves the rotational motion of the structure at the point of attachment unconstrained. The overall effect of the device is that the weight of the structure is supported while its motion is virtually unconstrained. Therefore, the structure can behave as though it were weightless.

Another basic suspension consideration is whether structures will be supported overhead or underneath. Overhead suspension is usually accomplished with cables. These are widely used, their overall vertical stiffnesses can be reduced with ZSRM's, and they offer simplicity for ground testing of structures undergoing only vibratory motions. Cable suspensions have pendular and axial stiffnesses, and if they are used to suspend rapid slewing or articulating structures, then complicated control devices and suspension hardware must also be used. With the ZSRM/air suspension from underneath, high overhead height needed for cables (to reduce pendular and axial stiffness) is not required. Therefore, only the size of the structure will dictate how tall a test facility should be. Though the mass of the suspension hardware couples horizontally with the structure, its dynamic effect can be easily modeled analytically.

This work was done by Stanley E. Woodard and Victor M. Cooley of **Langley Research Center**. *No further documentation is available.*

This invention is owned by NASA, and a patent application has been filed. Inquiries concerning nonexclusive or exclusive license for its commercial development should be addressed to the Patent Counsel, Langley Research Center *[see page 14]*. *Refer to LAR-14142.*

Adjustable Pitot Probe

The probe is readily positionable in the core of uniform flow in a hypersonic wind tunnel.

Langley Research Center, Hampton, Virginia

Pitot probes are generally used to measure the pressures of high-velocity fluid streams in wind tunnels. In a hypersonic wind tunnel, the air is heated up to about 3,000 °F (about 1,600 °C) to prevent liquefaction of the nitrogen and oxygen in the flow. The transducers used to measure the pitot pressures must be protected from the hostile temperatures to prevent thermally induced measurement errors and possible damage to the transducers. Therefore, the pressure transducers are usually mounted outside of the test section, connected to the tips of the probes through relatively long tubes. The large volume of such a connecting tube causes an undesirable increase in the "settling time" of the pressure probe, the shortness of which can be essential to accurate measurements. Also, a free-stream pitot pressure probe is typically mounted on the wall of a tunnel or on an injection mechanism, and its position can be adjusted within only a limited range. Accordingly, in the design of a new cooled, readily positionable pressure probe, the transducer is mounted relatively close to the tip of the probe.

The probe is formed of a pair of mating cylindrical housings: the transducer housing and the pitot-tube housing. A small hole is bored through the transducer housing along its centerline. A hole slightly larger than the body of the sensor portion of the transducer is bored from one end along the same line to a depth large enough to provide a pressure-sensing chamber beyond the tip of the transducer. The transducer mounting post, in the vicinity of the pressure-sensing chamber, is surrounded by a cooling-water annulus, which has full-depth webbing 180° apart to divide it in half. It also has cross-connecting water passages at full depth to force the water to flow completely around the volume area to be cooled. A thermocouple sheathed in stainless steel is inserted from the other end into the pressure-sensing chamber to monitor the temperature. The transducer housing also contains a pressure annulus and a larger annulus that accommodates a boss on the pitot-tube housing.

The pitot-tube housing has a pressure annulus that matches the boss. The pitot pressure is delivered from the pitot tube, which points into the free stream, to the pressure-sensing chamber via a metal bellows that connects the pitot tube to its housing. The pitot tube is supported by an adjustable wedge fairing attached to the top of the pitot-tube housing with a semicircular foot. This foot extends over the transducer housing with a radial clearance and allows the pitot tube to rotate to any orientation within 360°.

Because of the design of the wedge fairing, the probe can be adjusted both radially and circumferentially. In addition, the pressure-sensing transducer in the adjustable probe is cooled internally by water or other cooling fluid passing through the annulus of the cooling system.

This work was done by George C. Ashby, Jr., W. Eugene Robbins, and Lewis A. Horsley of **Langley Research Center**. *For further information, Circle 113 on the TSP Request Card.*

This invention is owned by NASA, and a patent application has been filed. Inquiries concerning nonexclusive or exclusive license for its commercial development should be addressed to the Patent Counsel, Langley Research Center [see page 14]. Refer to LAR-14232.

Calculating Dynamics of Helicopters and Slung Loads

Motions of multiple lifting helicopters, spreader bars, cables, and loads can be simulated numerically.

Ames Research Center, Moffett Field, California

General equations have been derived for numerical simulations of the motions of multiple-lift, slung-load systems that consist of two or more lifting helicopters and loads slung from them by various combinations of spreader bars, cables, nets, and attaching hardware. The use of multiple (usually, two) helicopters to lift loads too heavy for one of them has been advocated for decades. However, with the exception of some limited flight tests and a few isolated commercial operations, the dual-lift technique remains largely undeveloped because of the complexity of motion and the consequent difficulty of stabilizing and coordinating the motion, both along the flightpath and in precise hover. New general equations are readily programmable for efficient computation of the motions; thus, they lend themselves well to the analysis and design of control strategies for stabilization and coordination.

In the mathematical model of a multiple-lift system, the helicopters, spreader bar(s), and load are treated as rigid bodies. The attaching hardware and nets are not modeled. The cables are treated as massless straight-line links that can be either inelastic (in the sense of unstretchable) or elastically stretchable. The aerodynamics of the cables are neglected. This model is expected to represent motions adequately at the frequencies up to a few hertz that are of interest in controlling the trajectories of the helicopters.

The derivation begins with the application of the Newton and Euler equations of motion to each rigid body, the definition of vectors that describe the configuration of the system, the introduction of generalized velocity coordinates, and the application of D'Alembert's principle to each body in the system. This approach leads to three formulations, two of which are generalized versions of formulations developed previously for specific cases involving inelastic and elastic cables. The third formulation is a new one obtained by choosing the generalized coordinates in the elastic-cable formulation in such a way that they are partitioned into (1) d coordinates that represent the motion of the system as though the cables were inelastic and (2) c coordinates that describe the component of the motion due to stretching of the cables (where c is the number of constraints that would be imposed by the cables if they were inelastic). For inelastic suspensions, the cable tensions are obtained from the equations governing the stretching-motion coordinates, and this solution is used in the equation for the remaining coordinates. In comparison with the conventional formulation, the new formulation is computationally more efficient.

The new formulation has been applied to obtain equations for the dual-lift system illustrated in the middle of the figure. The other dual-lift systems shown at the left and right can be treated as special cases of the system in the middle by appropriate simplifications of the equations to account for elimination of the bridle cables (left) or elimination of the spreader bar and tether cables (right). In each case, the equations are written in terms of the natural vectors and matrices of the dynamics of three-dimensional rigid bodies and are tractable for both analysis and programming.

This work was done by Luigi Cicolani

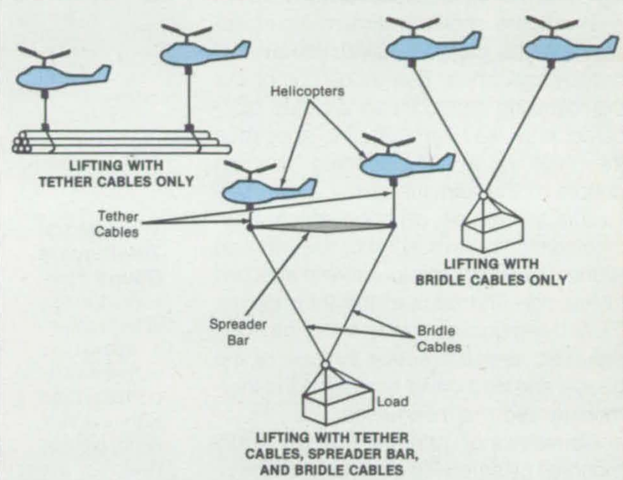

Two Helicopters Lift One Load with the help of cables and, optionally, a spreader bar. The motions of suspension systems like these are complicated and must be simulated numerically for analysis and control.

and Gerd Kanning of **Ames Research Center**. *Further information may be found in NASA TM-102246 [N90-17641], "Equations of Motion of Slung Load Systems with Results for Dual Lift."*

Copies may be purchased [prepayment required] from the National Technical Information Service, Springfield, Virginia 22161, Telephone No. (703) 487-4650. Rush orders may be placed for an extra fee by calling (800) 336-4700.
ARC-12755

Integral Plug-Type Heat-Flux Gauge

The integral construction reduces the components of error caused by discontinuities.

Lewis Research Center, Cleveland, Ohio

A new heat-flux gauge eliminates measurement errors caused by temperature discontinuities associated with conventional gauges. The new gauge yields more accurate surface heat-flux data for verifying aerodynamic and heat-transfer models.

The figure shows a schematic of the new heat-flux gauge mounted into a metal or alloy specimen. The gauge comprises the following items: (1) an annulus fabricated part way through the specimen thickness, (2) a wall extending from the bottom of the annulus to the active surface of the gauge, (3) a cylindrical thermoplug that is surrounded by the annulus, (4) thermocouple thermoelements attached to the side and back of the thermoplug, (5) a thermocouple with a hot junction mounted near the active surface of the gauge, and (6) a cover enclosing the thermoplug and thermocouples.

Conventional gauges are generally mounted by screwing or welding them into position. Sharp temperature changes are possible across the temperature discontinuities formed by the resulting threads or seams. These temperature discontinuities can produce large errors of measured surface heat flux. Unlike a conventional gauge, the new gauge is not screwed or welded into place, but instead a thermoplug and annulus are electrical-discharge-machined (EDM) into the specimen material. The EDM process leaves no interface between the material and the thermoplug, thus inherently increasing gauge accuracy by eliminating the interface and the associated temperature discontinuity. The EDM process is also conducive to accurate fabrication of minute gauges.

Gauges can be fabricated in a variety of sizes. Thermoplug diameters are currently 0.040 in. (1.02 mm), and lengths are about 0.060 in. (1.52 mm). Wall thicknesses nominally vary from about 0.010 in. (0.25 mm) to 0.020 in. (0.51 mm) (see figure). Annulus depths range from 0.060 in. (1.52 mm) to 0.100 in. (2.54 mm). Annulus widths are typically 0.020 in. (0.51 mm).

Temperatures are measured with commercial coaxial (single-wire) thermocouple assemblies, which are modified by swaging them to a diameter of 0.010 in. (0.254 mm) and then by stripping them to expose a 0.0015 in. (0.038 mm) diameter Chromel* or Alumel* (or equivalent) thermoelement (wire). Pairs of Chromel and Alumel wires are joined and spotwelded to the sides of the thermoplug to form hot junctions. The junctions are located circumferentially 120° from each other along the length of the thermoplug. The wires are extended from the junctions in a direction perpendicular to the cylindrical plug surface and are then routed through the annulus to the back of the gauge. The wires are carefully positioned so that they do not touch metal surfaces. The coaxial thermocouple assemblies are then extended from the rear of the material gauge (see figure) and laid side by side within grooves electrical-discharge-machined into the material. The grooves and assemblies are covered with metallic, material welded to the specimen. The thermocouple assemblies are extended to remote data systems for temperature-data storage. A cover is welded over the plug to seal thermally insulating air within the annulus. The air minimizes heat loss from the thermoplug. To measure temperature near the active surface, individual Chromel and Alumel thermoelements in the coaxial thermocouple assemblies are joined and spotwelded to the bottom of a hole electrical-discharge-machined from the annulus side into the wall (see figure). The hole is nominally located 0.010 in. (0.254 mm) below the active surface.

The **Integral Thermoplug Gauge** measures the flux of heat across a specimen of material. In comparison with conventional gauges that are screwed or welded in place, the integral thermoplug gauge is more accurate.

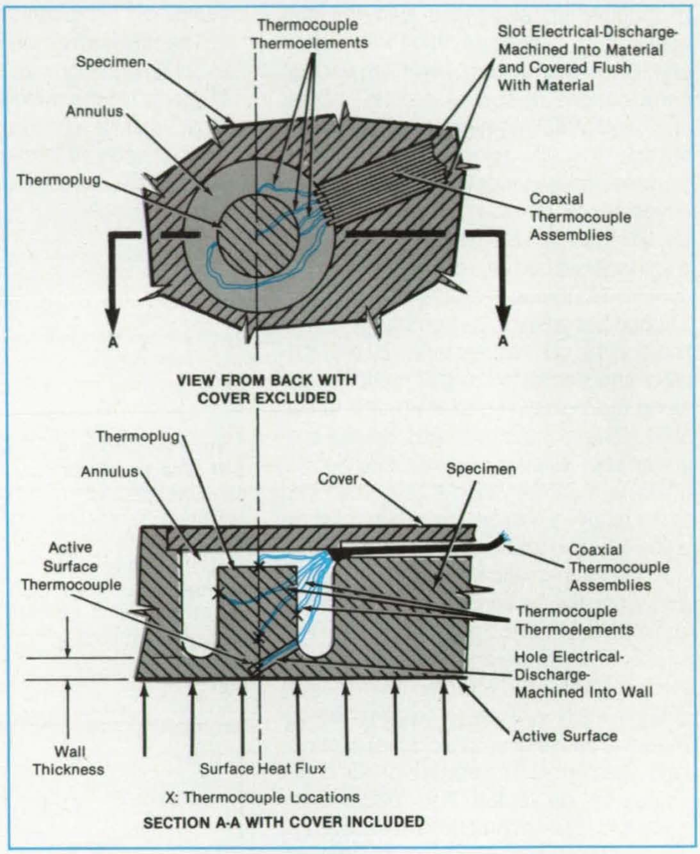

HEAT FLUX GAUGE

The gauges measure both transient and steady-state surface heat flux. Temperature as a function of time is recorded at each thermocouple location. The surface heat flux and rate of change of surface heat flux are calculated from temperature-vs.-time data, known properties of the gauge material, thermocouple positions measured from the active surface of the gauge, and thermoplug length. A gauge of this type functions at temperatures ranging from cryogenic to the melting temperatures of metals and alloys.

This work was done by Curt H. Liebert and John Koch, Jr., of **Lewis Research Center**. *For further information, Circle 28 on the TSP Request Card.*

This invention is owned by NASA, and a patent application has been filed. Inquiries concerning nonexclusive or exclusive license for its commercial development should be addressed to the Patent Counsel, Lewis Research Center [see page 14]. Refer to LEW-14967.

Mixed-Mode-Bending Delamination Apparatus

Double-cantilever-beam and end-notch-flexure loads are applied simultaneously.

Langley Research Center, Hampton, Virginia

Failures in structural composites often develop as delamination between laminated plies. Typically these delaminations are initiated and grow as a result of combined peeling (opening) stresses and sliding (shear) stresses. Therefore, studies of resistance to delamination should account for the effects of combined opening and shear stresses, referred to as mode I and mode II stresses, respectively.

Although most delamination tests are currently conducted by use of single-mode specimens, various mixed-mode test procedures have been introduced. Unfortunately, each of these mixed-mode test procedures has one or more limitations. For example, with some tests, only a narrow range of mode I/mode II ratios can be tested, and others require difficult time-consuming numerical analyses of the test results. Therefore, the mixed-mode-bending delamination apparatus was developed to apply mode I and mode II loads simultaneously to a simple test coupon to measure delamination resistance.

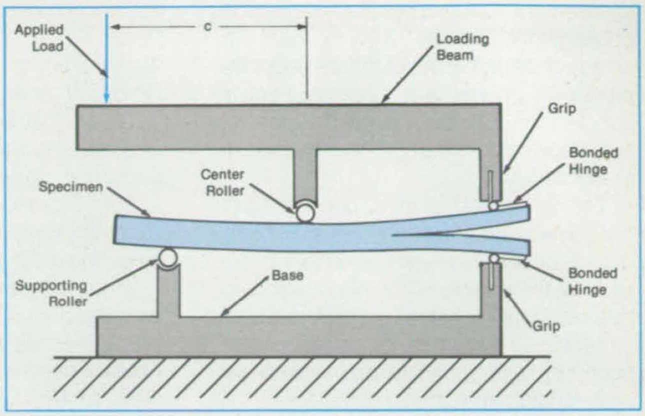

The **Mixed-Mode-Bending Delamination Apparatus** generates two types of delamination stress simultaneously in the specimen from a single externally applied point load.

The figure illustrates a test conducted with the apparatus. The specimen is loaded in a manner that represents a combination of two well-known procedures used in pure mode I and mode II testing. The upward load on the right end is like that used in a double-cantilever-beam (DCB) test for mode I delamination. The downward load is like that used in an end-notch-flexure (ENF) test for mode II delamination. These loads can be applied simultaneously to produce combined mode I and mode II delamination in the specimen.

The combined load is produced by applying a single load to a beam attached to the specimen. Bonded hinges on the end of the specimen are attached to the loading beam and to the base of the apparatus by use of grips. The left end of the specimen rests on a supporting roller. A center roller loads the specimen downward, and, simultaneously, the right end of the specimen is loaded upward. These two loads are in proportion to the applied load, and their relative magnitudes depend on the loading distance, *c*. By varying *c*, a wide range of mode I/mode II ratios for mixed-mode delamination testing can be produced.

The mode I and mode II loading on the specimen can be expressed in terms of the applied load, which can be measured by use of a conventional test machine. Then simple equations related to DCB and ENF testing can be used to resolve the measured mixed-mode response into its mode I and mode II components. For example, mixed-mode delamination toughness can be determined by measuring the applied load during an increment of delamination growth and can then be resolved into mode I and mode II components. Also, these simple equations for pure mode I and mode II testing provide for selection of *c* to obtain desired mode I/mode II test ratios.

In this technique, the individual mode I and mode II contributions to delamination in the specimen can be analyzed by use of simple beam-theory equations, thereby eliminating the need for time-consuming, difficult numerical analysis. Also, this technique allows a wider range of mode I/mode II ratios than are possible with many other methods. Mixed-mode delamination testing is of interest in all fields that utilize composite materials. Composite materials are used mostly in the aerospace field, but are also used in automobiles, lightweight armored military vehicles, boats, and sporting equipment. This technique could also be useful in the general lumber, plywood, and adhesive industries.

This work was done by John H. Crews Jr., and James R. Reeder of **Langley Research Center**. *Further information may be found in NASA TM-100662 [N89-10945], "A Mixed-Mode Bending Apparatus for Delamination Testing."*

Copies may be purchased [prepayment required] from the National Technical Information Service, Springfield, Virginia 22161, Telephone No. (703) 487-4650. Rush orders may be placed for an extra fee by calling (800) 336-4700.

This invention is owned by NASA, and a patent application has been filed. Inquiries concerning nonexclusive or exclusive license for its commercial development should be addressed to the Patent Counsel, Langley Research Center [see page 14]. Refer to LAR-13985.

Books and Reports

These reports, studies, handbooks are available from NASA as Technical Support Packages (TSP's) when a Request Card number is cited; otherwise they are available from the National Technical Information Service.

Incompressible, Viscous Flow About an Ogive/Cylinder

Calculated flow patterns agree closely with experimental ones.

Theoretical predictions and observations of incompressible viscous flow about a body of revolution at an angle of attack are compared in a report. This study was a test of modern numerical methods for the solution of the equations of fluid dynamics, and was conducted as a step toward future work on more difficult problems.

The body consisted of a solid circular cylinder at the downstream end and tapered in an ogive of revolution to a point on the axis at the upstream end. The cylinder had a length-to-diameter ratio of 1, and the ratio of the length of the ogive to the diameter of the cylinder was 3.5, yielding an overall length-to-diameter ratio of 4.5.

The ogive/cylinder was placed in a towing tank and a camera was mounted to move along with it. The tank was filled with salt water seeded with small particles. When illuminated by a fan of laser light and photographed, the particles produced streak images, the lengths and directions of which indicated the local velocity of the flow about the body. Observations were made at angles of attack of 30° and 45°. Previous studies had shown that the flow is steady at angles of attack up to 60°.

For the simulation, the flow was represented by the Navier–Stokes equations in mass-averaged variables, with terms for pseudocompressibility. The pseudocompressibility allows the use of an implicit finite-difference scheme and relaxes the requirement of incompressibility during the convergence process. Upon reaching the steady state, the effect of the pseudocompressibility on a solution becomes negligible, and the solution is essentially that of the Navier–Stokes equations of incompressible flow.

The computational mesh conforming to the ogive/cylinder was generated by a two-dimensional Poisson-grid generator in the plane of the body axis. The plane was then rotated about the axis to generate a three-dimensional wrapped mesh. The outer boundary was spherical and located six body lengths from the tip of the ogive.

The equations were solved numerically by use of the INS3D computer code. Implicit second-order and explicit fourth-order numerical dissipation was added to damp out high-frequency oscillations. The solution was advanced in time until the steady state was reached.

The computed and photographed crossflows at various positions along the ogive and at both angles of attack were in qualitative agreement. In general, the crossflow, which develops along the body, produces a pair of leaside vortices. An analysis of the development of the symmetric vortical flow field reaffirms the utility of the impulsive-flow analogy in understanding the qualitative nature of the flow.

This work was done by Gregory G. Zilliac of **Ames Research Center**. *Further information may be found in NASA TM-88329 [N90-11254], "A Computational/Experimental Study of the Flow Around A Body of Revolution at Angle of Attack."*

Copies may be purchased [prepayment required] from the National Technical Information Service, Springfield, Virginia 22161, Telephone No. (703) 487-4650. Rush orders may be placed for an extra fee by calling (800) 336-4700.

Inquiries concerning rights for the commercial use of this invention should be addressed to the Patent Counsel, Ames Research Center [see page 14]. Refer to ARC-11793.

Research in Helicopter Noise

Progress in aeroacoustical theory and experiments is reviewed.

A report summarizes continuing U.S. Army programs of research into the causes of noise generated by helicopters. There are many such causes, most of which are related to aerodynamic phenomena around rotor blades and fuselages. Among the most notable advancements of recent decades have been computer codes for the prediction of high-speed impulsive noise, a technique for the measurement of noise in flight, and a joint Army/helicopter-industry test program in an anechoic wind tunnel.

One of the three main topics discussed in the report is high-speed impulsive noise. Experimental data have been taken by a quiet airplane instrumented with microphones, flying in formation with a helicopter. High-speed impulsive noise manifests itself in such measurements as strong negative pressure peaks observed during level flight at high speeds. This type of noise has been shown to be caused by effects of the thicknesses of rotor blades and transonic flow around the blades. High-speed impulsive noise has also been studied with models in wind tunnels. From flight and wind-tunnel tests, it has become clear that high-speed impulsive noise can be scaled and that the primary scaling parameter is the mach number of the advancing tip of the rotor blade.

The theoretical analysis of high-speed impulsive noise is based on an equation for the far-field acoustic pressure in terms of monopole and dipole integrals over the surfaces of rotor blades and the surrounding volume. Comparisons between theoretical predictions and experimental data are presented.

The second main topic is noise caused

by interactions between rotor blades and vortices. This phenomenon is not as well understood as is high-speed impulsive noise. It is known, however, that this type of noise can be scaled for low advance ratios and that the scaling parameters are the mach number of the advancing tip of the rotor blade, the advance ratio, the coefficient of thrust of rotor colitity, and the angle of the plane defined by the path of the tips of the rotor blades. Techniques of computational fluid dynamics are now emerging for the understanding of the interactions between blades and vortexes and the noise caused by them.

The third topic is the joint Army/helicopter-industry test program. Acoustic and aerodynamic measurements are taken in a wind tunnel with advanced, dynamically scaled, pressure-instrumented model rotor systems to relate the important aerodynamic phenomena to near- and far-field acoustic radiation. Topics of study include high-speed impulsive noise, blade/vortex-interaction noise, and low-frequency harmonic noise.

This work was done by Yung H. Yu, Frederic H. Schmitz, and Andrew H. Morse of **Ames Research Center**. *To obtain a copy of the report, "Aeroacoustic Research Programs at the Army Aviation Research and Technology Activity," Circle 15 on the TSP Request Card.*
ARC-12171

Growth of Instabilities in Two Types of Mixing Layers

Effects of feedback are examined.

A report discusses issues involved in the computation of the growth of instabilities and vorticity in the mixing (shear) layer between two parallel flows that have different speeds and are separated initially by a flat surface. The study focusses upon the degree to which these growing flow structures hasten or retard their own further growth, and upon the related question of the differences between flows computed according to mathematical models of S-layer and T-layer mixing.

An S (for "space") layer is a shear layer that develops downstream of a point where the two streams are brought into tangential contact. This kind of shear layer is better suited to experimental study in a laboratory where, for example, it can be formed at the downstream edge of a thin splitter plate. A T (for "time") layer is a shear layer in which infinitesimal wrinkles grow and roll up into vortexes, developing in time from an initial tangential velocity discontinuity at the plane separating the half spaces that contain the initial uniform flows. A T-layer is better suited to theoretical study because the differential equations that describe its development are parabolic in time (as opposed to elliptic for the S-layer) and, therefore, an initial perturbation can be specified according to the linear theory and its growth treated by linear/weakly nonlinear and computational techniques.

The author notes that despite the similarities between S- and T-layers, the common practice of interpreting observations of S in terms of calculations with T may be misleading. One of the physical questions associated with the difference between T- and S-layers is whether distant vortexes, which have already paired once or several times downstream in the S-layer, can induce perturbations upstream that seed the subharmonic instability. If so, the downstream development of the S-layer would not depend on perturbations imposed upstream but the S-layer would create its own perturbations and continue to develop downstream. To examine this question, the author offers a model of the S-layer that introduces the elliptic nature of real flow indirectly to some level of approximation in the solution for the T-layer.

The method of comparison between the S- and T-models is to assume that the vorticity of the S-layer is given parabolically by a Galilean mapping of that of the T-layer, to satisfy the appropriate boundary conditions in the S-layer and compute the velocity induced at any point in the S-layer by its vorticity field, and to compare this velocity to that which can be derived from the velocity of the T-layer at corresponding points by a Galilean transformation of the velocity itself. The purpose of these calculations is to assess approximately how far the flow in the S-layer is from parabolic and, in particular, to what extent the perturbations induced upstream by large downstream concentrations of vorticity exert the retarding or hastening effect described above. The results of the calculations suggest that this elliptic influence, or the feedback, in a mixing layer is relatively small, at least for flows in which the normalized difference between the two initial velocities is relatively small. Thus, the transformation method used in this study offers a suitable tool for the study of such flows.

This work was done by Upender K. Kaul of Sterling Federal Systems for **Ames Research Center**. *To obtain a copy of the report, "Do large structures control their own growth in a mixing layer? An assessment," Circle 89 on the TSP Request Card.*
ARC-12567

Block Lanczos Algorithm for Gyroscopic Systems

Vibrations of rotating structures are calculated more efficiently.

A report describes the details of implementation of a procedure for the accurate and economical computation of natural frequencies and associated vibrational modes of an elastic structure rotating along an arbitrary axis (e.g., a rotating, vibrating artificial satellite). A block version of the Lanczos algorithm is derived for the solution of the eigenvalue and eigenvector problems. This version fully exploits the sparsity of the associated matrices and employs only real numbers in all relevant computations. It is also capable of determining multiple roots and proves to be most efficient when compared to other similar existing techniques.

The equations of motion are usually put in the form

$$(A + \omega B)y = 0$$

where A is a matrix that contains the inertia matrix M and the stiffness-and-centrifugal-force matrix K as two blocks on the diagonal, B is a matrix that contains off-diagonal antisymmetric blocks $-M$ and $+M$ and an antisymmetric Coriolis matrix C on the diagonal, y is a displacement-and-velocity vector, and ω represents the natural frequencies (purely imaginary for steady oscillations).

The conventional solution process involves the implicit inversion of A to reduce the eigenvalue problem to one in terms of a single matrix of twice the original size. However, this procedure is inefficient due to the nonsparse character and increased order of the matrix.

To obtain the new block Lanczos algorithm, the equation is first rewritten as

$$(A - \lambda D)y = 0$$

where $D = iB$ is a pure imaginary Hermitian matrix, the roots $\lambda = i\omega$ are real and occur in pairs $\lambda_1, -\lambda_1, \ldots, \lambda_n, -\lambda_n$, and the corresponding eigenvectors occur in complex-conjugate pairs. To obtain a single matrix from the set of two matrices that define this equation, one performs a Choleski decomposition

$$A = L_A L_A^T$$

in which

$$L_A = \begin{bmatrix} L_M & 0 \\ 0 & L_K \end{bmatrix}$$

and L_M, L_K are the lower triangular forms of matrices M and K, respectively. The equation is then transformed to

$$(H - \gamma I)y = 0$$

in which $\gamma = 1/\lambda$, $\omega = 1/i\gamma$, and the matrix H is expressed as

$$H = \begin{bmatrix} 0 & -iL_M^T L_K^{-T} \\ iL_K^{-1} L_M & iL_K^{-1} C L_K^{-T} \end{bmatrix}$$

At this point, several new constituent matrices and matrix operations are defined and used to describe a procedure to recast the block Lanczos algorithm in terms of real numbers.

The method was demonstrated by application to a spinning cantilever beam and a spinning cantilever plate. While each step in the block algorithm is costlier than in the conventional nonblock Lanczos method, fewer steps are needed. The overall saving in solution time is comparable to that effected by block multivector inverse iteration in place of the single-vector iteration process. Furthermore, this procedure is capable of effective determination of multiple roots in which the usual nonblock procedure is deficient. Also, although some experience may be necessary in choosing an optimum block size, a range between 2 and 4 has been found to be effective.

This work was done by Kajal K. Gupta of **Ames Research Center** *and Charles L. Lawson of Harvey Mudd College. Further information may be found in NASA TM-88290 [N87-19753], "Implementation of a Block Lanczos Algorithm for Eigenproblem Solution of Gyroscopic Systems."*

Copies may be purchased [prepayment required] from the National Technical Information Service, Springfield, Virginia 22161, Telephone No. (703) 487-4650. Rush orders may be placed for an extra fee by calling (800) 336-4700.
ARC-12147

Placement of O-Rings in Solid Rocket Booster

Outward bowing of the wall would tighten the seal.

A brief report proposes to modify the placement of the O-ring seals in the joints of the Solid Rocket Booster of the Space Shuttle. This proposal is one of the suggestions derived from analysis of the Space Shuttle Challenger disaster, which has been attributed to the failure of these O-ring seals.

The analysis showed that the pressure from the burning propellant caused the wall of the booster to bow outward. Because the outward bowing is greater in the portions of the wall between the joints than at the joints, the joints bend a little: this is the phenomenon known popularly as "joint rotation." The joint consists of a tang ring locked by pins into a clevis ring, and in the old configuration, the O-rings are placed between the tang and the clevis on the inner side of the tang. The joint rotation causes the tang to pull away from the O-rings, with consequent loss of seal.

The modified joint and seal would be essentially an "inside-out" version of the old joint and seal. In the modified joint, the O-rings would be placed between the outer side of the tang and the clevis. The joint rotation would push the tang harder against the O-rings, thereby making an even tighter seal.

This work was done by Charles Wood of Caltech for **NASA's Jet Propulsion Laboratory**. *To obtain a copy of the report, "Placement of O-Rings in the Space Shuttle Solid Rocket Booster," Circle 12 on the TSP Request Card.*
NPO-18008

Machinery

Hardware, Techniques, and Processes

Books and Reports

Bearing-Cartridge Damping Seal

Ball bearings would carry reduced loads and be cooled more effectively.

Marshall Space Flight Center, Alabama

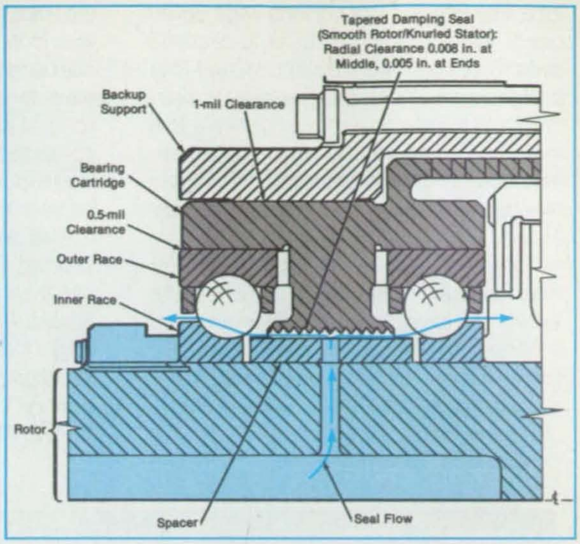

The **Damping Seal** would be incorporated into the bearing cartridge to divert loads from the ball bearings and damp vibrations of the rotor.

In a proposed design for an improved ball-bearing cartridge, a damping seal in the form of a thin-layer fluid journal bearing would be incorporated into the cartridge. The damping seal would act as an auxiliary bearing, relieving the bearing balls of significant portions of both the static and the dynamic bearing loads. The damping from the seal would reduce the dynamic loads even further by reducing the amplitude of vibrations in the second vibrational mode of the rotor, which mode occurs when the rotor is turning at nearly the full operating speed. The damping-seal-cartridge design is intended for use in the high-pressure-oxygen turbopump of the Space Shuttle main engine, but the design concept should also be applicable to other turbomachinery bearings.

The bearing cartridge would be mounted with 0.001-in. (0.025-mm) radial clearance in the backup support attached to the stator. The outer races of the bearing would be mounted with 0.0005-in. (0.013-mm) radial clearance in the bearing cartridge (see figure). Because the static lateral loads would remain greater than the dynamic lateral loads throughout each turn of the rotor, the bearings and cartridge would be held to one side within their radial clearances.

The damping seal would be formed by the fluid in the gap between the knurled inner surface of the cartridge and the smooth outer surface of a spacer on the rotor. The damping seal would be 1 in. (2.54 cm) long and located between the two ball bearings. A small volume of the pumped fluid (in this case, liquid oxygen) would flow along the axis of the rotor, then along six radial roles to holes in the spacer that are aligned 50° from radial backward from the rotation. This arrangement would partly deswirl the flow as it entered the damping-seal gap. Deswirling would reduce the undesired cross-coupling stiffness while maintaining the desired direct stiffness and damping for optimum rotordynamic performance. As it emerged from the damping-seal gap, this flow would discharge directly into the heat-generating zone of the ball bearings, thereby helping to remove heat from the bearings and consequently prolonging their operating life.

The design of the seal is limited by the available supply pressure and rate of flow. The seal is designed to impose the controlling resistance in its flow circuit and to provide maximum stiffness versus leakage, thus providing maximum support for the rotor in the face of the limited supply flow. The design that results from this combination of requirements calls for the knurled cartridge surface and a gap that tapers from 0.008 in. (0.20 mm) radial clearance at the middle to 0.005 in. (0.13 mm) at the ends. (The gap and the knurl are exaggerated for clarity in the figure.)

This work was done by David G. Goggins, Joseph K. Scharrer, and Wei C. Chen of Rockwell International Corp. for **Marshall Space Flight Center**. *For further information, Circle 85 on the TSP Request Card.*

Inquiries concerning rights for the commercial use of this invention should be addressed to the Patent Counsel, Marshall Space Flight Center [see page 14]. Refer to MFS-29657.

Books and Reports

These reports, studies, handbooks are available from NASA as Technical Support Packages (TSP's) when a Request Card number is cited; otherwise they are available from the National Technical Information Service.

Damping Seals Would Help Support Turbopump Rotor

Tentative designs are presented.

A report describes an engineering study of the proposed use of damping seals as major load-carrying members of the high-pressure-oxygen turbopump of the Space Shuttle main engine. The damping seals would be incorporated into the bearing packages at the preburner-pump and turbine-end locations on the pump rotor. This exploration of the damping-seal concept was motivated by the need to increase the operating lives of the ball bearings that support the rotor by relieving them of damaging transient lateral loads.

A damping seal of the type in question is a leaky thin-layer liquid bearing somewhat reminiscent of a labyrinth seal. It is formed by directing some of the pumped fluid (in this case, liquid oxygen) into the volume defined by the roughened or pocketed inner surface of a stator member and the smooth outer surface of a rotor member that fits in the stator member with a small radial clearance. The damping seals are required to act in parallel with, and remove most or all of the radial load from, the ball bearings during operation. The damping seals and ball bearings must act in concert to suppress the bending-mode vibrations of the rotor. The overall result should be longer bearing lives and a rotor-supporting system that is almost fully redundant.

The modified bearing packages are required to be robust and simple and to allow the proper transfer of loads to the damping seals. This means, among other things, the smooth transfer of loads from the ball bearings to the seals as the pump approaches the operating speed. The installation of the seals must not impose any additional bearing loads (for example, because of slight misalignments caused by accumulations of manufacturing tolerances) and must not compromise the integrity of the pump in any other way. The seals are required to function with the pressure gradients available in the unmodified pump design. The damping seals are also required to prevent rotation of the outer races of the ball bearings.

During the design study, specifications for the required performance, design envelope, and boundary conditions were developed. Various seal and bearing-package design concepts were evaluated, and final designs were selected and analyzed. Alternatives to standard damping seals were also evaluated. After selection of the best bearing-package design concepts, preliminary mechanical designs were prepared and analyzed.

Three damping-seal designs — two at the preburner-pump location and one at the turbine-end location — were developed and analyzed. An alternative that was developed for the turbine-end location consisted of a pocketed hydrostatic bearing with an unique geometry of stationary pockets and a rotating feed. The dynamic performance of the rotor/bearing system was evaluated. It was found that two critical speeds that excite bending-mode vibrations of the rotor will have to be traversed below the running speed. However, the dynamic behavior was computed to be very well controlled, and the response of the rotor was computed to be very heavily damped.

This work was done by O. Pinkus, J. Walowit, C. Lee, and F. Gillham of Mechanical Technology, Inc., and P. Buckman of Aerojet TechSystems for **Marshall Space Flight Center**. *To obtain a copy of the report, "Damping Seal Rotor Support in Turbomachinery," Circle 3 on the TSP Request Card. MFS-27227*

Carrying Humans to and from Mars

A proposed spacecraft would incorporate advanced technologies.

A document presents a conceptual design for a space vehicle to carry human explorers from Earth to Mars, then back to Earth. The design takes into account promising — and sometimes conflicting — new technologies that would make Mars missions possible. Some new technologies like radiation-storm shelters and advanced cryogenic propulsion can readily be integrated into familiar vehicles. Others, however, demand fundamentally new vehicles. Such technologies include modular hardware, robotic assembly and maintenance, rotating artificial gravity, and high-energy aerobraking.

The vehicle would be an assembly of discrete, often modular, systems. With simple modifications, the systems can be reconfigured to accommodate the widely varying transfer energies of the phases of the mission (from Earth to orbit about the Earth, from orbit about the Earth to orbit about Mars, from orbit about Mars to landing on Mars, and so forth).

The crew would occupy a triangular racetrack of three Space-Station modules: one for dormitory and garden; one for galley, wardroom, operations, and recreation; and one for science and the maintenance of health. The crew modules would be mounted on an aerobrake that would be used for arrival at Mars and return to Earth. An auxiliary vehicle would carry four crewmembers from orbit about Mars to the surface of that planet for 60 days of exploration, then carry them back to the main vehicle.

For most of the time in transit between Earth and Mars, except during changes in course, systems would be extended from tethers and rotated to generate artificial gravitation for the crew. A tether crawler, powered by its own solar cells, would reposition scientific instruments as necessary to keep them at the center of gravity.

Robotic manipulators would be used to reconfigure the vehicle for the various phases of the mission and to perform maintenance in flight. The robot arms would travel along the rim of the aerobrake and be able to reach all points on the exterior of the spacecraft.

This work was done by Brent Sherwood of Boeing Huntsville Advanced Civil Space System for **Marshall Space Flight Center**. *To obtain a copy of the report, "Manned Mars Mission Vehicle Concept," Circle 64 on the TSP Request Card.*

Inquiries concerning rights for the commercial use of this invention should be addressed to the Patent Counsel, Marshall Space Flight Center[see page 14].Refer to MFS-28453.

Fabrication Technology

Hardware, Techniques, and Processes

Computerized Profilometer for Inspection of Welds

Subjective inputs in inspection are reduced with consequent enhancement of precision.

Marshall Space Flight Center, Alabama

A third-generation profilometer for the inspection of butt welds includes a hand-held probe unit that operates in conjunction with a computer. In comparison with first- and second-generation profilometers, this one increases precision by reducing subjective inputs and the concomitant variations in outputs among different operators. In addition, the training of operators is simplified.

A contour gauge in the hand-held probe unit acquires a surface profile or cross section (see figure) and reproduces the profile mechanically in the input-image aperture of an array of optoelectronic sensors. A microprocessor in the hand-held probe unit collects the raw image data (64 pairs of x, y coordinates) and sends them to the computer via a standard serial data link. The computer processes these data into a dimensionally correct cross section of the weld, locates the centerline, and computes the peak angle and mismatch of the weld. The results of these computations are sent over a parallel data port to a printer/plotter, which prints the peak angle and mismatch and plots the cross section.

The computerization of the third-generation profilometer retains the capabilities of the first- and second-generation profilometers to measure the peak angles and mismatches of butt welds and extends measurement capabilities into the field of image analysis. This makes the profilometer an expandable system in the sense that the computer program can be made to extract and quantify subtle features in a weld profile. For example, it could be made to detect a weld bead, measure its width and height, and assess its symmetry. With modifications of the hand-held probe and further modifications of the software, the profile-analysis capability could be extended to include such other inspection functions as rapid, objective measurements of diameters, concentricities, angles, and general profiles, as well as tooling-setup functions for which rapid, objective measurements are required.

Yet another advantage of computerization is that output data are more readily processable into forms that can be used by the same or another computer. This feature is desirable for the development of data bases and for the development of systems that perform other analyses; e.g., to determine statistics on the qualities of manufactured products for use in controlling manufacturing processes.

This work was done by M. A. Badinger, F. N. Stone, and G. J. Drouant of Martin Marietta Corp. for **Marshall Space Flight Center**. *For further information, Circle 59 on the TSP Request Card.*

Inquiries concerning rights for the commercial use of this invention should be addressed to the Patent Counsel, Marshall Space Flight Center [see page 14]. Refer to MFS-28548.

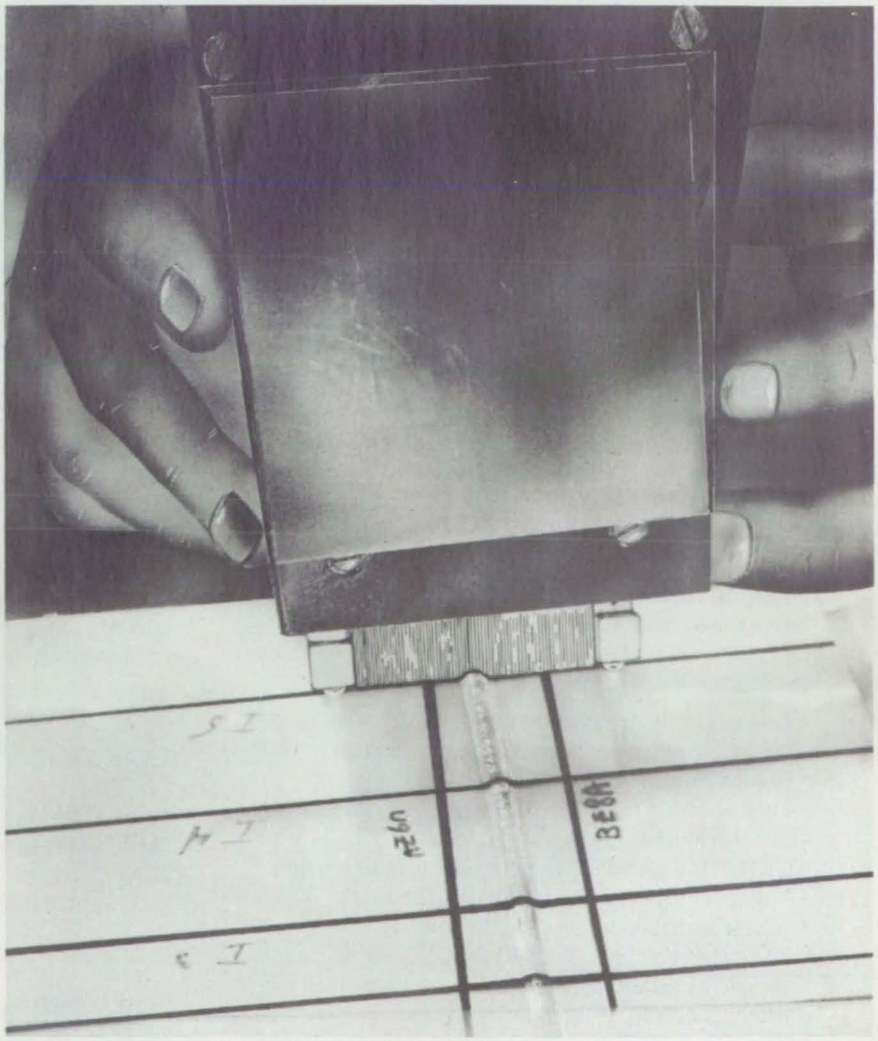

The **Hand-Held Probe Unit** is positioned across a weld, in contact with the workpiece, to obtain a profile.

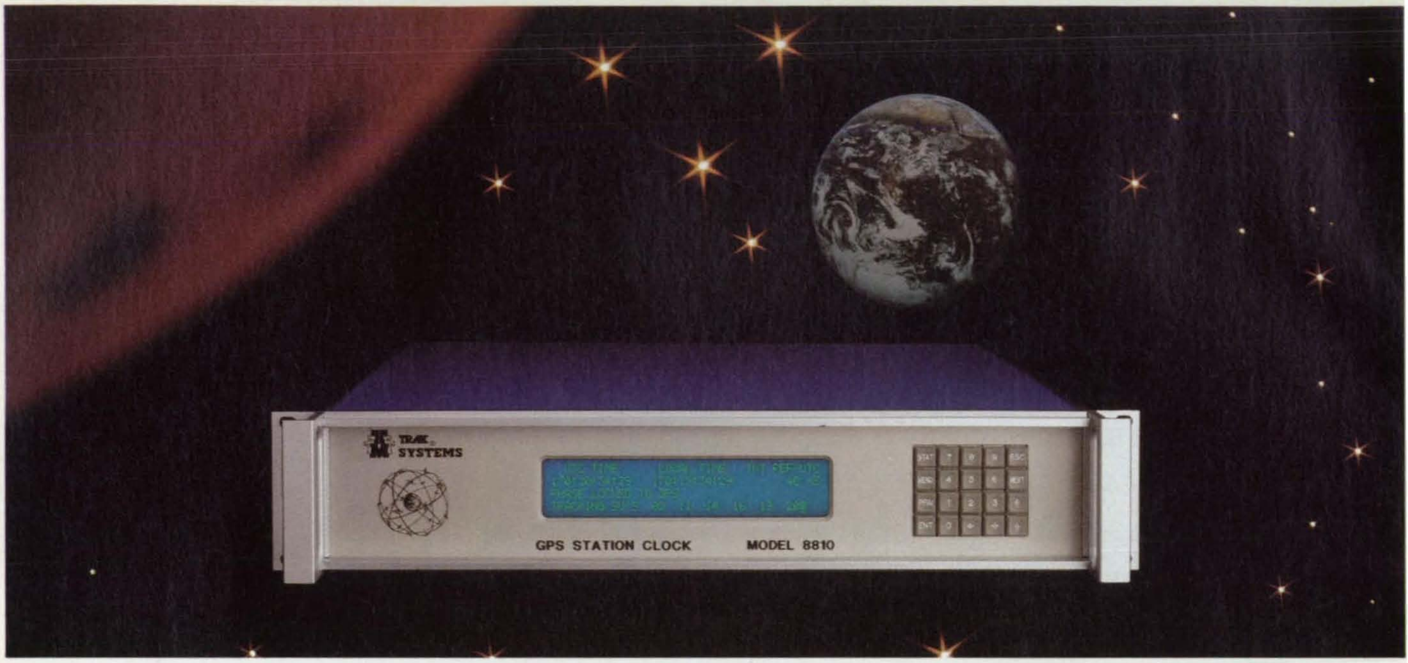
TRAK SYSTEMS
GPS STATION CLOCK
MODEL 8810

Computer-Aided Design of Sheet-Material Parts

The old manual graphical "development" technique is computerized.

Marshall Space Flight Center, Alabama

A computer-aided-design system partly automates the tedious process of designing and guiding the assembly of small pieces of flat sheet material into large surfaces that approximate smoothly curved surfaces that have complicated three-dimensional shapes. The system was conceived for use in making rocket-engine nozzles — specifically, for designing the small pieces of brazing foil, called "preforms," that are assembled edge to edge to cover the surface of each nozzle prior to brazing in a furnace. Previously, the foil covers were patchworks of manually trimmed, small pieces that had random, nonoptimum shapes and did not fit the surfaces of the nozzle in some spots. Clearly, computer-aided design can be used to advantage not only in the rocket-engine application but in other applications that require the design of sheet-material parts.

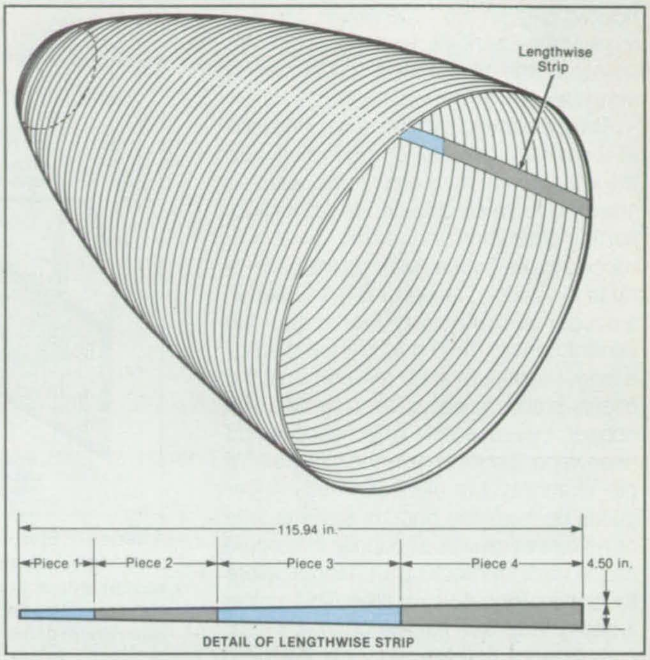

A **Curved Surface of Revolution** is approximated by flat lengthwise strips that can be cut with the help of templates and assembled edge to edge. In this case, each strip is divided into four pieces.

In effect, this computer-aided design system provides an improved, accelerated version of the old technique of manual graphical "development" of flat sections of sheet metal that are to be joined at their edges and/or folded to make three-dimensional vessels, ducts, and the like. In contrast with the manual graphical technique, the computer-aided technique rapidly yields accurate dimensions for the small pieces. This capability provides for flexibility in that it enables the designer to assess quickly and easily the effects of changes in design in making engineering compromises among various sizes and shapes.

At the beginning of the design process, the data that specify the three-dimensional surface to be covered or constructed are fed into the computer from an engineering drawing of the surface or from an equivalent computer data file. From this base of information and with the help of the computer, the designer can develop the geometric data on the pieces. Different shapes can be created, then translated and/or rotated onto the surface as required. This process enables the designer to obtain an optimized design fairly quickly.

The system can plot the outline of a tentatively designed piece in full size; the shape can be cut out of the plotting paper and placed on a model of the surface to determine whether the tentative design provides a good fit. The system can create drawings of templates that are used to cut out the pieces (see figure). It can also create indexing-aid drawings, which assist in assembly by showing how to mark each piece to show where to place it on the surface to be covered or constructed.

The system can save time and money in both design and fabrication. For example, it can be used to maximize the sizes and/or optimize the shapes of parts in such a way as to reduce the amount of scrap left after cutting the parts out of sheet stock. Alternatively, it could help the designer achieve an acceptable fit with fewer parts, thereby reducing the fabrication time.

This work was done by Jeffrey L. Gilbert, Vincent Y. Paternoster, Maureen L. Levitt, and Mark R. Osterloh of Rockwell International Corp. for **Marshall Space Flight Center**. *For further information, Circle 13 on the TSP Request Card.*

Inquiries concerning rights for the commercial use of this invention should be addressed to the Patent Counsel, Marshall Space Flight Center [see page 14]. Refer to MFS-29759.

Making High-Pass Filters for Submillimeter Waves

A process makes a thick metal mesh.

NASA's Jet Propulsion Laboratory, Pasadena, California

A micromachining-and-electroforming process makes rigid metal meshes with cells that range in size from 0.002 in. (0.05 mm) to 0.05 in. (1.27 mm) square. The meshes are electrically thick; that is, thicknesses are comparable to the sizes of the cells. These meshes are used as high-pass filters (dichroic plates) for submillimeter electromagnetic waves.

The figure illustrates some of the steps in the process. First, a standard undoped silicon wafer is cut to a shape (usually square) and to a size large enough to provide a 0.05-in. (1.27-mm) border around the mesh. To provide for an integral frame that will support the mesh during the process, the wafer is made at least 0.010 in. (0.25 mm) thicker than the final mesh is expected to be.

A high-speed dicing saw cuts parallel channels in the wafer. The wafer is rotated 90° on the saw table, and the saw cuts another set of channels parallel to each other and perpendicular to the first set of channels, forming a waffle pattern. The distance between adjacent channels defines the size of a cell, and the width of a channel defines the thickness of the wall between adjacent cells. The channels are cut to a depth slightly greater than the intended thickness of the grid. The saw blade is exchanged for a much thicker grinding wheel, and a swath 0.05 in. (1.27 mm) wide is ground off around the edge of the wafer to provide for the frame. At this stage, the wafer forms the inverse of the final mesh.

The wafer is cleaned and placed in a vacuum evaporation channel with the channel side facing a vapor-deposition source and with a collimating baffle between the wafer and the source boat. A layer of titanium 50 to 100 Å thick is deposited on the wafer and is followed by a layer of gold

2,500 to 5,000 Å thick. (The thin titanium layer helps the gold adhere to the silicon.) The baffle, with its 10:1 ratio of length to width, causes most of the metal to be deposited only on the edge swath, the bottoms of the channels, and the tops of the squares; little or no metal condenses on the sidewalls of the channels.

The evaporated metal layers on the tops of the squares are cut or ground off, and the wafer is cleaned again. The wafer is attached to an electrically insulating supporting plate, and a cathodic contact is clipped to the copper layer on the perimeter of the wafer. The wafer is immersed in a copper electroforming bath at an initial current density of 30 mA/cm^2 followed by a longer exposure at 20 mA/cm^2 until the channels and the edges become filled with copper. Because little or no copper had been vapor-deposited on the sidewalls of the channels, the electroformed copper builds up from the bottom; there is little or no lateral growth of copper that could cause voids by blocking a channel before the bottom is completely filled. This makes it possible to use narrow channels and, consequently, to make thin walls; the thickness of a wall can be as little as one-fifth the thickness of the mesh (the height of the wall).

When the channels are filled with copper, the wafer is removed from the electroforming bath and rubbed on fine emery paper to remove any copper that has grown on the squares and to flatten out any asperities on the frame. The silicon is etched away in hot potassium hydroxide, leaving the copper mesh and its frame.

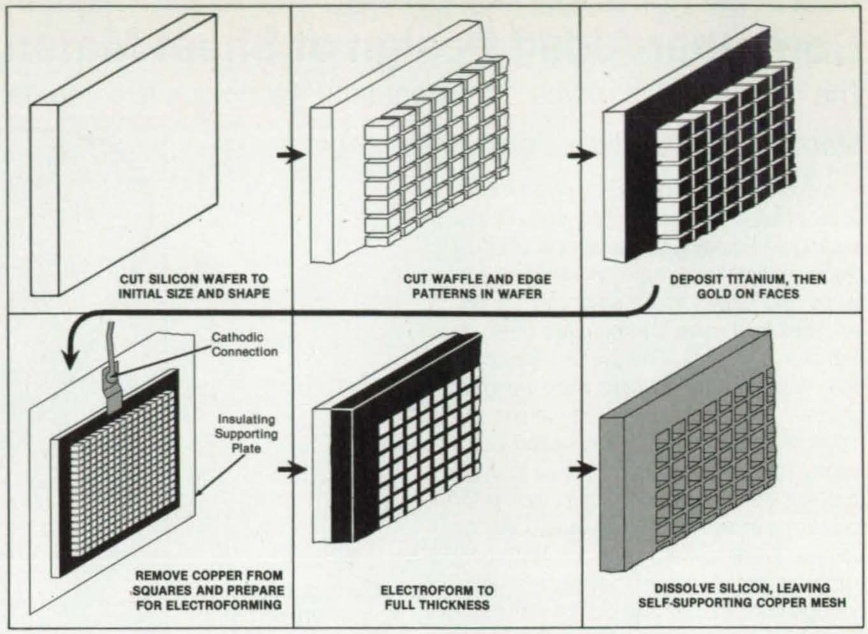

A **Series of Steps** involving cutting, grinding, vapor deposition, and electroforming creates a self-supporting, electrically thick mesh. The width of the holes is typically 1.2 times the cutoff wavelength of the dominant waveguide mode in a hole. To obtain a sharp frequency-cutoff characteristic, the thickness of the mesh should be made greater than one-half of the guide wavelength of the mode in the hole.

The new process is not limited to square silicon wafers. Round wafers can also be used, with slightly more complication in grinding the periphery. The grid can be in any pattern that can be produced in an electroforming mandrel. Any platable metal or alloy can be used for the mesh.

This work was done by Peter H. Siegel of Caltech and John A. Lichtenberger of Metaplate Co. for **NASA's Jet Propulsion Laboratory**. *For further information, Circle 127 on the TSP Request Card. NPO-17992*

Stiff, Strong Splice for a Composite Sandwich Structure

Layers of alternating fiber orientation are interposed between thin ears in an adhesive joint.

Ames Research Center, Moffett Field, California

A new type of splice for a composite sandwich structure reduces the peak shear stress in the structure. The splice, which was developed for a structural joint in the spar of a helicopter rotor blade, also increases the precision of control over the thickness of the adhesive at the joint.

The spar consists of two pieces — a leading-edge half and a trailing-edge half, both having C-shaped cross sections. The new splice (see figure) bonds the halves together to form a structural spar that can carry high torsional shear; high bending moments from aerodynamic loads; and additional loads from flap shear, chord shear, and related bending moments. The joint is easy to make, requires no additional pieces, and adds little weight. The bending stiffness across the joint remains high so that deflections of the airfoil surface under aerodynamic loads are minimized. The new joint supplants single- and double-overlap joints. The single-overlap joint suffers from low bending stiffness and high peak shear and tension stresses. The double-overlap joint is superior to the single-overlap version but is difficult to make.

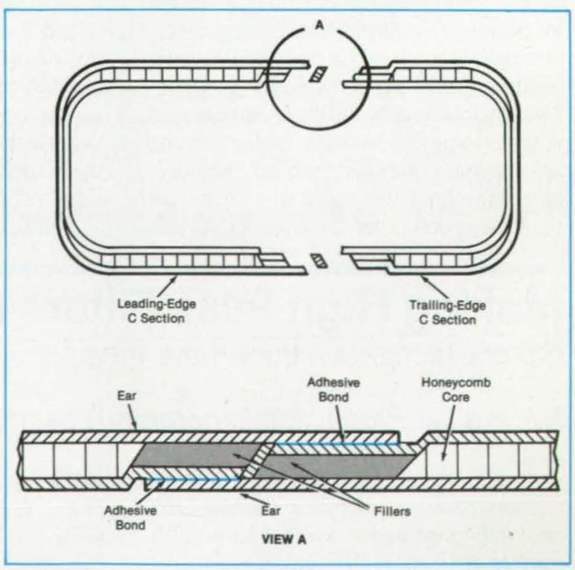

Thin Ears Join Sections of the spar of a helicopter rotor. A thick graphite filter laminate is sandwiched between the thin laminate ears by an adhesive.

The new joint includes a pair of ears bonded with a graphite filler laminate. The thin ears can conform to the curvature of the thicker graphite laminate between them, yielding a spatially gradual and therefore more uniform distribution of tension stress across the bond lines and consequently smaller tension peaks. The cross-sectional area that provides bending stiffness is reduced by only the thickness of an ear.

The ears are relatively stiff laminates of 90° and 45° fiber orientations, while the filler laminate with its ±45° fiber orientations is relatively compliant. The combination of stiff ears and compliant filler contributes further to the spatially and temporally gradual transfer of loads to reduce the peak shear stresses.

This work was done by D. Schmaling of United Technologies, Sikorsky Aircraft, for **Ames Research Center**. *For further information, Circle 149 on the TSP Request Card.*

Title to this invention, covered by U.S. Patent No. 4,793,727, has been waived under the provisions of the National Aeronautics and Space Act [42 U.S.C. 2457(f)]. Inquiries concerning licenses for its commercial development should be addressed to

Robert Kline
Sikorsky Aircraft Division
United Technologies
6900 North Main Street
Stratford, CT 06601-1381

Refer to ARC-11743, volume and number of this NASA Tech Briefs *issue, and the page number.*

Verification of Tooling for Robotic Welding

Computer simulations, robotic inspections, and visual inspections are performed to detect discrepancies.

Marshall Space Flight Center, Alabama

A method for the verification of tooling for robotic welding involves a combination of computer simulations and visual inspections. The verification process ensures the accuracy of a mathematical model that represents the tooling in an off-line programming system that numerically simulates the operation of the robotic welding system. In so doing, the process helps to prevent damaging collisions between the welding equipment and the workpiece, to ensure that the tooling is positioned and oriented properly with respect to the workpiece, and/or to determine whether the tooling has to be modified or adjusted to achieve the foregoing objectives.

The mathematical model for a tool to be used in welding a given workpiece is first developed on a computer-aided-design system (e.g., Computervision or equivalent). The model is transferred to another computer-aided-design system (e.g., Unigraphics or equivalent) for the generation of test points at various known locations on the tool. These are points to which a tool-inspecting robot will subsequently be commanded to move.

The model of the tool and the test-point information are then viewed with the help of commercially available simulation software (e.g., PLACE or equivalent). The position and the orientation of the surface are verified at each test point. If the orientation at a point is improper, it could cause the inspecting robot to attempt to reach beyond the limits of its joints. Consequently, it may be necessary to alter the mathematical model of the tool. Once the model and the test points are satisfactory, they are saved in a computer file. From this file, the locations of the test points (relative to where the tool is attached to a positioning table) are computed and used to create a trajectory for the inspecting robot.

The off-line programming system is used to create a program to move the inspecting robot to the desired test points on the real tool. To do this, another simulation is performed — this time taking account of the entire collection of equipment in the robotic work cell, including the robot and its end effector, the positioning table, and the tool. The trajectory created in the previous step must be within the reach of the robot, and the limits of the joints are examined to verify this.

To prevent damage to the tool or the inspecting robot, collisions are detected during this simulation. The alignment and location of the tool on the positioning table are also watched to determine whether the mathematical model has to be adjusted further. At the completion of a successful simulation (that is, when there are no collisions and no joint limits are exceeded), the program for the robot is created and transmitted electronically to the robot controller.

The tool is mounted on the positioning table. A special end effector that measures the position of the robot relative to the surface under inspection is mounted on the robot. This measurement is then performed at each test point. The resulting measurement data are used to determine whether the mathematical model of the tool matches the real tool. If necessary, the model can be revised and the process repeated until the differences between the model and the tool are acceptably small.

This work was done by Mark R. Osterloh, Karen E. Sliwinski, and Ronald R. Anderson of Rockwell International Corp. for **Marshall Space Flight Center**. *For further information, Circle 148 on the TSP Request Card.*

Inquiries concerning rights for the commercial use of this invention should be addressed to the Patent Counsel, Marshall Space Flight Center [see page 14]. Refer to MFS-29725.

Automated Scheduling Via Artificial Intelligence

The Operations Mission Planner approach is based on iterative refinement.

NASA's Jet Propulsion Laboratory, Pasadena, California

Artificial-intelligence software that automates scheduling has been developed in the Operations Mission Planner (OMP) research project. The OMP approach differs from the classical artificial-intelligence approach to scheduling, in which a schedule is built-up in straightforward incremental fashion and if any proposed change in a schedule could give rise to a conflict in a subsequent scheduled event, the entire part of the schedule beyond the change must be rebuilt to take account of the change. OMP software can be used in both the generation of new schedules and the modification of existing schedules in view of changes in tasks and/or available resources. Although the OMP project focused upon the scheduling of operations of scientific instruments and other equipment aboard a spacecraft, the OMP approach is also applicable to such terrestrial problems as scheduling production in a factory.

The OMP approach is based on iterative refinement like that practiced by expert human schedulers: the scheduling software builds and refines a schedule by making a series of passes over the entire schedule, learning from each pass and modifying both the schedule and the scheduling technique as it learns. In the multiphase OMP approach, the planning phases can be interleaved, enabling the scheduling software to look globally over the whole schedule or focus locally on a given part of the schedule at its discretion. The principal innovations of OMP iterative refinement are the following:

- Unlike in the classical approach, illegal schedules (those that contain conflicts) are representable.
- The schedule is refined and conflicts are resolved by modifying an existing schedule, not by building a new schedule from the beginning.
- Information about the state of the schedule from prior passes is used to guide the scheduling actions in subsequent passes.
- Different strategies are used during different passes.
- Backtracking is not required. If a poor decision is made, it can be unmade through an appropriate action. The valid parts of the schedule developed after the mistake are not affected, although they may be causally related.
- Replanning is reduced to selecting the appropriate scheduling phase and reinitiating planning with the additional tasks or resource changes.

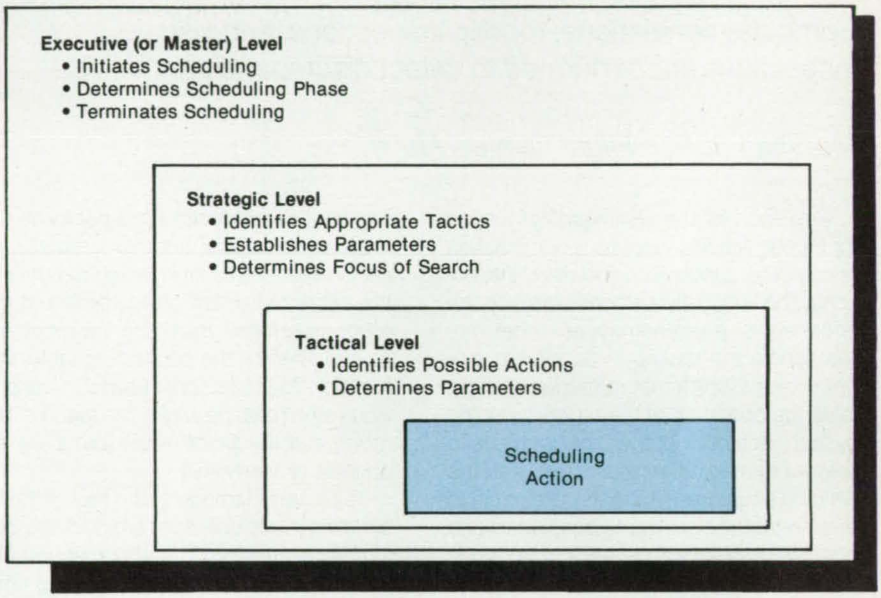

Three Levels of Control of scheduling activities impart flexibility to the OMP scheduling software in that the generation of schedules is not bound to a single, all-encompassing, general-purpose control algorithm.

To summarize briefly, the OMP approach is first to construct a rough schedule to identify the problems, then refine the schedule. In a significant departure from classical planning software, the OMP software allows illegal schedules to be developed and conflicts to exist within a schedule during its evolution. By first building schedules that help to identify the areas of high contention for resources and interactions among tasks (denoted as "bottlenecks"), the software can focus its scheduling efforts. This parallels the expert human approach. Human schedulers first throw everything onto timelines, which are data structures that represent usage of resources and assignments of tasks over time, to identify the potential problem areas. Once they have identified these areas, they begin focusing their efforts there, jumping back and forth from one area to another to narrow the problems. A schedule without conflicts is produced only as a final output.

To implement iterative refinement, it has been necessary to develop and incorporate some new artificial-intelligence concepts. These include highly interdependent, advanced concepts of the multilevel control of scheduling functions (see figure), the representation of scheduled tasks, and chronologies (limited histories of scheduling activities and the effects of them on the schedule). Chronologies are needed to support assessment heuristics, which identify and classify bottlenecks and are required to support the multilevel control mechanisms. In turn, the multilevel control mechanisms are necessary to support knowledge-intensive searches, which in turn are necessary because of the enhanced representation of scheduled tasks. The integration of all these pieces into a working model of an iterative-refinement scheduling system is the most significant achievement of the OMP research.

This work was done by Eric W. Biefeld and Lynne P. Cooper of Caltech for **NASA's Jet Propulsion Laboratory**. *For further information, Circle 8 on the TSP Request Card. NPO-18209*

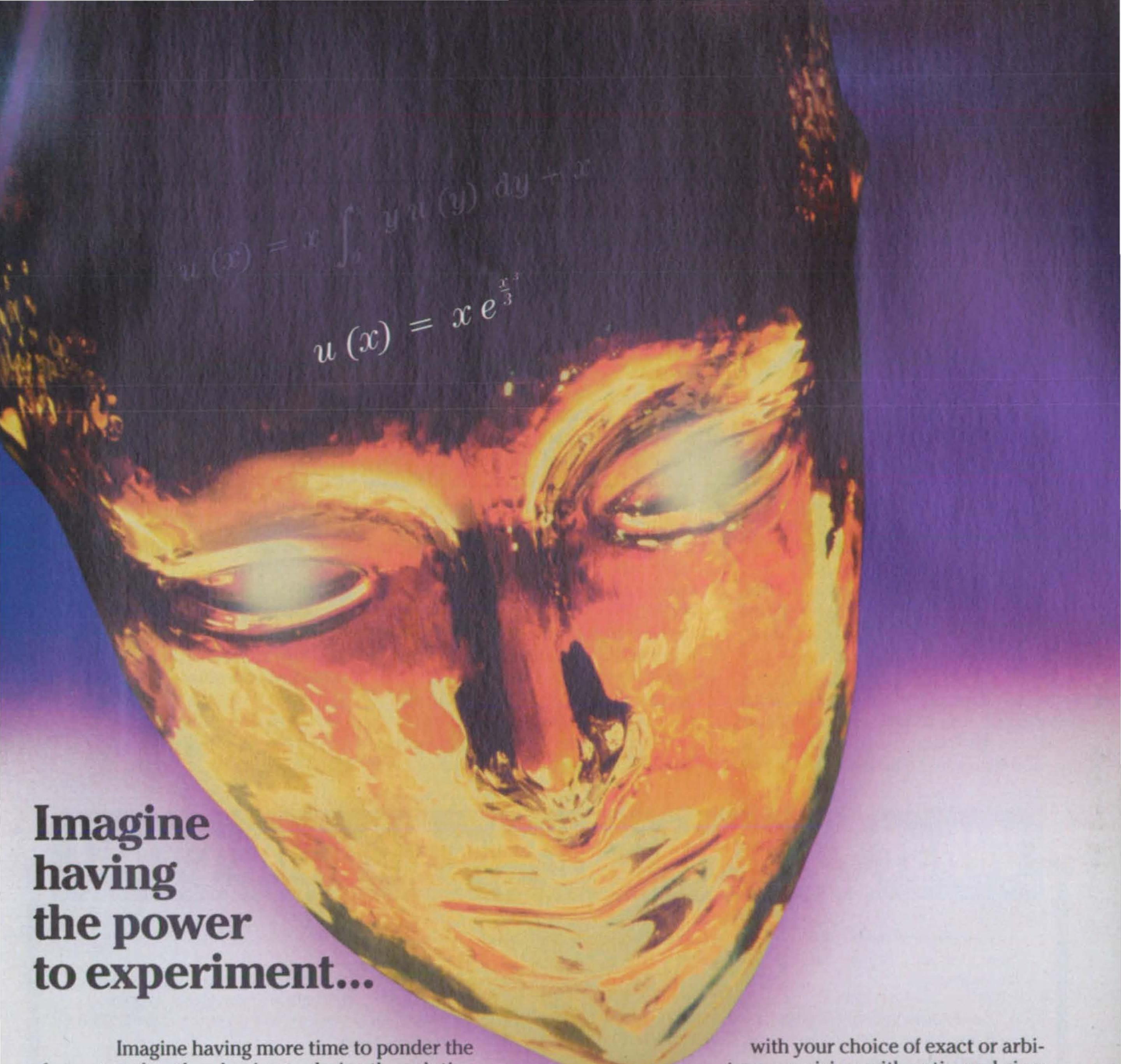

Imagine having the power to experiment...

Imagine having more time to ponder the abstract, rather than having to derive the solution.

With MACSYMA® *symbolic math software* you can!

No other software today packs the computational power, versatility, and reliability of MACSYMA. MACSYMA can tackle any mathematical application you may have, whether in algebra, calculus, trigonometry, or practically any other branch of higher mathematics. It gives you problem-solving tools such as Laplace and Fourier transforms, Taylor and Poisson series, solution of first and second order differential equations, solutions to integrals, and more. It gives you sophisticated 2-D and 3-D graphics, and can convert your equations into Fortran or 'C' for optimal numeric performance, or $\mathrm{T_EX}$ for inclusion in publications.

MACSYMA provides unequalled accuracy too, with your choice of exact or arbitrary precision arithmetic, and gives you results at speeds from 10 to 100 times faster than traditional methods.

All this power is remarkably easy to use. With the help of the User's Guide, extensive on-line documentation, executable examples and demonstrations, and the Quick Reference Card, a beginning MACSYMA user can quickly become proficient, tackling problems that might otherwise have been too difficult or time-consuming.

Whatever your application — engineering, science, economics or pure math — your work is too important to trust to any other math software. You deserve MACSYMA.

More than just a system for doing mathematics by computer, it's the power tool for mathematics.

symbolics, Inc.

MACSYMA Division

8 New England Executive Park East, Burlington, MA 01803 USA • 1-800-622-7962 (in Massachusetts, 617-221-1250.)

Circle Reader Action No. 524

Books and Reports

These reports, studies, handbooks are available from NASA as Technical Support Packages (TSP's) when a Request Card number is cited; otherwise they are available from the National Technical Information Service.

Spatial-Operator Algebra for Robotic Manipulators

Transitions from abstract formulations to detailed solutions of problems are simplified.

A report discusses a spatial-operator algebra that has been developed in recent studies of the mathematical modeling, control, and design of the trajectories of robotic manipulators. This algebra provides a succinct representation of the mathematically complicated interactions among multiple joints and links of a manipulator, thereby relieving the analyst of most of the tedium of detailed algebraic manipulations. The report presents an analytical formulation of the spatial-operator algebra, describes some specific applications, summarizes current research, and discusses implementation of the spatial-operator algebra in the Ada programming language.

The elements of this algebra are certain linear operators that are always present in the equations that describe the dynamic and kinematic behavior of manipulators. The domain and range spaces of these operators consist of forces, velocities, and accelerations. They are called "spatial" operators because they show how forces, velocities, and accelerations propagate through space from one rigid body (e.g., a link of a manipulator) to the next. Not only do such operators have obvious physical interpretations, but they are also implicitly equivalent to recursions from link to link along the manipulator arms. These recursions can be turned immediately into implementable algorithms by projecting onto appropriate coordinate frames.

The spatial operators are elements in the algebra of linear bounded operators that map between finite-dimensional Hilbert spaces. The algebra of these operators is known as a Banach algebra in the theory of linear operators. The inversion of an operator can, of course, be achieved by the traditional techniques of linear algebra. In addition, many important spatial operators can be factored as the product of a causal, a diagonal, and an anticausal operator. For such an operator, inversion can be achieved by the inward/outward-sweep solutions of spatially recursive Kalman filtering.

The spatial-operator algebra provides a high-level mathematical framework for the description of the kinematic and dynamic behavior of a manipulator and for the corresponding control and trajectory-design algorithms. Expressions interpreted within the algebraic framework lead to enhanced conceptual and physical understanding of the dynamics and kinematics of manipulators. The spatial-operator algebra can be used to solve any problem in the dynamics of multiple interacting rigid bodies; in so doing, it enables the equations of motion to be manipulated at a very high level of abstraction in which many of the quantities being manipulated are causal or anticausal linear operators. As a consequence, at any stage of an abstract manipulation of operators, spatially recursive algorithms to implement the operator expressions can be obtained readily by inspection. As a further consequence, the transition from abstract-operator mathematics to practical implementation is relatively easy, requires only a simple mental exercise, and can be automated readily with a computer program.

This work was done by Guillermo Rodriguez, Kenneth K. Kreutz, and Mark H. Milman of Caltech for **NASA's Jet Propulsion Laboratory**. *To obtain a copy of the report "A Spatial Operator Algebra for Manipulator Modeling and Control," Circle 87 on the TSP Request Card.*
NPO-17770

Life Sciences

Hardware, Techniques, and Processes

Software for Design of Life-Support Systems

A special-purpose computer program combines conventional mathematical models with an expert software system.

Ames Research Center, Moffett Field, California

The Design Assistant Workstation (DAWN) computer program is the prototype of an expert software system for the analysis and design of regenerative, physical/chemical life-support systems that will revitalize air, reclaim water, produce food, and treat waste. DAWN incorporates both conventional software for quantitative mathematical modeling of physical, chemical, and biological processes and an expert system that offers the user its stored knowledge about materials and processes. DAWN enables a user to jump from one design level to another — for example, from a detailed evaluation of reaction kinetics to an overall concept of the process to an overall energy balance.

The user can call on the conventional software for help in solving clearly defined problems for which ample data are available. Then the user can ask the expert system for qualitative, common-sense reasoning and rules of thumb in developing new concepts for which few empirical data are available.

For example, if a designer wished to consider the separation of water from salt, DAWN would propose two alternatives: centrifuging or flashing (see figure). Suppose that the designer decides to consider flashing. DAWN then leads the designer through an evaluation. It informs the designer that flashing is a viable alternative if the boiling points of the components are far away from each other. It finds that heat must be added to the stream to effect flash separation and that the first effect of the addition of heat would be a change of phase (it would not be a change of temperature; DAWN "knows" that in this case the water must first change from a solid to a liquid). DAWN continues to simulate the effect of the addition of heat and defines each change of state until the goal of separation is reached. The user can ask to see the characteristics of the mixture at any state.

This example illustrates how DAWN accepts a goal (separation), breaks it down into possible subgoals (flash, centrifuge), and simulates the effects (a sequence of states) of the process associated with the chosen subgoal (in this case, the addition of heat associated with flashing). The user can control the path of the design and simulation. For example, the path can be varied by addition of subgoals or by beginning with a higher-level goal like an incineration process or a lower-level goal like a change of phase of water.

At the process level, DAWN has a "smart front end," wherein the user defines a process in some detail, and a "smart back end," wherein the user compares the results of a quantitative simulation (based on conventional software models) with the predictions made by the smart front end. The smart back end helps the user make rough calculations, suggests basic assumptions, offers some quantitative reference data, and explains equations.

This work was done by Mary R. Rudokas and Elizabeth R. Cantwell of **Ames Research Center** *and Peter I. Robinson and Timothy W. Shenk of RECOM. For further information, Circle 5 on the TSP Request Card. ARC-12665*

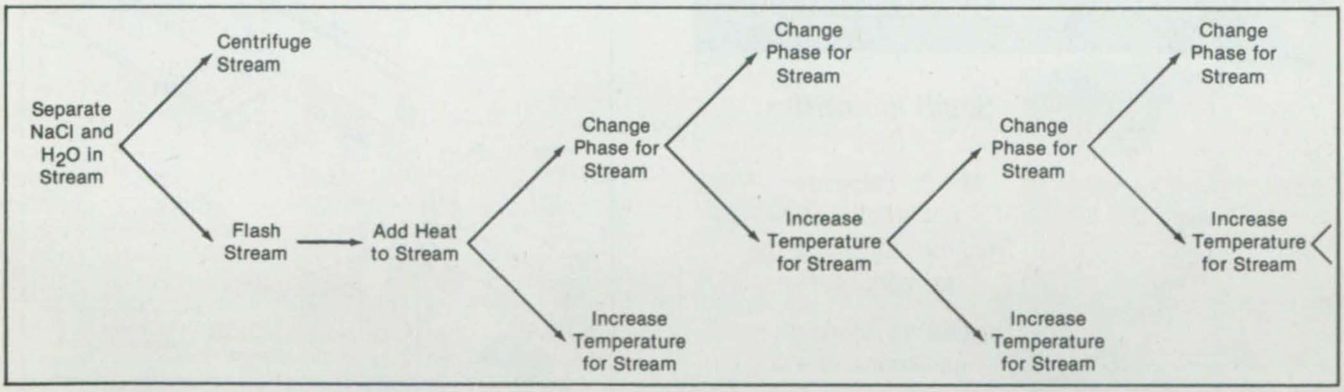

DAWN Constructs a Task Tree as it leads a user through a simulated process, offers alternatives (centrifuge stream or flash stream, for example), and indicates where an alternative is not feasible (e.g., an increase in the temperature of the stream is impossible at the first addition of heat because the water is ice at this stage and must first be melted).

Research Animal Holding Facility Prevents Space Lab Contamination

A healthy environment for both rodents and human researchers is maintained.

Ames Research Center, Moffett Field, California

A research animal holding facility (RAHF) and rodent cage prevent solid particles (feces, food bits, hair), micro-organisms, ammonia, and odors from escaping into the outside environment during spaceflight. The cage (see figure) houses two rodents in separate compartments. When installed in a cage module, the cage mates with gaskets that form a barrier for internal gases and particles. In addition, the cage is maintained at a pressure slightly below ambient to prevent gases and particles from flowing outward.

A removable waste tray at the base of

the cage contains a layer of porous polyester padding treated with phosphoric acid to inhibit the production of ammonia during the decomposition of rodent urine. A layer of charcoal-impregnated fibers is placed under the polyester pad to control odors. Under that is a thin, electrically charged woven-fiber pad supported by a fine screen and bottom stainless-steel grill. Urine and feces are dried by the flow of air through the tray to inhibit decomposition.

The tray can easily be removed and replaced with a clean one. An astronaut inserts a cover into the cage module to seal the tray, removes the tray, places it in a bag for later analysis and disposal, and inserts a new tray. To prevent food particles from escaping, the astronaut follows a similar procedure for removing and replacing a feeding tray.

During the removal or insertion of a cage or tray, an auxiliary high-flow centrifugal blower is turned on to generate a vigorous suction in the open module in addition to the small operating suction maintained in the module by the environmental control system. The additional inward flow helps to keep particles and gases inside until the tray or cage is returned to the module.

The cage is 1 of 12 in a cage module. An environmental control system behind the cage module circulates air through the cages, controls the temperature and humidity, exhausts filtered air to the outside environment through a charcoal bed and bacterial filter, and accepts fresh air from the outside.

The RAHF system passed a 12-day ground-based biocompatibility test. No particles larger than 150 μm and no micro-organisms in the laboratory environment outside the holding facility could be traced to the holding facility. No odors were detected by a panel of qualified subjects. No ammonia was detected, and carbon dioxide buildup was less than 0.35 percent.

This work was done by P. D. Savage, Jr., G. C. Jahns, B. P. Dalton, R. P. Hogan, and A. E. Wray of **Ames Research Center**. *For further information, Circle 66 on the TSP Request Card. ARC-12599*

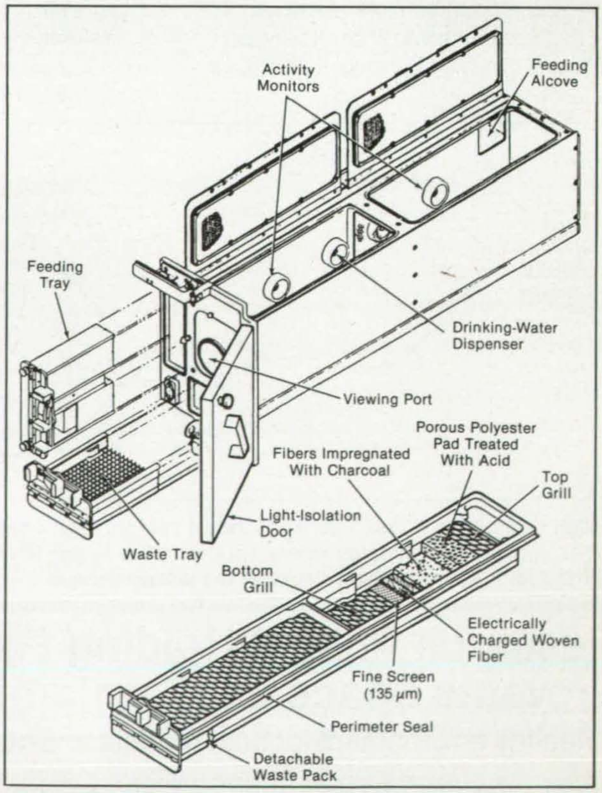

The **Rodent Cage Contains Compartments** for two animals. For each, it provides a drinking-water dispenser, a feeding alcove, and an activity-monitoring port. The feeding and waste trays are removable. The layered structure of the waste tray inhibits the generation of ammonia and the decomposition of urine and feces.

New on the Market

A handheld, battery-operated **resolver meter** has been developed by Control Sciences Inc., Chatsworth, CA. Designed to simplify testing of resolver systems, the meter is useful for resolver alignment, field testing, troubleshooting, and system installation and checkout. Its LCD readout displays synchro angles from 0° to 359.9°, with 0.1° resolution and 0.2° accuracy.
Circle Reader Action Number 796.

CHI Systems Inc., Pleasanton, CA, has introduced a user-programmable **interface board** that connects VME workstations with 100- and 200-MByte/sec supercomputer HIPPI (high-performance parallel interface) ports. It provides both input and output channels and can be configured to support dual simplex operations for both 32- and 64-bit data path widths. The 9U interface connects systems such as Sun and Silicon Graphics with supercomputers from Cray, IBM, and others.
Circle Reader Action Number 774.

Xmath™, an interactive, object-oriented **mathematical analysis and scripting environment** for X-Windows workstations, is offered by Integrated Systems Inc., Santa Clara, CA. Features include a spreadsheet-style editor for matrices, point-and-click graphics annotation, on-line hypertext help, and a built-in source-level debugger window for script-based programming. Xmath automatically generates plots from data or computations, including 2D scatter plots, 3D surface plots, multiple X and Y plots, and multi-curve strip charts.
Circle Reader Action Number 792.

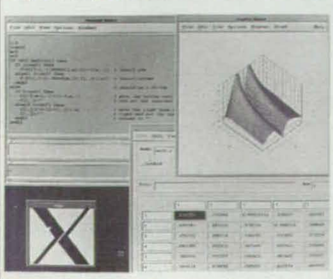

Automatix Inc., Billerica, MA, has introduced Autovision®, a high-resolution, gray-scale **machine vision system** for on-line gaging, assembly verification, and machine guidance. Autovision can automatically inspect up to 1200 parts per minute with accuracy to ±0.0002". Built-in gauging tools enable reporting of over 200 measurement types including point-to-point and line-to-point distances, area, centroid, radius, angle, and object location.
Circle Reader Action Number 780.

A new six-channel **Global Positioning System receiver** from Magnavox, Torrance, CA, is built onto a single pocket-size printed circuit board. Called the GPS Engine, it simultaneously tracks and processes navigational signals and carrier phase from six satellites with sensitivity 4-5 dB better than sequencing receivers and 8 dB better than multiplexed receivers. It can be adopted in vehicle tracking systems, avionics suites, handheld radios, personal locators, marine navigation systems, and other applications requiring precise position updates and time measurements.
Circle Reader Action Number 800.

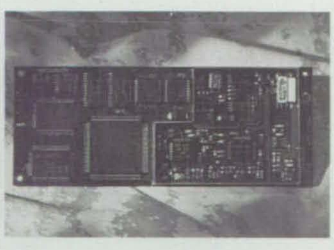

A new **bolt stress analyzer** from Zendex Intl., Dublin, CA, uses ultrasonic waves to measure bolt fatigue. Designated the JAG-2000, the computer-based system processes and displays information on tensile and structural conditions. It can gauge the fatigue of embedded bolts and record stress conditions of previously-installed bolts for future comparative analysis.
Circle Reader Action Number 786.

The Big Blu **leak reactant** from Refrigeration Technologies, Fullerton, CA, is a topical spray coating that detects points of gas leakage as small as 10^{-7} cc/sec. The test fluid forms a soap-like foam cocoon visible for up to two hours. The solution is nontoxic, biodegradable, noncorrosive, and leaves no residue.
Circle Reader Action Number 782.

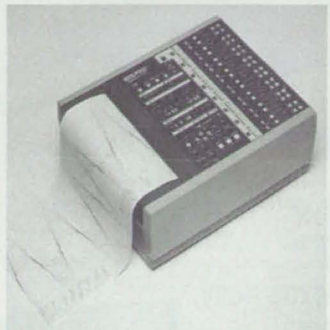

SOLTEC Corp., San Fernando, CA, has developed a **thermal array recorder** with a 400 dots per inch thermal print head. The TA260 recorder offers up to 32k word/channel memory capacity with battery backup of set-up conditions and a 5 µsecond maximum memory recording sampling interval for recording transient and high-speed signals. It features real-time waveform, logging, and trigger recording.
Circle Reader Action Number 778.

Integrated Engineering Design, Columbus, OH, has announced the Parallax III SE, a **3D wire frame modeler** that runs under Microsoft Windows 3.0™. Priced at $350, the CAD/CAM system uses hand-written symbol or written letter recognition, temporary construction lines, icons, and heads-up operation.
Circle Reader Action Number 794.

Millitech Corp., South Deerfield, MA, has announced a new family of **millimeter wave communication systems** for use in cellular radio interconnects, crowded spectrum inter-city links, secure data links, and personal communications networks. Covering the frequency spectrum from 24 to 320 GHz, the systems offer simplex, half duplex, and full duplex transceivers, as well as repeaters and translators. Modulation options include AM, FM, FSK, BPSK, and QPSK, using direct or heterodyne conversion.
Circle Reader Action Number 788.

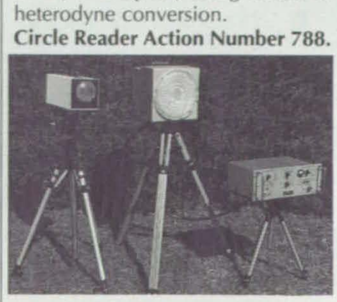

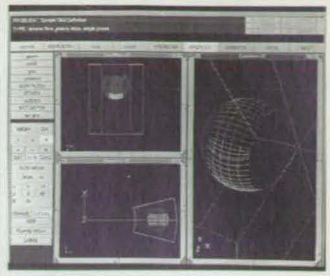

CHAM of North America, Huntsville, AL, has introduced EasyMesh-3D™, a **three-dimensional grid generation software package** for computational fluid dynamics simulation and analysis. Using body-fitted coordinates, the software allows engineers to define complex grids and structures. It features a graphical user interface and point-and-click, pull-down menus.
Circle Reader Action Number 798.

Krohn-Hite Corp., Avon, MA, has developed a **tunable active low-pass filter** with a frequency range to 25.6 MHz. Offering 2.5 digits of resolution over the 170 Hz to 25.6 MHz range, the four-pole, maximally-flat filter has an attenuation slope of 24 dB/octave and a stopband attenuation of 100 dB. It features selectable AC or DC coupling and 1m or 50 ohm input impedance.
Circle Reader Action Number 790.

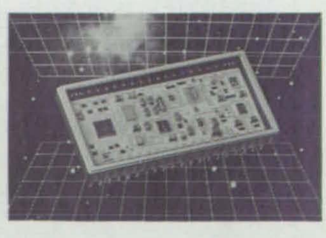

A new 14-bit, 200-nsec **track/hold and A/D converter hybrid** is available from ILC Data Device Corp., Bohemia, NY. Packaged in a small 40-pin TDIP or flatpack, the ADC-00145 contains track/hold, tri-state output buffers, and timing circuits. The hybrid operates over a temperature range of -55° to +125° C. It has applications in military and industrial data conversion, including radar and sonar digitizing, vibration and FFT analysis, and high-speed data acquisition.
Circle Reader Action Number 776.

NASA's Innovators

(continued from page 11)

units during space station construction, it could be customized for Earth applications such as equipment or waste transfer.

Other state-of-the-art technologies can be used in tandem with telerobotic hardware to expand its applications. Holography, another of Marzwell's research interests, could prove especially fruitful. Three-dimensional holographic images—with data on position, depth, and intensity—provide a detailed picture often inaccessible through other means. A holographic display system developed under an SBIR contract by Computer Sciences Corporation provides near-real-time, full-parallax images of a remote work site, enabling human supervisors to more accurately monitor and control mechanical systems.

When a task is particularly difficult, simulations can provide a safe and inexpensive training ground. KMS Fusion Inc., under contract to JPL, has created the Global Local Environment Telerobotics Simulator (GLETS), which immerses an operator in a real-time, interactive simulation. By superimposing the real image on the recorded simulation, GLETS can update the virtual environment and alert the robot and operator to variances and impending errors. Specialized software allows the robot to correct and learn from its mistakes, update its database, and proceed safely with the task. The system provides a means for remote handling operations in hazardous environments and serves as an aid to mission planning.

As robotics technology becomes more sophisticated, human assistance will be summoned to solve problems only when the robot has exhausted its own store of possible solutions. This will free humans to oversee teams of robots engaged in increasingly complex activities from ever greater distances. Marzwell envisions robotic systems expanding in trainability, retention, self-learning, and self-organization. With these developments, he said, will come the autonomy needed to enhance performance and safety, increase productivity, and reduce costs in countless fields of human endeavor. ❐

Editor's note: Dr. Marzwell will discuss several of these advanced robotic systems at Technology 2001, the second national technology transfer conference, December 3-5 in San Jose, CA.

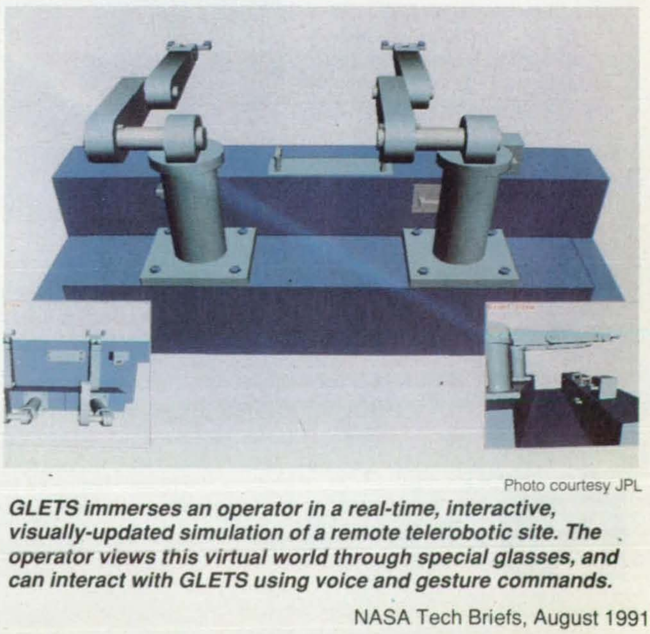

Photo courtesy JPL

GLETS immerses an operator in a real-time, interactive, visually-updated simulation of a remote telerobotic site. The operator views this virtual world through special glasses, and can interact with GLETS using voice and gesture commands.

New Literature

Lithium/thionyl chloride batteries for industrial, military, petrochemical, and medical applications are featured in a color brochure from Battery Engineering Inc., Hyde Park, MA. The batteries provide high energy density, high current and voltage, and low self-discharge rates, and operate over the -55° to +200° C range.
Circle Reader Action Number 724.

A 28-page booklet from APD Cryogenics Inc., Allentown, PA, offers basic technical instructions on **cryopumping** for new and potential users. The booklet describes applications in UHV systems, sputtering chambers, thin film production, evaporative coaters, molecular beam chambers, electron spectroscopy, and high-frequency crystal calibration.
Circle Reader Action Number 708.

A technical bulletin on **Ryton® sulfar fiber**, issued by Phillips Fibers Corp., Greenville, SC, details its performance and physical properties, and lists applications for the Ryton resin and fiber. The flame-retardant and heat-resistant materials are used in thermoplastic composites and filter bags for filtration of flue gas from coal-fired boilers. Performance in three commercial pulse-jet baghouse installations is described.
Circle Reader Action Number 704.

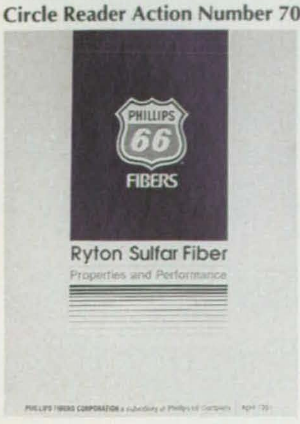

Avtech Electrosystems, Ogdensburg, NY, is offering a 113-page catalog of **nanosecond waveform generators** and accessories, including over 300 models of ultra-high-speed pulse generators, impulse generators, monocycle generators, samplers, and delay generators. The products are suited for use in optical communications, GHz logic, semiconductor switching, radar, ultrasonics, and medicine.
Circle Reader Action Number 710.

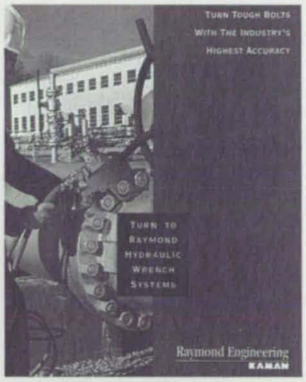

Hydraulic wrenches with a novel rack and pinion design for improved accuracy are featured in a brochure from Raymond Engineering Inc., Middletown, CT. The wrenches have drop-foot adaptors adjustable within a 360° range and swivel hydraulic fittings that ensure maneuverability without hose binding. The four-color brochure also describes heavy-duty multi-pin ratchet wrenches with torque to 75,000 ft.-lbs., Kerotest wrenches for nuclear globe and check valves, and accessories such as drives for impact sockets.
Circle Reader Action Number 720.

Austron Inc., Austin, TX, has released a color brochure on its **Global Positioning System** (GPS) products that briefly explains the GPS system, its operational advantages, and potential applications. Specifications for Austron's GPS time and frequency receivers are included.
Circle Reader Action Number 718.

Electrostatic Technology Inc., Branford, CT, has released a brochure describing its **powder coating systems for composite material manufacturing**. The systems, which are energy-saving and require no solvents, use dry powders to pre-impregnate reinforcing materials such as carbon fiber, aramid, and fiberglass, in the forms of fabric and tow.
Circle Reader Action Number 722.

The Microscope Book, from the Cambrex Group, Boston, MA, showcases state-of-the-art **microscope equipment and supplies**. It describes atomic force, electron, light, scanning electron, stereo, and transmission electron microscopes, as well as accessories such as cameras, video systems, printers, image acquisition equipment, diamond knives, and ergonomic chairs for microscope use.
Circle Reader Action Number 728.

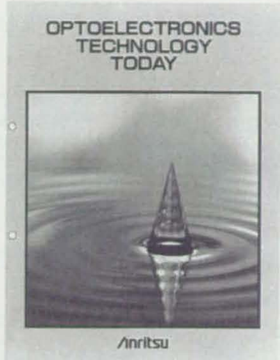

Anritsu America Inc., Oakland, NJ, has published a free 46-page booklet on **optoelectronics** detailing the latest advances in light source technology and its applications. The booklet includes studies by leading authorities on surface emitting lasers and active parallel microoptics, synchrotron radiation, remote laser detection of methane, current x-ray laser R&D, ultrafast optoelectronics, and the future of optical technology.
Circle Reader Action Number 702.

A color brochure published by Deft Chemical Coatings, Irvine, CA, describes environmentally-safe **coatings** for commercial and military aircraft applications. The brochure features a new VOC-compliant, fluid-resistant epoxy primer intended for corrosion protection of metal parts exposed to chemicals such as solvents and hydraulic fluids.
Circle Reader Action Number 726.

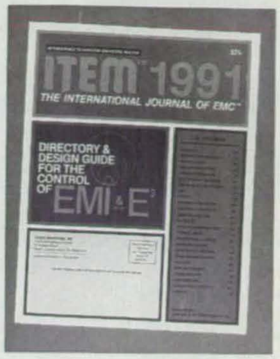

R&B Enterprises, West Conshohocken, PA, has published a design guide and directory covering the measurement, reduction, and control of all forms of electromagnetic interference (EMI) and electromagnetic environmental effects. The 420-page guide includes a product directory and features sections on shielding aids, filters, TEMPEST, EMP, lightning, electrostatic discharge, product safety, radiation hazards, and commercial and military EMI standards. A government directory lists federal agencies concerned with EMI.
Circle Reader Action Number 712.

A 700-page databook from GEC Plessey Semiconductors, Scotts Valley, CA, spotlights the company's **radiation-hard and silicon-on-sapphire (SOS) ICs**. SOS-based products include RAMs to 64 Kbits, logic, 1553 protocol devices, 29XX-bit slice, and a range of MIL-STD 1750A microprocessors and peripheral devices.
Circle Reader Action Number 714.

A new cost-effective **metal cutting system** is profiled in a booklet from Cybermation Cutting Systems Inc., Medford, MA. The RAZOR™ system uses a proprietary narrow-beam cutting head to produce precision metal parts at nearly half the cost of laser-based systems. It features advanced machine and numerical controls that support a 48" x 96" cutting range on a large, rigid machine tool bed.
Circle Reader Action Number 706.

A full-color brochure describes the IMAGE system, a universal test system from ACL Technologies, Santa Ana, CA, that provides **computer-aided testing** for a variety of aircraft components, including servovalves, servoactuators, pumps, and motors. Airlines can use the IMAGE system to quickly and accurately test components removed from aircraft to determine whether or not they should be sent to overhaul.
Circle Reader Action Number 716.

Subject Index

Computer controllable X-Y table only $1,890

Includes table, step motors & control / driver

- ✔ Compact & Simple Design
- ✔ Scanning and Feeding
- ✔ Testing and Manufacturing
- ✔ 747 Different Models
- ✔ Send for free catalog

CALL 800/642-6446 except NYS

VELMEX, INC. P.O. BOX 38 E. BLOOMFIELD, NY 14443 PHONE 716/657-6151

Circle Reader Action No. 447

Circle Reader Action No. 416

FREE! 130 Page Catalog "Optics for Industry"

Free 130 page product catalog from Rolyn, world's largest supplier of "Off-the-Shelf" optics. 24-hour delivery of simple or compound lenses, filters, prisms, mirrors, beamsplitters, reticles, objectives, eyepieces plus thousands of other stock items. Rolyn also supplies custom products and coatings in prototype or production quantities. **ROLYN OPTICS Co.,** 706 Arrowgrand Circle, Covina, CA 91722-2199, (818)915- 5707, FAX (818)915-1379

Circle Reader Action No. 551

3D MOTION CONTROL FOR MACs

THREE-D MOTION is a multiple axis software package for step-motion applications such as engraving, milling, robotics and vision systems. Screen presentation consists of mouse-driven panel and pop-up windows.

Motion is controlled by Absolute (screen grid positions of x-y and z are selected by "clicks"), Relative (jogs the position along the selected path), Numeric (positions are entered as text with parameters, i.e. speed, acceleration and spindle), and PICT (creates a scan file that translates any screen image into x-y with z axis intensity). Demo disc available.

THREE-D is MultiFinder compatible. A comm port connects multiple controller/driver hardware.

Software: $235. **3-axis hardware: $895.**

ELECTRONIC PRODUCTS
P.O. Box 891, Mountain View, CA 94042
800-424-STEP

Circle Reader Action No. 409

Let AutoCAT drive your IEEE Bus for only $295.00!

Software for IBM™ or compatible computers to Automate Computer Aided Tests.

- Automatic test generation
- No programming knowledge required. Online help.
- Uses IEEE-488, RS232 and plug in cards
- Spreadsheet/database compatible files
- Menu and mouse driven
- Free demo disk

NEOS

4451B Enterprise Ct., Melbourne, FL 32934
Ph.: (407) 259-2090 Fax: (407) 255-0274

Circle Reader Action No. 577

Circle 301 For OEM Product Application.
Circle 556 For In-House Use.

Build Your Own Space Shuttle

This 1/72 scale model of the space shuttle Discovery features a huge 13" wingspan and includes engraved tile detail, movable rudder and flap, authentic NASA decals, adjustable manipulator arm, opening cargo bay doors, and detailed Spacelab payload. Molded in white. Kits are $24.95 each + $4.00 postage and handling. (NY residents add sales tax.) **Send check or money order to: NASA Tech Briefs, Dept. F, 41 East 42nd St., New York, NY 10017. For credit card orders, call (800) 258-0201 (NY state: 212-490-3999).**

More than 450 pages of tooling components!

FREE!

This illustrated complete line catalog includes component parts for jigs and fixtures, chuck jaws, plug gauges, threaded inserts, stainless steel tooling components, toggle clamps, SWIFTSURE power workholding devices, drill jig bushings, locking pins, and modular fixturing. Completely illustrated. **Send for your free copy.**

Carr Lane MANUFACTURING CO.

Circle Reader Action No. 429

EXPERTS IN FAR-IR INTERFEROMETERS

FOURIER TRANSFORM POLARIZING MICHELSON, MARTIN PUPLETT AND FABRY PEROT INTERFEROMETERS

- Range 17μm to 5mm (2-600cm^{-1})
- Fast Scan and Step Scan Versions
- High Resolution (up to 0.025cm^{-1})
- Phase, Amplitude or Polarization Modulation
- Detectors (room temp. or cryogenic)
- Software and Computer Interface
- Dispersive Accessory Option

OVER 20 YEARS EXPERIENCE

SPECAC

SPECAC ANALYTICAL INC.
301 Commerce Drive, Fairfield, CT 06430
Tel: (203) 366-5112 Fax: (203) 384-1524
A Cambridge Electronic Industries (CEI) Company

Circle Reader Action No. 621

ADVERTISERS INDEX

*RAC stands for Reader Action Card. For further information on these advertisers, please circle the RAC number on the Reader Action Card in this issue. This index has been compiled as a service to our readers and advertisers. Every precaution is taken to insure its accuracy, but the publiser assumes no liability for errors or omissions.

NASA Tech Briefs, ISSN 0145-319X, USPS 750-070, copyright © 1991 in U.S., is published monthly by Associated Business Publications Co., Ltd., 41 E. 42nd St., New York, NY 10017-5391. The copyrighted information does not include the individual tech briefs which are supplied by NASA. Editorial, sales, production and circulation offices at 41 East 42nd Street, New York, NY 10017-5391. Subscription for non-qualified subscribers in the U.S., Panama Canal Zone, and Puerto Rico, $75.00 for 1 year; $125.00 for 2 years; $200.00 for 3 years. Single copies $10.00. Foreign subscriptions one-year U.S. Funds $150.00. Remit by check, draft, postal, express orders or VISA, MasterCard, and American Express. Other remittances at sender's risk. Address all communications for subscriptions or circulation to NASA Tech Briefs, 41 East 42nd Street, New York, NY 10017-5391. Second-class postage paid at New York, NY and additional mailing offices.
POSTMASTER: please send address changes to NASA Tech Briefs, 41 East 42nd Street, Suite 921, New York, NY 10017-5391